PREVENTING RAPID PLATELET ACCUMULATION UNDER VERY HIGH SHEAR STRESS

A Thesis
Presented to
The Academic Faculty

by

Andrea N. Para

In Partial Fulfillment
of the Requirements for the Degree
Doctor of Philosophy in the
Woodruff School of Mechanical Engineering

Georgia Institute of Technology
August 2012

PREVENTING RAPID PLATELET ACCUMULATION UNDER VERY HIGH SHEAR STRESS

Approved by:

Dr. David Ku, Advisor
Woodruff School of Mechanical Engineering
Georgia Institute of Technology

Dr Hans Deckmyn
Interdisciplinary Research Center
Katholieke Universiteit Leuven

Dr Shannon Meeks
School of Medicine
Emory University

Dr Todd Sulchek
Woodruff School of Mechanical Engineering
Georgia Institute of Technology

Dr Gilda Barabino
Wallace H. Coulter Department of Biomedical Engineering
Georgia Institute of Technology

Date Approved: May 2, 2012

To my family and friends,

and the many friends who have become family.

ACKNOWLEDGEMENTS

I would like to begin by thanking my advisor, Dr Ku, for your guidance and encouragement over the last seven years. You have taught me the importance of constantly challenging myself and always pursuing my goals. Thank you for this incredible experience.

I would also like to thank my committee: Dr Deckmyn, Dr Meeks, Dr Sulchek and Dr Barabino as well as Dr Roberts, who funded this project. Your conversations, both personal and professional have been incredibly helpful. It is an honor to have gotten to work with you all.

I would also like to thank everyone in the Phlebotomy Lab at Georgia Tech (Jack Horner, LaShonna Stokes, Lisa Carr, Kenneth Butts and Richard Hoose) - you all have made this last seven years such a wonderful journey! The morning would not be the same without your wit, stories, and advice. Thanks for keeping me in line. You are all very special to me. Ken - All of the researchers and donors send you our very best wishes for a speedy recovery.

To my friends from the KULAK - Karen Vanhoorelbeke, Karen De Ceunynck, Bauke De Maeyer, Katleen Broos (and Benjamin and Casper), Hendrik Feys (and Jennifer and Nina) and Isabelle Salles - Thank you all for opening your homes to me and taking me through your cities. You all have created incredibly fond memories and Belgium would not have been the same without your kindness.

I have gotten to know a lot of people throughout this process, many of which have become family. To Mamtaben - thanks for being such an awesome sister and running buddy and for always reminding me how much flatter TX is than GA. Pooja - you already know from your real sister that you are an amazing person, so positive

and encouraging, but please know you have another fan. Rahul - I have missed our football games and gratuitous food binges, but consider myself very lucky for all of our conversations and visits. Srin - my other Indian bhaiya - you are probably one of the funniest, most outspoken people I know and I would be remiss in saying that I am a little surprised that the Secret Service allowed you into the Whitehouse. We are all so lucky that Pooja is a lawyer. To my other Indian family - Pritty, Murali, Kartik B, Smitha, Tanvi, Yash, Ayona, Avika, Popo and Kartik S - you guys have provided so much levity and fun to this experience, I can't thank you enough not to mention the food! I can't wait until our next reunion.

Further, I need to thank my wingmates who put up with my antics. Julia H - you are not only an incredible researcher, you are an amazing woman, confidant and Polish sister. Our "Finer Things" club was a sight to behold. To Rachel W - your amazing brunches, clothing outings and dinners were the setting dreams are made out of. It could only be topped by your amazing capacity for kindness and patient ear. I don't know how I did not meet you earlier, but I am so glad I finally found you! To Roxanne - you are an amazing and talented woman. I can't wait to be a customer at your bakery and get to see your amazing cakes in magazines! Katie M - I have thoroughly enjoyed our wildly productive coffee sessions. You are a woman I admire and I am very lucky to have gotten to know you better. Kelly S - We know each-other far too well to ever not be friends. You have been a great personal advisor, workout buddy and pub crawl coordinator - always providing a good laugh or helpful advice. To Tamera - you are completely my other half and I am so glad we got to work in the lab for 2 years together. You are an amazing person; it almost makes up for the fact that JP is always wrong. JP - you are hilarious and have been so fun to get to know over the years but, I am sorry, Tamera is funnier. Andrew S - I want to thank you for always providing levity and putting up with my practical jokes. I could always count on you for a coffee break and an interesting conversation. Thanks

for introducing me to the other half of "Team Andrea". Chris H - you and Ally have been a blast to hang out with during this experience. I will miss our endless rides on the Emory bus, trading off the crossword, and having awesome Superbowl Sundays at your house.

To the Glezer lab - thank you guys for helping me feel like an honorary member, for the great talks and many meals we have shared. Your terrible taste in movies is easily made up for by being one of the most genuine groups of men I have ever met. Thank you for being so kind.

My current labmates: Marmar, Daniel, Mark and Susan - thank you for putting up with me. You have all been incredibly encouraging during this process. I will miss our random conversations and long walks. Thank you so much for your support. You have made this lab an easy place to come to every day.

A special thank you is reserved for my family, which has come to include not only my parents and brother, but now includes Teresa, Christopher, Joshua, and my "outlaws", Maud and David. You all have been so supportive during this process - your words of encouragement have gotten me through some very rough times and I cannot be thankful enough for having you in my life. Thanks for being brave enough to answer the phone. Please know I love you all.

Lastly, to Abe. I can't believe how lucky I was to have met you on the first day of grad school. You are an amazing man, my best friend, an incredible researcher and someone that I not only love, but admire. I am so glad I have had your support during this experience.

TABLE OF CONTENTS

LIST OF TABLES

LIST OF FIGURES

SUMMARY

Atherosclerosis is a major cause of mortality in industrialized nations. Atherosclerosis is characterized by plaque deposition which decreases the lumen diameter into a stenosis. The creation of a restriction increases shear rates pathologic levels exceeding 3,500s^{-1}. Following plaque cap rupture, thrombus may form from the accumulation of millions of platelets, occluding the vessel, leading to heart attack and stroke. Studies of high shear thrombosis show that platelet activation, $\alpha_{IIb}\beta_3$ and vWF are involved. However, some recent studies also suggest that high shear aggregation is not dependent on activation or $\alpha_{IIb}\beta_3$. Several antiplatelet pharmaceuticals against activation and $\alpha_{IIb}\beta_3$ have been proposed, but their efficacy in patients remain mixed. The overall objective of this project is to determine the factors necessary for thrombosis to occlusion in very high shear regions seen in diseased arteries. Our central hypotheses are that platelet activation and the subsequent conformational change in $\alpha_{IIb}\beta_3$ are necessary for thrombosis, and that higher concentrations of vWF in the plasma will increase thrombosis.

To this end, we developed a new high shear hemodynamic model utilizing 30mLs of whole blood and quantified thrombus thickness, volume accumulation and accumulation rates. We demonstrate that thrombosis to occlusion stems from a second phase of Rapid Platelet Accumulation (RPA). Thrombus accumulation is completely prevented by PGE_1 inhibition of platelet activation. Similarly, $\alpha_{IIb}\beta_3$ blockade via abciximab prevented significant thrombus deposition and RPA. We also found that increasing plasma vWF levels in high shear regions increased thrombus thickness and suggestively increased RPA rates. The results clarify the need for activation of mural platelets for long term thrombus accumulation without the activation of circulating

platelets.

CHAPTER I

INTRODUCTION

Cardiovascular disease is a major cause of mortality in industrialized nations.[9, 13, 25] Atherosclerosis is a form of cardiovascular disease, characterized by plaque deposition which decreases the elasticity of the arteries and potentially decreases the lumen diameter. A decrease in the lumen diameter can have a significant impact on the shear rate, with normal vasculature attaining shear rates $<$1,500s^{-1}, while pathologic, diseased arteries with restricted diameters are capable of shear rates exceeding 100,000s^{-1}.[1, 20] Following either endothelial damage or the rupture of the plaque, platelets deposit on the thrombogenic surface exposed. Platelet deposition can form a platelet-rich plug which occludes the vessel, precipitating myocardial infarction (MI) and stroke.[6, 28] The process of platelet accumulation, which may lead to occlusion, is mediated by many factors, including: high shear, platelet activation, Glycoprotein IIb/IIIa ($\alpha_{IIb}\beta_3$) and von Willebrand Factor (vWF).

Platelets in flow arrest onto a thrombogenic surface under arterial conditions via Glycoprotein Ib (GPIb) to vWF interactions.[2] Following initial adhesion, platelet activation ensues, aiding platelet-platelet accumulation. Platelet activation is an event which can lead to the release of platelet contents, shape change of the platelet and the conformational change of $\alpha_{IIb}\beta_3$.[24] Aside from being stimulated by mechanical forces via pathologic shear, activation can occur through pathways mediated by ADP and Ca^{2+}.[28]

The conformational change in $\alpha_{IIb}\beta_3$, one of the most abundant receptors on the platelet surface with over 40,000 copies present, allows the protein to bind other proteins such as vWF.[4, 7] vWF aids platelet-platelet attachment and is found in platelet

alpha granules and the plasma of whole blood.[15] vWF is a shear dependent protein, elongating at shear rates exceeding $6{,}000s^{-1}$.[23] Elongation exposes the many binding domains of vWF, allowing it to bind more readily than in its non-elongated globular form.[19, 26] vWF's A1, A3 and C1 domains, which bind GPIb, collagen and $\alpha_{IIb}\beta_3$ respectively, allow vWF to participate in thrombosis.[21, 22, 29] After activation, the expulsion of the alpha granule from the platelet creates vWF concentrations which are 50x higher on the surface of thrombotic growth than in whole blood.[10]

These proteins mediate thrombosis is differing ways - aiding platelet adhesion and aggregation. Platelet adhesion refers to the arrest of a platelet onto a surface from flow and, under the conditions of arterial thrombosis which include high shear stress and collagen exposure, is usually mediated via GPIb.[2, 8] Aggregation refers to the formation of a platelet-platelet mass (<100 platelets), sometimes due to shear prior to adhesion.[20]

Recent studies by Flannery and Para with porcine blood suggest that the process of thrombus formation occurs in two phases: an initial adherence of platelets onto a surface followed by a faster type of platelet accumulation, Rapid Platelet Accumulation (RPA).[12, 17] RPA is accumulation rates $\geq 1.6\ \mu m^3\ \mu m^{-2}\ min^{-1}$.[17]

Studies conducted at lower shear rates ($<3{,}000s^{-1}$) indicate proteins have shear dependent behaviours, with proteins such as fibrinogen dominating platelet to platelet aggregation at shear rates $<2{,}600s^{-1}$, but not above.[27] Under very high shear conditions ($20{,}000s^{-1}$), Ruggeri et al showed that platelet aggregation was activation independent, with both Ruggeri and Turitto further supporting the potential for a different protein mechanism contributing to platelet accumulation under very high shear stress.[20]

As $\alpha_{IIb}\beta_3$ is seen as the main receptor for adhesion and aggregation in the formation of a platelet plug and platelet activation is necessary for the conformational change required for $\alpha_{IIb}\beta_3$ to participate in high shear occlusion, it is important to

determine the effect that blocking them will have on RPA.[4, 5] Further, as vWF aids platelet to platelet deposition under high shear conditions it is important to determine if thrombosis can be increased by increasing vWF concentrations in the plasma and at the surface of thrombotic formation.[15, 18] Therefore, to study thrombosis in vitro, it is necessary to recreate the hemodynamic conditions that trigger arterial thrombosis.

Previous studies have utilized parallel plate chambers, stenosis models and the PFA-100® to study platelet deposition.[11, 12, 16, 17]

The parallel plate model is the most widely utilized model, often using fluorescence microscopy to measure the amount of deposited, fluoresced platelets on the surface of the chamber.[16] While parallel plates can create very high shear conditions, most utilize a recirculating blood arrangement that often activates all the circulating platelets.[14] Further, parallel plate chambers utilize abrupt geometries and a wide aspect ratio which may induce secondary flows not present in stenotic arteries. However, the biggest drawback of the parallel plate system is that thrombus growth in the depth direction is poorly resolved. The parallel plate chamber gives an *en face* view of platelet deposition. Thus, the common parallel plate endpoint is surface coverage of platelet attachment to an immobilized protein that may miss a different phenomenon of platelet-platelet attachment. While intravascular thrombosis requires the accumulations of hundreds of millions of platelets, this phenomenon is poorly measured in parallel plate chambers. The study of such large volumes of thrombosis requires high resolution thickness measurements in a range from 10 to thousands of microns.

Tubular glass stenosis models, such as the gravitationally model created by Flannery, et al, allow for the measurement of millions of platelet depositions accumulating to occlusion, although require 240mLs of blood.[12, 17] This large blood volume requirement is not a viable option for repeatable testing with human blood.

The PFA-100® uses small amounts of blood to occlude a small filter at high shear rates.[11] While the PFA-100® uses small amounts of blood under pathologic shear conditions, it does not measure the thickness of thrombus formation deposited which is necessary for the calculation of accumulation rates. Rather, it measures time to occlusion of the filter which may include an embolic event due to upstream platelet aggregation and not RPA. Further, the small aperture occludes within 5 minutes, a time scale that likely represents only Phase I of attachment by thousands of platelets instead of Phase II where millions of platelets accumulate to cause arterial thrombosis.

Therefore, we have created a syringe pump-fed stenosis model which allows for the measurement of thrombus thickness . The thickness vs time data can be converted into volume and accumulation rates. We utilize an in-vitro setup which exposes small volumes (<30mLs) of whole, human blood to high shear conditions (>3,500s^{-1}), creating an environment which promotes large scale thrombosis.[3]

It is the goal of this dissertation to utilize an in-vitro hemodynamic model to answer the following questions regarding the clinically-fatal, massive accumulation of platelets under high shear conditions associated with an atherosclerotic stenosis:

- Are platelet-to-platelet thrombosis rates different than platelet-surface attachment rates?
- Can we demonstrate stenotic thrombosis with less than 50 mls of whole blood with a high resolution measurement of volume?
- Does human shear induced platelet thrombosis differ from porcine thrombosis?
- What are the rates of shear induced platelet accumulation in human blood?
- Is shear induced thrombus from human blood composed of mainly platelets?
- Does blocking $\alpha_{IIb}\beta_3$ prevent thrombosis under high shear stress conditions?

- Does blocking $\alpha_{IIb}\beta_3$ prevent significant thrombus thickness deposition under high shear stress conditions?
- Does blocking $\alpha_{IIb}\beta_3$ prevent significant thrombus volume deposition under very high shear stress conditions?
- Does blocking activation prevent large-scale thrombosis under high shear stress conditions?
- Does blocking activation prevent large-scale thrombus thickness deposition under high shear stress conditions?
- Does blocking activation prevent large-scale thrombus volume deposition under very high shear stress conditions?
- Does adding a high concentration of vWF to whole blood increase thrombosis under high shear conditions?
- Does adding vWF to whole blood significantly increase thrombus thickness under high shear conditions?
- Does adding a high concentration of vWF to a surface with initial deposition increase thrombosis under high shear conditions?
- Does adding vWF to a surface with initial deposition significantly increase thrombus thickness under high shear conditions?

1.0.1 References

REFERENCES

[1] Bark, David Ku, D., "Wall shear over high degree stenoses pertinent to atherothrombosis," *Journal of Biomechanics*, vol. 43, pp. 2970–2977, 2010.

[2] Cauwenberghs, N., Meiring, M., Vauterin, S., van Wyk, V., Lamprecht, S., Roodt, J. P., Novak, L., Harsfalvi, J., Deckmyn, H., and Kotze, H. F., "Antithrombotic effect of platelet glycoprotein Ib - blocking monoclonal antibody fab fragments in nonhuman primates," *Arteriosclerosis, Thrombosis, and Vascular Biology*, vol. 20, pp. 1347–1353, 2000.

[3] Chow, T. W., Hellums, J. D., Moake, J. L., and Kroll, M. H., "Shear stress-induced von willebrand factor binding to platelet glycoprotein Ib initiates calcium influx associated with aggregation," *Blood*, vol. 80, no. 1, pp. 113–120, 1992.

[4] Coller, B., "Blockade of platelet gpIIb/IIIa receptors as an antithrombotic strategy," *Circulation*, vol. 92, pp. 2373–2380, 1995.

[5] Dav, G. and Patrono, C., "Platelet activation and atherothrombosis," *New England Journal of Medicine*, vol. 357, pp. 2482–2494, 2007.

[6] Davies, M. J. and Thomas, A. C., *Plaque fissuring-the cause of acute myocardial infarction, sudden ischaemic death, and crescendo angina*, vol. 53. London, ROYAUME-UNI: BMJ Publishing Group, 1985.

[7] de Walle, G. R. V., Schoolmeester, A., Iserbyt, B. F., Cosemans, J. M. E. M., Heemskerk, J. W. M., Hoylaerts, M. F., Nurden, A., Vanhoorelbeke, K., and Deckmyn, H., "Activation of $\alpha_{IIb}\beta_3$ is a sufficient

but also an imperative prerequisite for activation of $\alpha_{IIb}\beta_1$ on platelets," *Blood*, vol. 109, pp. 595–602, 2007.

[8] Doggett, T. A., Girdhar, G., Lawshe, A., Schmidtke, D. W., Laurenzi, I. J., Diamond, S. L., and Diacovo, T. G., "Selectin-like kinetics and biomechanics promote rapid platelet adhesion in flow: The gpIb α-vwf tether bond," *Biophysical Journal*, vol. 83, pp. 194–205, 2002.

[9] Eikelboom, J. W., Lonn, E., Jr., J. G., Hankey, G., and Yusuf, S., "Homocyst(e)ine and cardiovascular disease: A critical review of the epidemiologic evidence," *Annals of Internal Medicine*, vol. 131, pp. 363–375, 1999.

[10] Harrison, P. and Cramer, E., "Platelet alpha-granules," *Blood Review*, vol. 7, pp. 52–62, 1993.

[11] Kratzer, M. and Born, G., "Simulation of primary haemostasis in vitro.," *Haemostasis*, vol. 15, pp. 357–62, 1985.

[12] Ku, D. N. and Flannery, C. J., "Development of a flow-through system to create occluding thrombus," *Biorheology*, vol. 44, no. 4, pp. 273–284, 2007.

[13] Larson, M. G., Atwood, L. D., Benjamin, E. J., Cupples, L. A., Sr, R. B. D., Fox, C. S., Govindaraju, D. R., Guo, C.-Y., Heard-Costa, N. L., Hwang, S.-J., Murabito, J. M., Newton-Cheh, C., O'Donnell, C. J., Seshadri, S., Vasan, R. S., Wang, T. J., Wolf, P. A., and Levy, D., "Framingham heart study 100k project: genome-wide associations for cardiovascular disease outcomes," *BMC Medical Genetics*, vol. 8, p. S5, 2007.

[14] Meiring, M. S., Litthauerb, D., Harsfalvic, J., van Wyka, V., Badenhorsta, P. N., and d, H. F. K., "In vitro effect of a thrombin inhibition peptide selected by phage display technology," *Thrombosis Research*, vol. 107, pp. 365 – 371, 2002.

[15] Moake, J. L., Tumer, N. A., Stathopoulos, N. A., Nolasco, L. H., and Hellums, J. D., "Involvement of large plasma von willebrand factor (vwf) multimers and unusually large vwf forms derived from endothelial cells in shear stress-induced platelet aggregation," *Journal of Clinical Investigation*, vol. 78, pp. 1456–1461, 1986.

[16] Muggli, R., Baumgartner, H., Tschopp, T., and Keller, H., "Automated microdensitometry and protein assays as a measure for platelet adhesion and aggregation on collagen-coated slides under controlled flow conditions.," *The Journal of Laboratory and Clinical Medicine*, vol. 95, pp. 195–207, 1980.

[17] Para, A., Bark, D., Lin, A., and Ku, D., "Rapid platelet accumulation leading to thrombotic occlusion," *Annals Of Biomedical Engineering*, vol. 39, pp. 1961–1971, 2011.

[18] Peterson, D. M., Stathopoulos, N. A., Giorgio, T. D., Hellums, J. D., and Moake, J. L., "Shear-induced platelet aggregation requires von willebrand factor and platelet membrane glycoproteins Ib and IIb-IIIa," *Blood*, vol. 69, no. 2, pp. 625–628, 1987.

[19] Ruggeri, Z. M., "The role of von willebrand factor in thrombus formation," *Thrombosis Research*, vol. 120, pp. S5 – S9, 2007.

[20] Ruggeri, Z. M., Orje, J. N., Habermann, R., Federici, A. B., and Reininger, A. J., "Activation-independent platelet adhesion and aggregation under elevated shear stress," *Blood*, vol. 108, no. 6, pp. 1903–1910, 2006.

[21] Sadler, J. E., "Biochemistry and genetics of von willebrand factor," *Annual Review of Biochemistry*, vol. 67, no. 1, p. 395, 1998.

[22] Savage, B., Saldivar, E., and Ruggeri, Z. M., "Initiation of platelet adhesion by arrest onto fibrinogen or translocation on von willebrand factor," *Cell*, vol. 84, pp. 289 – 297, 1996.

[23] Schneider, S. W., Nuschele, S., Wixforth, A., Gorzelanny, C., Alexander-Katz, A., Netz, R. R., and Schneider, M. F., "Shear-induced unfolding triggers adhesion of von willebrand factor fibers," *Proceedings of the National Academy of Sciences*, vol. 104, no. 19, pp. 7899–7903, 2007.

[24] Shattil, S. J., Hoxie, J. A., Cunningham, M., and Brass, L. F., "Changes in the platelet membrane glycoprotein IIb/IIIa complex during platelet activation," *Journal of Bioligical Chemistry*, vol. 260, no. 20, pp. 11107–11114, 1985.

[25] Shiffman, D., Mikita, T., Tai, J. T. N., Wade, D. P., Porter, J. G., Seilhamer, J. J., Somogyi, R., Liang, S., and Lawn, R. M., "Large scale gene expression analysis of cholesterol-loaded macrophages," *the Journal of Biological Chemistry*, vol. 275, pp. 37324 – 37332, 2000.

[26] Siedlecki, C. A., Lestini, B. J., Kottke-Marchant, K., Eppell, S. J., Wilson, D. L., and Marchant, R. E., "Shear-dependent changes in the three-dimensional structure of human von willebrand factor," *Blood*, vol. 88, pp. 2939–2950, 1996.

[27] Weiss, H. J., Hawiger, J., Ruggeri, Z. M., Turtto, V. T., Thiagarajan, P., and Hoffmann, T., "Fibrinogen-independent platelet adhesion and thrombus formation on subendothelium mediated by glycoprotein lIb-Illa complex at high shear rate," *Journal of Clinical Investigation*, vol. 83, pp. 288–297, 1989.

[28] Wootton, D. M. and Ku, D. N., "Fluid mechanics of vascular systems, diseases, and thrombosis," *Annual Review Of Biomedical Engineering*, vol. 1, pp. 299–329, 1999.

[29] Wu, D., Vanhoorelbeke, K., Cauwenberghs, N., Meiring, M., Depraetere, H., Kotze, H. F., and Deckmyn, H., "Inhibition of the von willebrand (vwf)-collagen interaction by an antihuman vwf monoclonal antibody results in abolition of in vivo arterial platelet thrombus formation in baboons," *Blood*, vol. 99, pp. 3623–3628, 2002.

CHAPTER II

RAPID PLATELET ACCUMULATION LEADING TO THROMBOTIC OCCLUSION

2.0.2 Introduction

An occluding, platelet-rich thrombus can cause sudden cardiac ischemic death in under an hour.[11] The sequence of events in acute arterial thrombosis is poorly understood as the clinical event is rapid and difficult to observe. Many investigators have utilized parallel plate chambers to study the formation of platelet deposition under shear.[1, 24] In parallel plate systems, investigators typically study lower, physiologic wall shear rates (<3500 s^{-1}) with experimentation times of <5 min.[1, 19] Platelet deposition under shear is thought to occur from Glycoprotein Ib (GPIb) on circulating platelets adhering to collagen via fibrinogen or von Willebrand Factor (vWF).[8, 10] Following the initial adhesion to the damaged vascular endothelium, Glycoprotein IIb/IIIa ($\alpha_{IIb}\beta_3$), mediated by fibrinogen and vWF, enables attached platelets to bind more firmly to other platelets following activation.[13, 22]

Alevriadou et al. measured a maximum deposition of approximately $20 * 10^6$ platelets cm^{-2} (0.5 μm^3 μm^{-2} min^{-1}) in a parallel plate flow chamber using 2 min experimentation times and low, physiologic shear (1500 s^{-1}).[1] Badimon et al. measured higher deposition rates at an increased shear (3380 s^{-1}) to achieve a deposition rate of 8 μm^3 μm^{-2} min^{-1}, while utilizing experimental times of 5 min.[3] Further increasing shear, Barstad et al. reported deposition rates of 12 μm^3 μm^{-2} min^{-1} utilizing high pathologic wall shear rates (10,500 s^{-1}) after times of 5 min.[5] Others have observed that platelet deposition increases with increasing wall shear rate up to about 10,000 s^{-1}.[29] In parallel plate systems, platelet attachment to a modified

surface is best for detecting surface area coverage, but is not well suited for volume growth that requires depth measurements. Further, parallel plate systems have difficulty exceeding 32,000 s^{-1} .

Thrombus formation can be optically visualized in a tubular test section with high spatial and time resolution.[21] The volume growth of thrombus can be clearly seen as perpendicular to the walls, as compared with the en face view of parallel plates. A stenosis can be used to create a focal area of very high shear stress that has pathologic relevance. The focal wall shear rates in a coronary stenosis can be >600,000 s^{-1} that is imposed on blood for a physiologic short duration instead of hours to minutes with a recirculating cone- and-plate or parallel plate system.[4] Occlusion can be verified by complete cessation of blood flow, a relevant endpoint with catastrophic clinical consequences. However, the location of platelet-rich thrombus formation within a stenosis has been difficult to identify, as Schoephoerster et al. and Bluestein et al. report partial platelet accumulation in regions away from the apical point, while others such as Badimon and Badimon and Markou co-workers observe thrombus formation at the apex in the region of highest shear.[2, 6, 27, 30]

Currently, there is a need in the field for a flow- based assay which utilizes high shear, whole blood and minimal anticoagulation in which thrombus forms to serve as a point of care system for physicians in an effort to provide better diagnostic care for patients.[31, 32]

In this article, we measure platelet deposition rates in an in vitro flow system with high resolution in real time. It is our goal to quantify thrombus formation rates with high spatial and time resolution in an in vitro system of single-pass blood flow under conditions of pathologic shear stress in a stenosis. We propose a new method for creating occlusive thrombosis under very high shear stress for more effective patient care.

2.0.3 Experimental Design and Methods

2.0.3.1 Flow Chamber

An in vitro flow system was designed to create very high shear stress in a test section that could be visualized under a microscope. Whole, porcine blood was perfused through the test section using a gravity pressure head of 30 mmHg (Figure 1 a). This single-pass flow-through hemodynamic system is similar to that previously described by Ku and Flannery.[21]

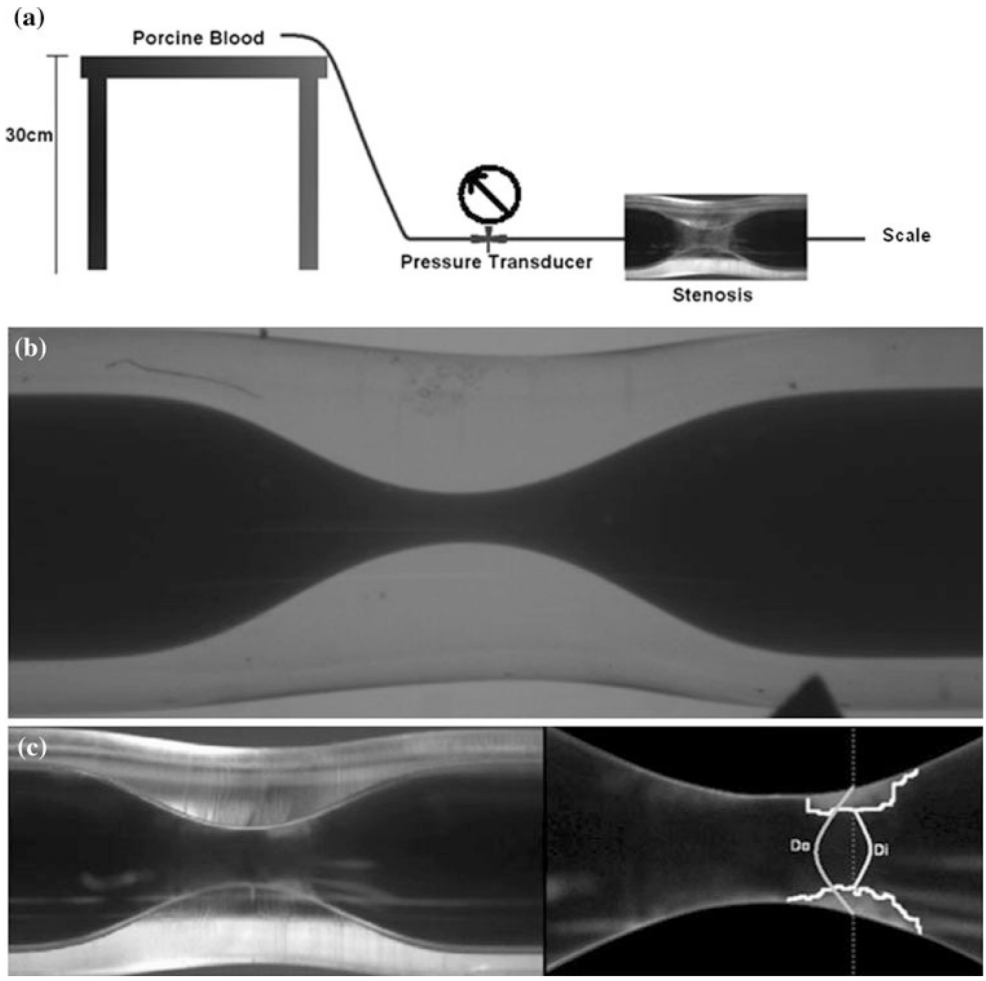

Figure 1: (a) Schematic diagram of the in vitro hemodynamic system. Whole blood flow originates on a raised platform to provide a constant gravity head of 30 mmHg and flows through a stenotic tube to an open outlet. A pressure transducer is used to monitor the upstream pressure and a graduated cylinder and stopwatch are used to measure flow rate. A high resolution digital camera records thrombus formation in the test section through a low power binocular microscope. (b) Image of an 82% stenosis. The gradual geometry is characteristic of all stenoses used in these experiments. (c) Measurement of thrombus volume. Measurements of the thrombus lumen diameter are taken approximately every 0.17 mm of the outer diameter created by the lumen of the tube and the inner diameter created by thrombus growth into the tube.

The stenotic test section (Figure 1 b) created a well- defined location of very high shear stress, followed by an area of recirculation.[4] The test section was constructed from glass tubes with an original inside diameter of 1.5 mm. A variety of hour-glass shaped stenoses were made by a professional glass blower with a severity ranging from 70 to 83% by diameter. The upstream Reynolds number was between 14 and 130. We have used computational fluid dynamics (CFD) to quantify the shear and velocity in the stenotic test sections. The glass was coated with fibrillar Collagen Type I (1 mg/mL, Sigma-Aldrich, St. Louis, MO, prepared according to manufacturers instructions) within the stenosis section and downstream portions of the tube. The collagen was left in the tube for 24 h in a warm, moist environment to form a thin layer of $<$100 μm. Following incubation, tubes were rinsed with $1x$ PBS (Fisher Scientific, Fair Lawn, NJ). Two sets of controls were utilized: (i) those with a stenosis and no collagen coating and (ii) those without a stenosis and with collagen coating.

2.0.3.2 Whole Porcine Blood

Whole blood from pigs was used for the experiments. Porcine blood was collected directly from the aorta at an abattoir (Holifield Farms, Covington, GA) and lightly anticoagulated with 3.5 USP $units/mL$ heparin (Sigma-Aldrich, St. Louis, MO). This amount of heparin prevented blood clotting in the static upstream reservoir, but allowed thrombus formation in the flowing test section. For perfusion through the test section, 250 mL of blood was transferred to a Pyrex jar for each experiment. During experimenta- tion, blood flowed from PVC plastic tubing (Baxter Healthcare Corporation, Deerfield, IL) with an inner diameter of 3 mm to the test section. All porcine blood tests were run within 8 h of harvest. During the flow experiments, blood was placed on a VSN-5 nutating mixer (Pro Scientific, Oxford, CT) to prevent blood separation. Mass flow rates were measured using a scale downstream.

2.0.3.3 Image Processing and Histology

The test section was photographed through a microscope objective using a high resolution digital CCD camera (Pixelfly, Keleim, Germany) connected directly to the Zeiss Stemi 2000-C (Zeiss, Jena, Germany) stereo microscope. Images were sequentially stored at a rate of approximately 0.7 $s/frame$ for off-line analysis. The software programs for post- processing image analysis were CamWare (Cooke Corporation, Romulus, MI), Photoshop (Adobe, San Jose, CA), Toast (Roxio, Nevato, CA), and Matlab (The Mathworks, Natick, MA). The image subtraction provided a quantitative representation of thrombus area vs. stenosis lumen area during thrombosis progression.

The volume of thrombus can be quantified from the two-dimensional microscope images (Figure 1 c). The images of thrombus were segmented by the observer and the incremental volume of thrombus was calculated as:

$$Volume(cm^3) = \sum_{i=1}^{n} (\frac{(D_{O,i}^2 - D_{I,i}^2}{4})\pi L \tag{1}$$

The length of the thrombus was divided into 11 increments of equal length, $L = 0.17 \pm 0.015$ mm. The outer diameter, D_O, was the diameter of the inside of the glass stenosis and the inner diameter, D_I, was the diameter created by measuring the top of the thrombus growing from the bottom of the tube and the bottom of the thrombus growing from the top of the tube. By summing the cylinders, the volume was then integrated along the length of the thrombus. Occlusion was defined as cessation of flow and is verified by the pressure transducer as an incremental increase in upstream pressure. Embolus was defined as a rapid increase in pressure and a sudden stoppage of flow within seconds. Embolus was verified visually and experiments which terminated with embolus were not included in this study.

Following occlusion, samples were fixed in 10% formalin (Fisher Scientific, Pittsburg, PA) overnight. The samples were then dehydrated and fixed in paraffin. 5 μm

sections were cut longitudinally and placed on a slide until Carstairs staining was performed.[28] This stain differentiates platelets from fibrin and collagen. Estimations of platelet number were based on a platelet volume of 5 fL and the assumption that platelets consume 80% of the total thrombus volume.[18, 21]

Some experiments were terminated prior to thrombotic occlusion and the lumen was perfused with Microfil MV-122 (Flow Tech Inc, Carver, MA), a lead chromate-based polymerizing contrast agent. The resulting tube was subjected to microcomputed tomography imaging (μCT 40; Scanco Medical, *Brüttisellen*, Switzerland) to visualize the protrusion of thrombus into the lumen of the stenosis (20 μm voxel resolution, $E = 55kVp$, $I = 145\mu A$, integration time 200 ms).

2.0.4 Results

2.0.4.1 High Resolution Imaging of Thrombus in a Stenosis

The time-to-occlusion was approximately 17.36 ± 2.62 min ($n = 6$) for stenoses between 70 and 83% . In the top Row I of (Figure 2), three example stenoses (a - c) with varying diameters show that small, focal accumulations of platelets adhered to the collagen stenosis within the first 40% of experimentation time. The white thrombus often accumulated at the down- stream end of the stenoses, but some spots were visible upstream of the apex.

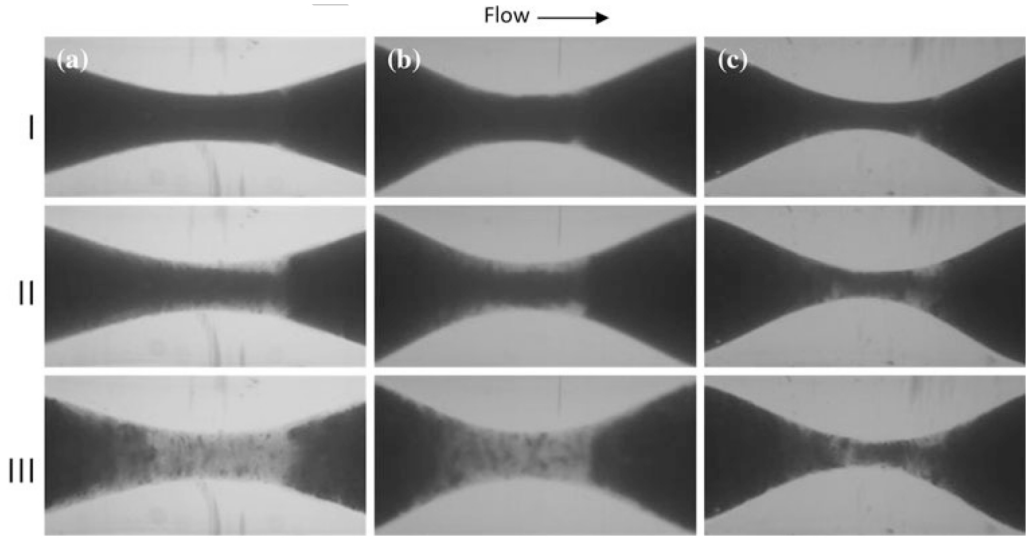

Figure 2: Series of photographs demonstrating the growth of thrombus under high shear stress in varying percent stenoses. Flow is from left to right. (a) A 70% stenosis by diameter is shown at 4.8, 9.3, and 15.8 min from the onset of flow. (b) A 75% stenosis by diameter is shown at 5.4, 8.0 and 14.4 min. (c) An 83% stenosis by diameter is shown at 3.82, 7.9, and 9.8 min.

After the initial focal spotting, thrombus formation appeared more diffuse, causing a generalized haziness that was concentrated near the apex of the stenosis and downstream (Figure 2 Row II). The thrombus accumulation after this time was rapid, visibly changing in real time. The rapid accumulation was no longer spotty, but extended both upstream and downstream of the apex for approximately 1 mm. Embolization of platelet aggregates was occasionally observed as a mass of white debris breaking off from the main structure. The embolic mass was large enough to be observed optically.

In some samples, the porcine blood would separate downstream of the throat, causing the high momentum red blood cells to separate from the low momentum recirculation flow, leaving a clear zone. The clear zone was not stagnant as an embolus could be seen rotating and the absence of thrombus in the downstream recirculation

zone was observed. A movie of this unusual hemodynamic phenomenon of a 42% stenosis can be seen online in the supplemental materials.

Row III of Figure 2 depicts the thrombus extent after total cessation of the blood flow. Thrombus spanned from wall-to-wall, but some areas devoid of platelets were occasionally seen. The bulk of the thrombus remained fixed at the apex with little volume in the downstream recirculation region.

Histologically, the apical thrombus was predominantly composed of platelets (Figure 3 a). Some red blood cells appeared to be in the downstream region beyond the platelet mass, likely due to red clot coagulation after cessation of flow. Microcomputed tomography provided an alternate view of the lumen and the thrombus surface before occlusion. In Figure 3 b, the positive casting of the lumen illustrates the irregular formation patterns of the thrombus surface, with uneven spacing between thrombus protrusions.

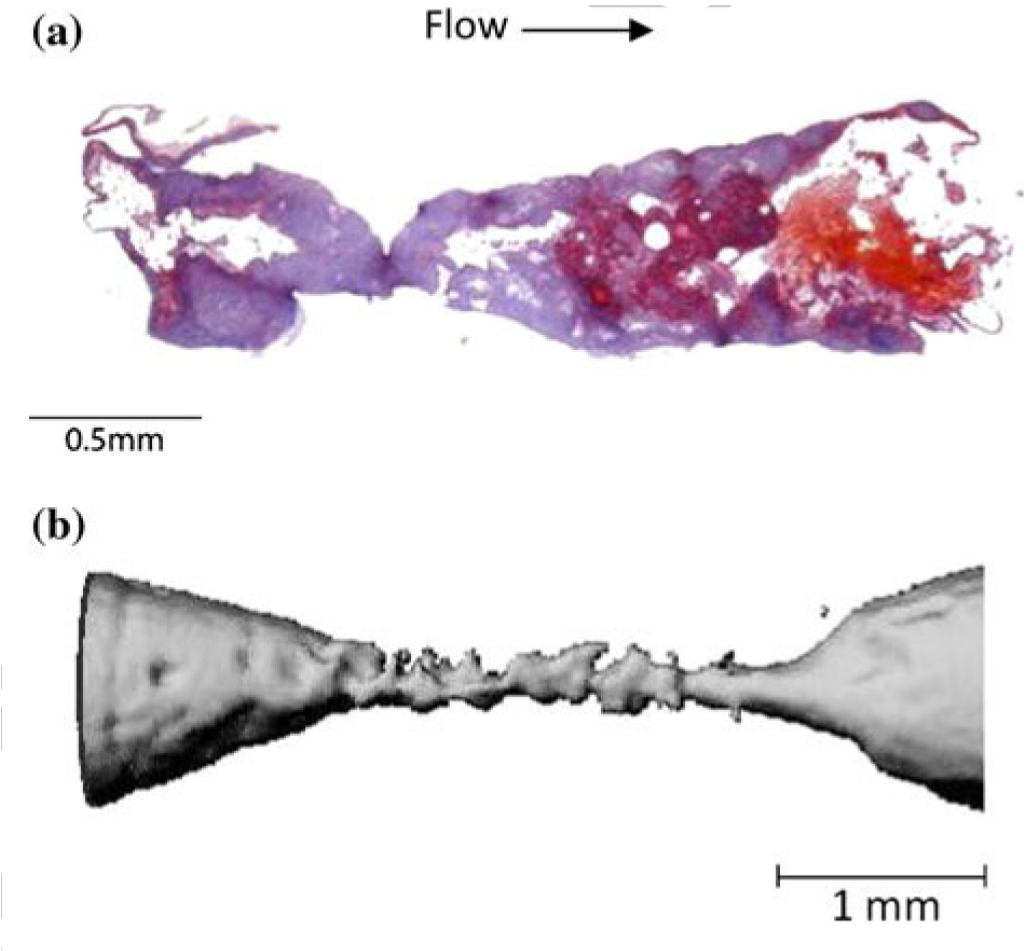

Figure 3: (a) Flow from left to right: Carstairs staining enables the composition of the thrombus to be observed. Platelets: gray-blue to navy; fibrin: deep red; red blood cells: yellow; collagen: bright blue. (b) Microcomputed tomography of the lumen of a 75% stenosis following partial thrombus growth into the lumen. The image shown is the shape of the lumen after thrombus has protruded into the flow.

2.0.4.2 Controls

1. Straight tubes were coated with collagen to isolate the independent effects of the focal stenosis (Figure 4 a). The wall shear rates in these tubes varied between 1000 and 2000 s^{-1}, a physiologic shear range for arteries. A thin layer of platelets attached to the collagen coated surface after several minutes. Little additional aggregation or

accumulation occurred after perfusion of 250 mL of whole porcine blood. Thus, rapid platelet accumulation (RPA) to occlusion appears to require very high shear stress conditions not present in flow through a straight tube with physiologic shear rates.

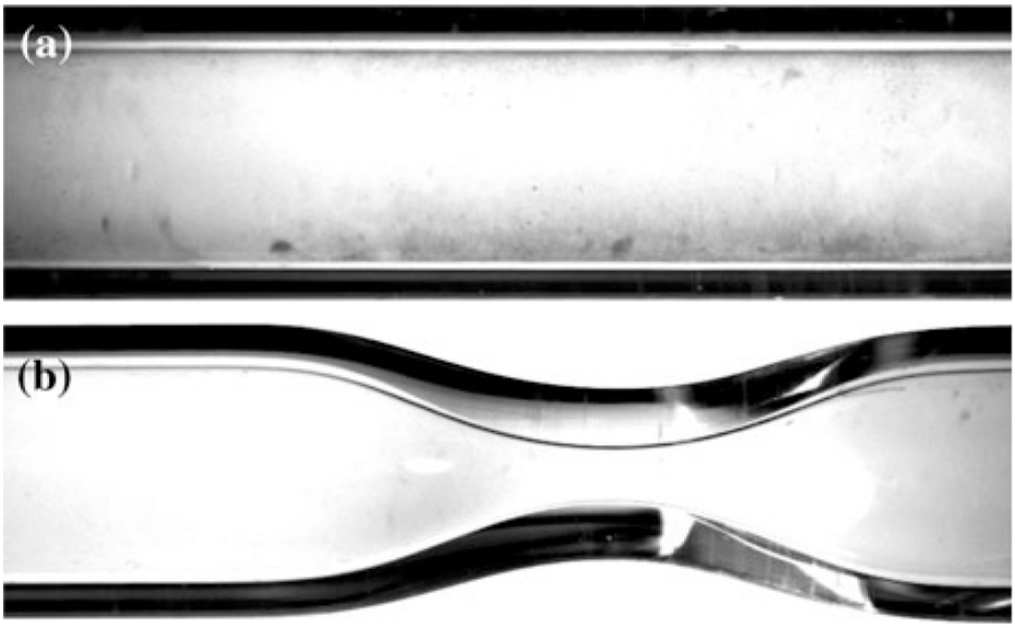

Figure 4: Two controls were utilized for this experiment: (a) collagen coated non-stenotic tubes. (b) Stenotic tube without collagen coating. It can be seen that no significant deposition forms on either the collagen coated or the stenosis without collagen. Deposition can be seen as areas stained with analine blue. As the tube is filled with PBS, some light reflections can be seen in the image.

2. Stenoses with no collagen coating were also used as a control. In these glass test sections, platelets did not adhere nor aggregate with whole blood perfusion (Figure 4 b). Thus, the collagen coating appears necessary for surface adherence, setting up the foundation for larger thrombosis.

2.0.4.3 Thrombus Position

Platelet accumulation was dominant in the throat of the stenosis where shear was greatest (Figure 5) and all occlusive thrombi occluded within the throat of the stenosis. Platelet-rich thrombus consistently formed in locations with high wall shear stress, such as those regions which reside within 1 mm upstream and downstream of the apex of the stenosis ($p<0.05, n = 6$). Dynamic thrombus accumulation in the lumen creates stenosis values of <80% by diameter that create wall shear rates in excess of 100,000 s^{-1}. The thrombus continues to grow with total occlusion in the face of these extreme shear rates.

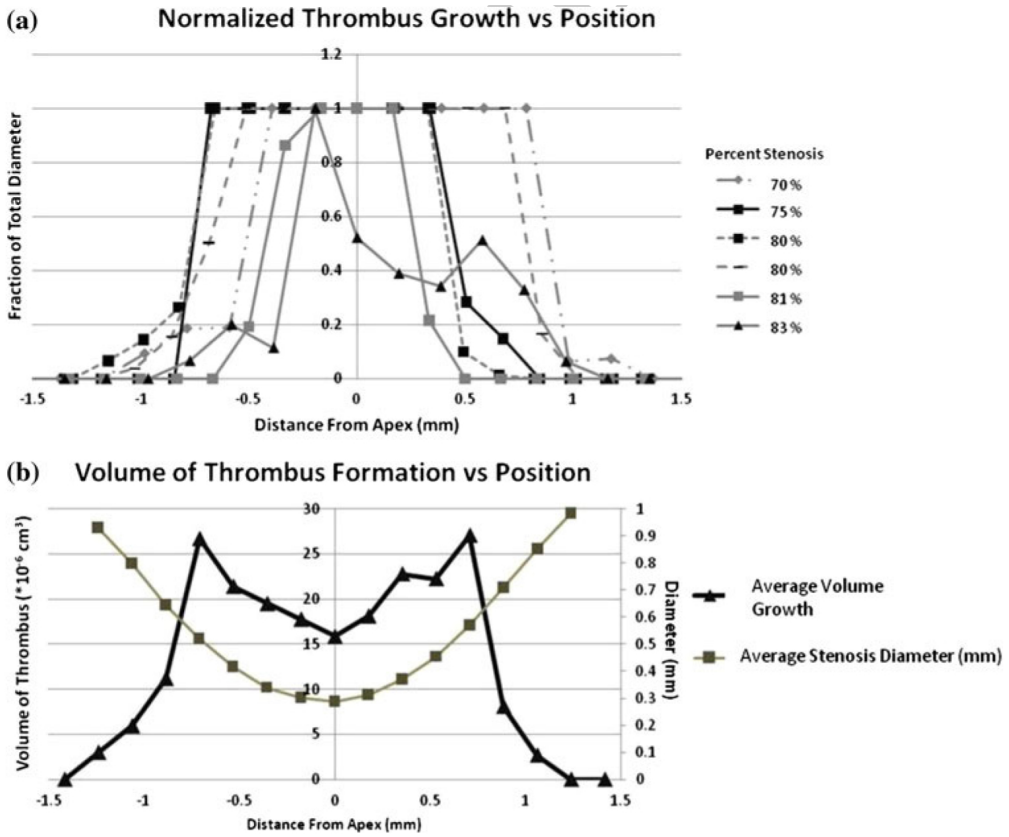

Figure 5: (a) This graph shows the fraction of the total diameter filled with thrombus at occlusion in relation to the apex of the stenosis. (b) This graph illustrates where the mean deposition of all of the stenotic test sections ($n = 6$) occurs with respect to the apex diameter at occlusion, with the average of all of the local stenosis diameters represented by the gray squares. Taking the mean of all of the inner diameters creates a representative stenosis that is 81% stenosed by diameter.

2.0.4.4 Thrombus Growth Accelerates to a Larger Rate in Phase II

The volume of thrombus growth is plotted over time, as shown in Figure 6. Thrombosis to occlusion can be broken into two phases: initial thrombus deposition of platelets to a collagen surface and RPA of platelets away from the surface. The differentiation of these two phases is further illustrated in Figure 6 b and Figure 7.

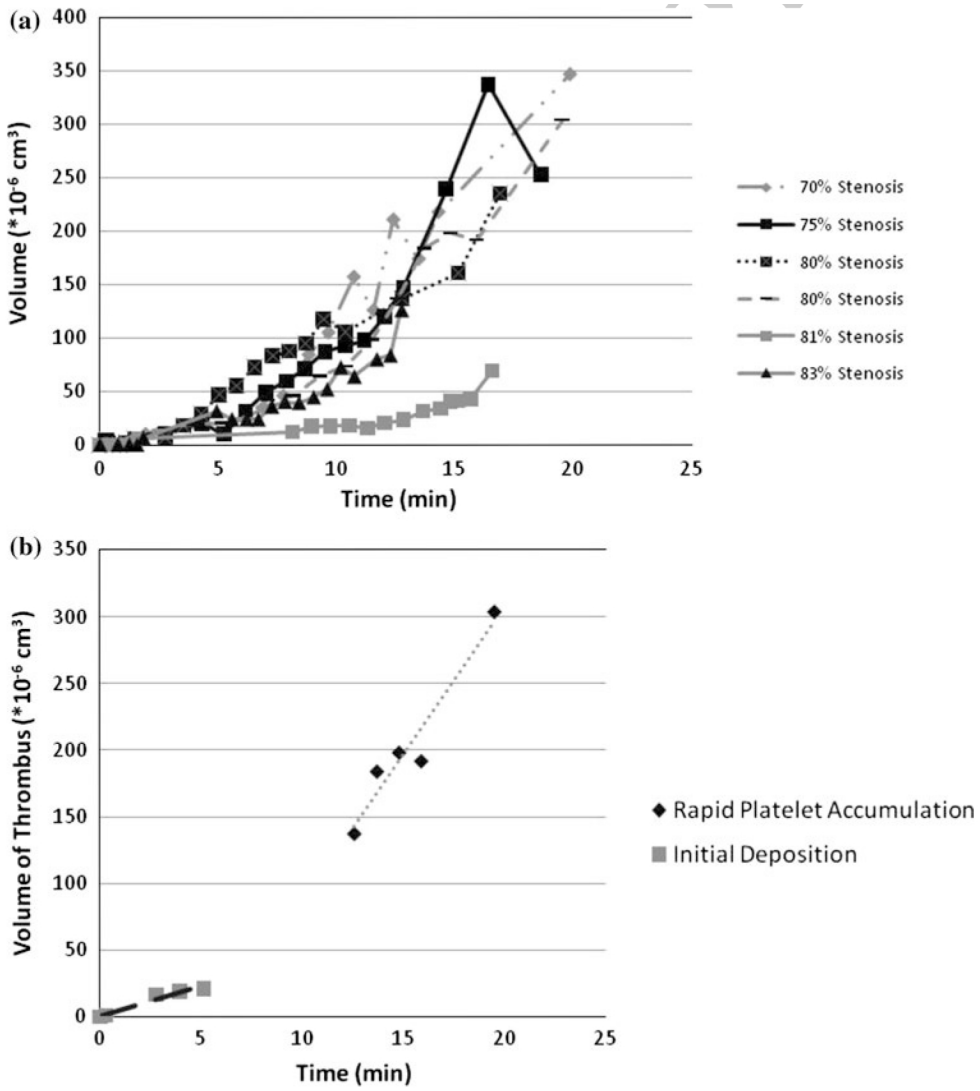

Figure 6: (a) Volume growth of thrombus over time until occlusion for six test sections. (b) Thrombus growth over time for an 80% stenosis. The initial rate of platelet deposition can be seen to have a visibly smaller slope (black dashed line) than the final rate of the half of formation leading to occlusion (RPA, gray dotted line).

All experiments exhibited initial deposition where few platelets could be observed at the macroscopic level for several minutes. Thrombus was first optically visible in the stenoses at 1.2 ± 0.76 min ($n = 6$). Initial deposition rates measured $3.1 \pm$

$1.7 * 10^{-6} cm^3 min^{-1}$. At this rate, a 70% stenosis would take approximately 6 h to completely occlude in the throat.

A second phase of RPA then followed in which mural thrombus grew rapidly. The RPA rates were significantly greater than the initial deposition rates, averaging 7.8 $\pm$ 3.5 μm^3 μm^{-2} min^{-1} ($20 \pm 4.5 * 10^{-6}$ cm^3 min^{-1} with an average surface area of $2.9 \pm 1.1 * 10^6 \mu m^2$, p<0.05, $n = 6$, Figure 7), with all occlusions occurring in <20 min (Figure 6 a). Our maximum RPA deposition rate of 13.7 μm^3 μm^{-2} min^{-1} (15.1 $*10^{-6}$ cm^3 min^{-1} in an 81% stenosis with an original surface area of 1.1 mm^2) is almost twice this.

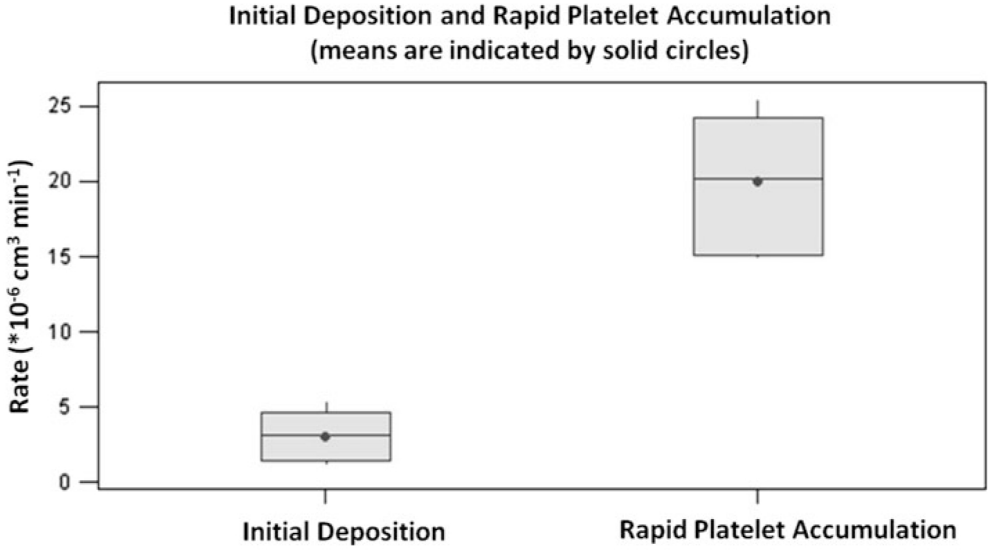

Figure 7: Initial deposition and rapid platelet accumulation formation rates in cm^3 $*10^{-6} min^{-1}$, $n = 6$. RPA ($20 \pm 4.5 * 10^{-6} cm^3 min^{-1}$) is significantly faster than initial deposition ($3.1 \pm 1.7 * 10^{-6} cm^3 min^{-1}$, p <0.05).

2.0.4.5 Intersection Determined Initial Deposition and RPA: Another Method for Calculating Rates

To serve as a check for the initial deposition rates and the RPA rates, we compared the intersection of the regression lines created for both of the rates. The regression lines for initial deposition and RPA of each stenosis intersected at 7.6 $\pm$ 3.6 min

($n = 6$), serving as a second method for dividing the initial phase of deposition from the second phase of RPA (Figure 8). Using the intersection time of the lines as a dividing point, initial deposition was $5.5 \pm 3.0 * 10^{-6}\ cm^3\ min^{-1}$ and RPA growth was $18 \pm 7.7 * 10^{-6}\ cm^3\ min^{-1}$ ($p<0.05$, Table 1).

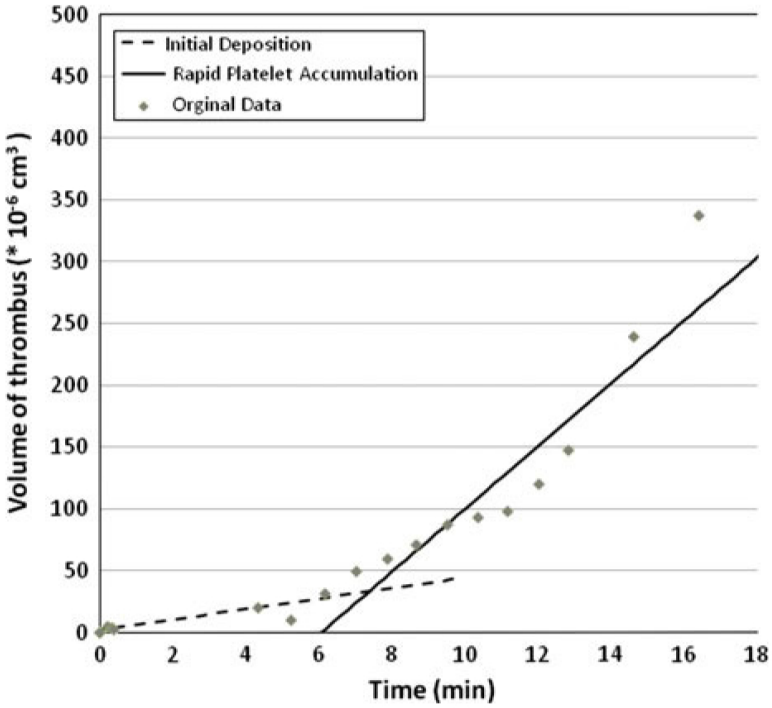

Figure 8: Regression lines describe a change in the rate of thrombus growth during initial deposition and rapid platelet accumulation. The intersection between the two lines occurred at approximately 7.6 min.

RPA rates determined using either the intersection definition or the last 50% of total thrombus volume, were similar ($p>0.05$, $n = 6$, Table 1). RPA accounts for the bulk of thrombus formation (77%). The slightly lower rate of RPA calculated using the intersection method could indicate some inclusion of the transition from the slow initial adhesion.

Using the intersection definition, initial deposition was greater than the initial deposition measured using the rate of formation to first visible thrombus ($p<0.05$,

Table 1: The percentage of final thrombus volume included in each definition of initial deposition and RPA as well as their respective rates of growth. It can be seen that initial deposition is faster than RPA when measured as first visible thrombus vs. last 50% of final thrombus volume (^{a}, $n = 6$, p<0.05) as well as first 7.6 min vs. last 7.6 min (^{b}, $n = 6$, p<0.05).

	Percentage of Final Thrombus Volume	Rate of Growth ($*10^{-6} cm^3 min^{-1}$)
Initial deposition (first visible thrombus)	$3.3 \pm 3.0\%$	3.1 ± 1.7^a
Initial deposition (intersection)	$19 \pm 10\%$	5.5 ± 3.0^b
Rapid platelet accumulation (last half)	$48 \pm 6.9\%$	20 ± 4.5^a
Rapid platelet accumulation (last half)	$48 \pm 6.9\%$	20 ± 4.5^b

$n = 6$). The intersection definition included the initial $19 \pm 10\%$ of thrombus volume, whereas deposition to first visible thrombus included only 3.3 ± 3.0% of the final thrombus volume. It is possible that the intersection definition includes some RPA growth, thereby increasing the initial deposition rate.

In our in vitro system, platelets pass through the stenosis only once. CFD calculations show that the velocity of platelets in the throat of the stenosis generally exceeds 1 m/s. The transit time of a platelet through the 2 mm stenosis would then be about 2 ms. This transit time is much too short for activation of the circulating platelet and is far below the threshold for shear-dependent activation. The CFD model quantifies the wall shear over the thrombus as reaching over 100,000 s^{-1} for all test sections described in this article.

2.0.5 Discussion

Our studies demonstrate that thrombus growth can be followed with high spatial and time resolution in an in vitro system of single-pass porcine blood flow under conditions of pathologic shear stress. Millions of platelets deposit within a stenosis to occlusion with local wall shear rates exceeding 100,000 s^{-1}. After an initial delay, RPA occurs with rates averaging $7.8 \pm 3.5 \mu m^3 \mu m^{-2} min^{-1}$ ($20 \pm 4.5 * 10^{-6} cm^3 min^{-1}$). With occlusion times of approximately 20 min and maximum deposition rates of

$13.7\mu m^3\mu m^{-2}min^{-1}$, the in vitro stenosis model is consistent with clinical observations of sudden cardiac ischemic death in under an hour.[11]

Our maximum deposition rate of $13.7\mu m^3\mu m^{-2}min^{-1}$ ($15.13*10^{-6}cm^3min^{-1}$) exceeds those found by previous reports.[1, 3, 5] The lowest rate, $0.5\mu m^3\mu m^{-2}min^{-1}$, measured by Alevriadou, occurred at the lowest wall shear rates (1500 s^{-1}) and shortest experimentation times (2 min).[1] Badimon and Barstad measured maximal deposition rates of 8 and 12 $\mu m^3\mu m^{-2}min^{-1}$, respectively, by increasing experimentation times to 5 min with high wall shear rates.[3, 5] By utilizing both very high, pathologic shear (100,000 s^{-1}) and longer timescales (>5 min), we were able to measure a maximum deposition rate which is on the high end of those previously reported. RPA in our single pass, stenosis system exceeds Barstad et al.s maximum deposition at 10,000 s^{-1} by only 1.3 $\mu m^3\mu m^{-2}min^{-1}$, indicating that platelets may accumulate in this rapid fashion once a threshold wall shear rate has been reached.

Contrary to results found by Schoephoerster et al. in a canine model where maximal platelet counts were assigned to the recirculation region downstream of the throat, thrombus formation was optically visible in the throat of the stenosis with the maximum platelet deposition within 1 mm of either side of the throat apex.[6] This indicates that platelet aggregation occurs around the highest shear in the stenosis model. Wootton found similar results in an un-anticoagulated, ex vivo baboon model, with thrombus forming at the apex of the stenotic test section.[30] Schoephoersters utilization of a swab sampling technique may not provide a precise location of mural thrombus, and their Lexan surface may be different from our collagen coated, glass stenosis model. Platelet accumulation in a murine model has been observed by Nesbitt et al. at the apex that may be pushed into the recirculation zone as the apex is quite short.[23] We also observed some migration of thrombus off the apex toward the downstream recirculation zone in the early phases of thrombus formation. Further experimentation will be pursued utilizing varying whole blood hematocrit that can alter

collision frequency and viscosity to determine shear effects on platelet margination. This stenosis model creates a new and clinically relevant endpoint of visual occlusion for in vitro studies with physiologic Reynolds numbers. Many current in vitro shear systems utilize a parallel plate chamber pioneered by Hellums et al. in the 1990s, the cone-and-plate viscometer, or the PFA-100.[9, 14, 15, 17, 26, 31, 32] A benefit of the stenosis model over these systems is that the geometry of the test section allows for continuous observation of thrombus formation until occlusion. Parallel plate chambers utilize a different aspect ratio for the test section: wide and long, but very shallow in depth. The perpendicular depth of field prevents accurate measurements of plateletplatelet accumulation beyond the first few layers of platelet deposition. The abrupt geometry of the parallel plate chamber corners may also influence deposition rates through alteration of the test section hemodynamics. Cone-and-plate systems expose blood for very long periods of high shear. The PFA-100 provides only a binary output without control of shear or continuous monitoring of the thrombotic process. While flow occlusion has been noted in animal studies, the opaque arteries do not allow visualization of the growing thrombus without the use of contrast or magnetic resonance imaging.[2, 7] The in vitro model described here allows for greater control of the blood sample and test section geometry, with quantitative measurement of thrombus thickness, thrombus shape, and time-to-occlusion.

Recent independent evidence supports the hypothesis that platelet adhesion and aggregation at very high wall shear rates may be different from the shear-dependent adherence at moderate shear. Ruggeri et al. have described parallel plate experiments in which platelet adhesion (but not occlusion) in human blood remained high with PGE treatment or blockade of $\alpha_{IIb}\beta_3$ adhesion was abolished by blockade of GPIb with monoclonal antibodies for very high wall shear rates of 20,000 s^{-1}.[25] Nesbitt et al. also reported that the adhesion of the initial hundred platelets is not prevented by PGE or antibodies to $\alpha_{IIb}\beta_3$, but is completely blocked by antibodies to GPIb

in a mouse capillary model.[23] Our studies indicate that the platelet transit time of 2 ms is far too short for activation of circulating platelets, but that the lag time of several minutes to RPA may be facilitated by activation by high shear on the mural platelets. Further identification of the mechanisms of high shear occlusion could lead to treatments that prevent RPA without blocking homeostatic hemostasis.

Our hemodynamic whole, porcine blood system has several limitations. The use of a single-pass flow-through system requires a large volume of blood. A smaller in vitro setup should be pursued for future experimentation on human blood. 3-D volumetric extrapolations of 2-D measurements are also problematic due to distortion and circumferentially non-uniform deposition of thrombus. This may be mitigated in the future with the use of a glycerin bath for the Pyrex stenosis and correlation between micro-CT and image measurements. As a separate check, the thrombus volume in the throat was compared with cylindrical volumes for the maximum and minimum diameters at the ends and middle of the hourglass shapes thrombus. For a representative thrombus, the maximum cylinder had a volume of 0.62 mm^3, the measured thrombus volume was 0.35 mm^3, and the minimum cylinder was 0.20 mm^3. Thus, the measured thrombus volume appears reasonable even in the face of optical refraction of index changes. Current measurements of error in the throat of the stenosis, however, show the error to be approximately 10%. The edges of the stenosis show the greatest error, which will be found in the initial adhesion measurements, or the first $5.0 \pm 3.2 * 10^{-6} cm^3$. The choice of heparin for baseline anticoagulation may affect platelet function and the local concentration of thrombin.[12] Heparin may decrease platelet affinity and weaken the thrombus, making it more likely to embolize.[12, 16] Our heparinization rate of 3.5 USP $units/mL$ was determined to be the minimum heparinization that would allow for the blood to be transported back to the laboratory and experiments to be completed without coagulation occurring.

Markous ex vivo baboon model of thrombosis measured deposition rates of 0.9

billion platelets $cm^{-2}min^{-1}$ which, using a platelet volume of 5 fL, converts to 0.75 $\mu m^3 \mu m^{-2} min^{-1}$, indicating that these light anticoagulation methods are not preventing platelets from reaching their maximal deposition rates.[18, 20] These differences in maximum platelet deposition rates may be attributed to variances in species as both Alevriadou and Barstad utilize human blood while porcine blood is used in the Badimon model and Markou uses a baboon model. Occlusion rates were never stated in the Markou model and occlusion was defined as cessation of flow before 2 h.[18, 20] The walls of the stenosis are rigid, unlike compliant, healthy arteries. However, arteries in diseased patients are also more rigid, therefore making compliance less important for modeling diseased artery hemodynamics.

2.0.6 Conclusion

In conclusion, we quantify the volume and rate of intravascular thrombosis under pathologically high shear conditions of a focal stenosis over 100,000 s^{-1}. The thrombosis proceeds to occlusion in 17 ± 2.6 min ($n = 6$) from the rapid accumulation of 44 million platelets. Average RPA rates $7.8 \pm 3.5 \mu m^3 \mu m^{-2} min^{-1}$ ($20 \pm 4.5 * 10^{-6} cm^3 min^{-1}$) in these experiments are significantly greater than initial deposition rate $1.1 \pm 0.49 \mu m^3 \mu m^{-2} min^{-1}$ ($3.1 \pm 1.7 * 10^{-6} cm^2 min^{-1}$) in 70 to 83% stenoses ($p<0.05$, $n = 6$). During RPA, platelet-rich thrombus forms at the apex of the stenosis where the shear remains the greatest but not in the large recirculation region further downstream. The capture of circulating platelets occurs on a very short time scale of <2 ms, much shorter than the time scale for activation in the single-pass system. This in vitro model of rapid capture of millions of platelets from whole, porcine blood can be used to study the mechanisms of thrombotic occlusion under arterial hemodynamics as well as be applied in a clinical setting to improve patient treatment by studying dose responsiveness, individual blood differences for personalize treatments, and to assess synergistic/deleterious effects of new pharmaceuticals

with existing medications.

2.0.7 References

REFERENCES

[1] Alevriadou, B. R., Moake, J. L., Turner, N. A., Ruggeri, Z. M., Folie, B. J., Phillips, M. D., Schreiber, A. B., Hrinda, M. E., and McIntire, L. V., "Real-time analysis of shear-dependent thrombus formation and its blockade by inhibitors of von willebrand factor binding to platelets," *Blood*, vol. 81, no. 5, pp. 1263–1276, 1993.

[2] Badimon, L. and Badimon, J. J., "Mechanisms of arterial thrombosis in nonparallel streamlines: platelet thrombi grow on the apex of stenotic severely injured vessel wall. experimental study in the pig model," *The Journal Of Clinical Investigation*, vol. 84, no. 4, pp. 1134–1144, 1989.

[3] Badimon, L., Badimon, J. J., Galvez, A., Chesebro, J. H., and Fuster, V., "Influence of arterial damage and wall shear rate on platelet deposition. ex vivo study in a swine model," *Arteriosclerosis, Thrombosis, And Vascular Biology*, vol. 6, no. 3, pp. 312–320, 1986.

[4] Bark, David Ku, D., "Wall shear over high degree stenoses pertinent to atherothrombosis," *Journal of Biomechanics*, vol. 43, pp. 2970–2977, 2010.

[5] Barstad, R. M., Kierulf, P., and Sakariassen, K. S., "Collagen induced thrombus formation at the apex of eccentric stenoses–a time course study with non-anticoagulated human blood.," *Thrombosis And Haemostasis*, vol. 75, no. 4, pp. 685–92, 1975.

[6] Bluestein, D., Niu, L., Schoephoerster, R. T., and Dewanjee, M. K., "Fluid mechanics of arterial stenosis: relationship to the development of mural thrombus," *Annals Of Biomedical Engineering*, vol. 25, no. 2, pp. 344–356, 1997.

[7] Cadroy, Y., Horbett, T. A., and Hanson, S. R., "Discrimination between platelet-mediated and coagulation-mediated mechanisms in a model of complex thrombus formation in vivo," *Journal of Laboratory and Clinical Medicine*, vol. 113, no. 4, pp. 436–448, 1989.

[8] Clemetson, K. and Clemetson, J., "Platelet collagen receptors," *Thrombosis And Haemostasis*, vol. 86, no. 1, pp. 189–97, 2001.

[9] Colman, R. W., Marder, V. L., Clowes, A. W., George, J. N., and Goldhaber, S. Z., *Hemostasis and Thrombosis: Basic Principles and Clinical Practice*. Philadelphia: Lippincott Williams & Wilkins, fifth ed., 2006.

[10] Cranmer, S. L., Ulsemer, P., Cooke, B. M., Salem, H. H., de la Salle, C., Lanza, F., and Jackson, S. P., "Glycoprotein (gp) Ib-IX-transfected cells roll on a von willebrand factor matrix under flow. Importance of the gpIb/actin-binding protein (ABP-280) interaction in maintaining adhesion under high shear," *Journal of Bioligical Chemistry*, vol. 274, no. 10, pp. 6097–6106, 1999.

[11] Davies, M. J. and Thomas, A., "Thrombosis and acute coronary-artery lesions in sudden cardiac ischemic death," *The New England Journal Of Medicine*, vol. 310, no. 18, pp. 1137–1140, 1984.

[12] Folie, B. J. and McIntire, L. V., "Mathematical analysis of mural thrombogenesis. Concentration profiles of platelet-activating agents and effects of viscous shear flow," *Biophysical Journal*, vol. 56, no. 6, pp. 1121–1141, 1989.

[13] Fullard, J. F., "The role of the platelet glycoprotein IIb/IIIa in thrombosis and haemostasis," *Current Pharmaceutical Design*, vol. 10, no. 14, pp. 1567–1576, 2004.

[14] Harrison, P., Robinson, M., Liesner, R., Khair, K., Cohen, H., Mackie, I., and Machin, S., "The PFA-100: a potential rapid screening tool for the assessment of platelet dysfunction," *Clinical And Laboratory Haematology*, vol. 24, no. 4, pp. 225–232, 2002.

[15] Hellums, J., "1993 whitaker lecture: Biorheology in thrombosis research," *Annals of Biomedical Engineering*, vol. 22, no. 5, pp. 445–455, 1994.

[16] Hubbell, J. A. and McIntire, L. V., "Platelet active concentration profiles near growing thrombi. a mathematical consideration," *Biophysical Journal*, vol. 50, no. 5, pp. 937–945, 1986.

[17] Jurk, K., Clemetson, K. J., De Groot, P. G., Brodde, M. F., Steiner, M., Savion, N., Varon, D., Sixma, J. J., Van Aken, H., and Kehrel, B. E., "Thrombospondin-1 mediates platelet adhesion at high shear via glycoprotein Ib (gpIb): an alternative/backup mechanism to von willebrand factor," *FASEB Journal*, vol. 17, no. 11, pp. 1490–1492, 2003.

[18] Kamath, S., Blann, A. D., and Lip, G. Y. H., "Platelet activation: assessment and quantification," *European Heart Journal*, vol. 22, no. 17, pp. 1561–1571, 2001.

[19] Kroll, M. H., Hellums, J. D., McIntire, L. V., Schafer, A. I., and Moake, J. L., "Platelets and shear stress," *Blood*, vol. 88, no. 5, pp. 1525–1541, 1996.

[20] Ku, D., "Blood flow in arteries," *Annual Review of Fluid Mechanics*, vol. 44, pp. 399–434, 1997.

[21] Ku, D. N. and Flannery, C. J., "Development of a flow-through system to create occluding thrombus," *Biorheology*, vol. 44, no. 4, pp. 273–284, 2007.

[22] Marco, L. D., Girolami, A., Zimmerman, T. S., and Ruggeri, Z. M., "von willebrand factor interaction with the glycoprotein IIb/IIIa complex. its role in platelet function as demonstrated in patients with congenital afibrinogenemia.," *Journal of Clinical Investigation*, vol. 77, no. 4, pp. 1272–1277, 1986.

[23] Nesbitt, W. S., Westein, E., Tovar-Lopez, F. J., Tolouei, E., Mitchell, A., Fu, J., Carberry, J., Fouras, A., and Jackson, S. P., "A shear gradient-dependent platelet aggregation mechanism drives thrombus formation," *Nature Medicine*, vol. 15, no. 6, pp. 665–673, 2009.

[24] Reininger, A. J., Heijnen, H. F. G., Schumann, H., Specht, H. M., Schramm, W., and Ruggeri, Z. M., "Mechanism of platelet adhesion to von willebrand factor and microparticle formation under high shear stress," *Blood*, vol. 107, no. 9, pp. 3537–3545, 2006.

[25] Ruggeri, Z. M., "Platelet interactions with vessel wall components during thrombogenesis," *Blood Cells, Molecules & Diseases*, vol. 36, no. 2, pp. 145–147, 2006.

[26] Sakariassen, K. S., Aarts, P. A., de Groot, P. G., Houdijk, W. P., and Sixma, J. J., "A perfusion chamber developed to investigate platelet interaction in flowing blood with human vessel wall cells, their extracellular matrix, and purified components," *The Journal Of Laboratory And Clinical Medicine*, vol. 102, no. 4, pp. 522–535, 1983.

[27] Schoephoerster, R. T., Oynes, F., Nunez, G., Kapadvanjwala, M., and Dewanjee, M. K., "Effects of local geometry and fluid dynamics on regional platelet deposition on artificial surfaces," *Arteriosclerosis, Thrombosis, And Vascular Biology*, vol. 13, no. 12, pp. 1806–1813, 1993.

[28] Sheehan, D. and Hrapchak, B., *Theory and Practice of Histotechnology*. St. Louis, MO: C.V. Mosby Company, 2nd ed., 1980.

[29] Wootton, D. M. and Ku, D. N., "Fluid mechanics of vascular systems, diseases, and thrombosis," *Annual Review Of Biomedical Engineering*, vol. 1, pp. 299–329, 1999.

[30] Wootton, D., Markou, C., Hanson, S., and Ku, D., "A mechanistic model of acute platelet accumulation in thrombogenic stenoses," *Annals of Biomedical Engineering*, vol. 29, no. 4, pp. 321–329, 2001.

[31] Zwaginga, J. J., Nash, G., King, M. R., Heemskerk, J. W. M., Frojmovic, M., Hoylaerts, M. F., Sakariassen, K. S., and Biorheology Subcommittee Of The Ssc Of The ISTH, "Flow-based assays for global assessment of hemostasis. part 1: biorheologic considerations," *Journal of Thrombosis and Haemostasis*, vol. 4, no. 11, pp. 2486–2487, 2006.

[32] Zwaginga, J. J., Sakariassen, K. S., Nash, G., King, M. R., Heemskerk, J. W., Frojmovic, M., Hoylaerts, M. F., and Biorheology Subcommittee Of The Ssc Of The ISTH, "Flow-based assays for global assessment of hemostasis. part 2: current methods and considerations for the future," *Journal of Thrombosis and Haemostasis*, vol. 4, no. 12, pp. 2716–2717, 2006.

CHAPTER III

A LOW-VOLUME, SINGLE PASS IN-VITRO SYSTEM TO STUDY HIGH SHEAR THROMBOSIS WITH HUMAN BLOOD

3.0.8 Introduction

Thrombus formation contributes to myocardial infarction (MI) and stroke, the leading causes of death in developed countries. Following plaque rupture, platelets initially adhere to the damaged arterial subendothelium in the region of very high shear stress and subsequently, rapidly accumulate to previously adhered platelets, a process known as thrombosis. We have recently described a phenomenon of Rapid Platelet Accumulation (RPA) whereby millions of platelets accumulate per minute that can lead to occlusion and mortality within an hour after symptomatic onset of MI.[3, 11] This is in strong contrast to common platelet adhesion studies in parallel plate systems whereby surface area coverage of hundreds of platelets over 5 minutes is the typical endpoint.[15]

As mortality occurs quickly, due to RPA, patients experiencing MI are often treated based on general evidence.[4] Unfortunately, not every patient is responsive to common treatments, with some patients being aspirin resistant and others being Plavix® resistant, the leading prescribed pharmaceutical for patients with atherosclerosis.[6, 19] This being the case, it is necessary to develop a device which utilizes low volumes of human blood (30mLs) in which RPA can be measured. This device would be single pass to ensure that platelets are not activated prior to experiencing the region of high shear stress, and have a pathologically similar, smooth transition to the region of highest shear. The goal of our study is to create an apparatus

that uses low volumes of whole blood in which RPA occurs as well as directly compare any species differences existing between porcine and human blood with regard to thrombus formation morphology, composition and RPA. If successful, this device may be used to analyze human blood samples and contribute to patient-specific therapy creation.

As such, it is important to review previous hemodynamic systems which have been used to study platelet accumulation.

3.0.8.1 Aggregometry

Clinically, it is important to utilize low volumes of blood to test platelet accumulation as 100mLs is approximately the largest amount of blood which can be collected from a patient on a routine basis. The VerifyNow aggregometer utilizes very low (2mLs) volumes of blood to test patient specific response to different platelet receptors.[9] However, VerifyNow® does not utilize shear conditions such as those found pathologically. Shear rates in diseased arteries are very high ($1{,}500s^{-1}$ - $100{,}000^{+}s^{-1}$) compared to those seen physiologically ($<1{,}500s^{-1}$).[11, 12] As large proteins, such as von Willebrand Factor (vWF), which contribute to thrombosis behave differently under increased shear rates, high shear is an important factor to studying RPA.[7]

3.0.8.2 Cone and Plate Viscometer

Cone and plate viscometers utilize small volumes of blood and very high shear stress. However, the cone and plate viscometer subjects the blood to continuously high shear rates that can activate all of the platelets.[5] This does not allow for a physiologically similar response, as platelets in the body are not exposed to a sustained, pathologically high shear. The advantage of a single pass system is that platelets are only exposed to the critical shear region a single time.

3.0.8.3 PFA-100®

A low volume, high shear (>5,000s^{-1}), single pass system currently used to test platelet dysfunction clinically is the PFA-100®.[1] In the system, blood is pulled through a capillary and over an undefined internal membrane. It is unclear whether the closure time listed is definitively time to thrombotic occlusion or potentially embolic occlusion of the membrane. The short closure time of 5 minutes may also not be long enough for RPA to occur.

3.0.8.4 Parallel Plate

Parallel plate models utilize low volumes of blood, high shear, single pass and optical measurement. Due to an *en face* view of the chamber during experimentation, measurement of subsequent platelet-to-platelet deposition characteristic of millions of platelets is quite difficult, with some experiments terminating after 5 minutes measuring only hundreds of platelets.[15] Even with fluorescence, measurement of platelet-to-platelet deposition is only possible until saturation, after which additional fluoresence cannot be measured. Further, the parallel plate model utilizes a wide aspect ratio that is not anatomic, creating unusual secondary flows in the corners of the chamber.

3.0.8.5 Stenosis Model

The stenosis model created by Flannery and Ku utilizes single pass flow, measures optically from RPA to occlusion, and creates a region of very high, pathologic shear stress in a smooth, rounded stenosis which mimics the shape of an atherosclerotic plaque.[8] The stenosis is approximately 2mm in length, creating an anatomically similar shear region to that of a coronary or carotid stenosis. While advantageous due to a defined, very high, pathologic shear region and anatomic similarity to a carotid stenosis, the stenosis model requires 240mLs of blood for each experiment.[8, 11] This

assay has only been tested with porcine blood due to porcine's pathological similarities and suitability as a direct comparison to human blood for ex-vivo coagulation studies.[8, 14, 16, 17, 20] However, faster clot formation times for porcine blood than human blood have been shown.[10, 17] This may indicate the requirement of more than 240mLs for experimentation with humans when utilizing this system which is unacceptable when considering a patient may need multiple tests conducted.

To this end, a low volume (30mLs), high shear stress (>3,500 $s^{-}1$), single pass, constant volume, glass capillary model of occlusive thrombosis which utilizes whole blood for experimentation has been created. It is the aim of this syringe pump apparatus to achieve RPA using low volumes of whole human blood. Thrombus formation morphology, initial formation rates, RPA rates and thrombus composition will be measured and compared to porcine blood.

3.0.9 Experimental Design and Methods

3.0.9.1 Experimental Setup: Gravitationally Fed and Syringe Pump Apparatuses

The gravitationally fed, single pass system was run as previously described, with 240mL of porcine blood flowing through PVC plastic tubing (Baxter Healthcare Corporation, Deerfield, IL) with an inner diameter of 3 mm to the test section from a raised platform, past a pressure transducer and through a collagen coated stenosis (Figure 9 A).[8, 11] Mass flow rates were measured using a scale downstream.

A syringe pump fed, in-vitro flow system (Figure 9 B) was designed to create high, pathologic shear rates ($3{,}500s^{-1}$), exceeding shear induced platelet activation, in a test section that could be visualized under a microscope.[2] Whole, lightly heparinized (3.5 IU/mL) blood was perfused past a pressure transducer (Harvard Apparatus, South Natwick, MA) and through a transparent, pyrex test section using a syringe pump to maintain constant flow. For porcine blood experiments, 30mLs of whole blood was used. Human blood experiments also did not exceed 30mLs.

During the flow experiments, excess blood was placed on an Orbit LS orbital mixer

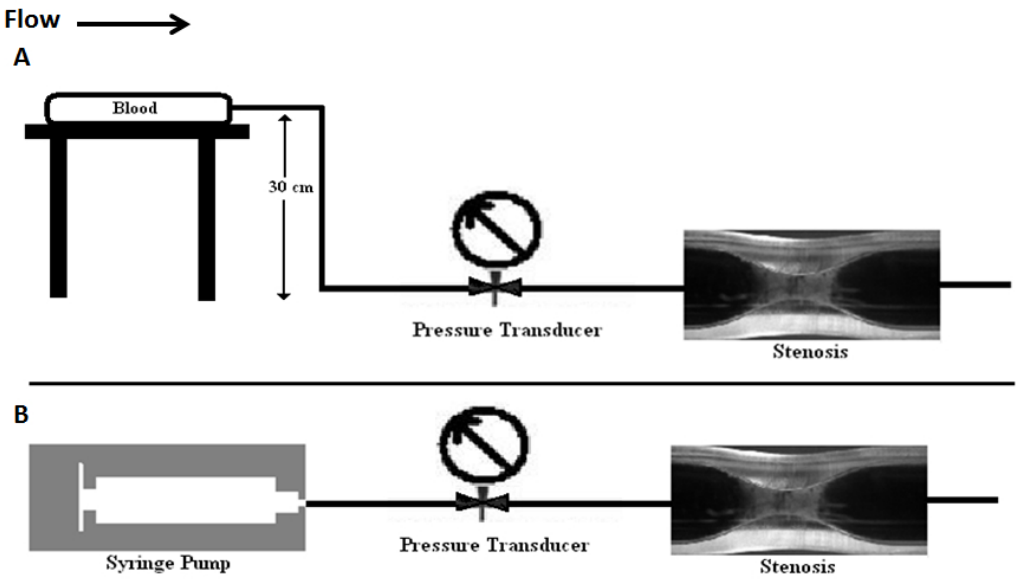

Figure 9: (A) Gravitationally fed experiments required an initial 240mLs of blood to be placed on a platform 30cm above the stenosis. During experimentation, blood flowed from the raised platform, past a pressure transducer, through the collagen coated test section and onto a scale where mass flow measurements were taken in real time. (B) The syringe pump experiment required a maximum of 30mLs of blood for experimentation to occlusion. Blood flowed, driven by a syringe pump, from a syringe, past a pressure transducer and through the collagen coated test section. Both systems are single pass.

(Labnet, Woodbridge, NJ) to prevent blood separation. All blood was used within 8 hours of harvest.

The test section was constructed from glass tubes with an original inner diameter of 1.5mm. A variety of hour-glass shaped stenoses were made by a professional glass blower with a severity ranging from 75 to 92% ($n = 34$) by diameter for all experiments with initial flow rates between 0.04 mL/min for highly stenosed test sections and 1.1mL/min for the larger diameter test sections.

Initial flow rates for the syringe pump experiments are programmed using Poiseuille assumptions:

$$\dot{\gamma} = \frac{32Q}{\pi D^3} \tag{2}$$

where d is the smallest inner diameter in the test section and $\dot{\gamma}$ is 3,500 s^{-1}. Shear

rates were highest at the throat of the stenosis and not upstream.

3.0.9.2 Collagen Coating

Stenoses were coated with fibrillar Collagen Type I (1 mg/mL, Sigma-Aldrich, St. Louis, MO, prepared according to manufacturer's instructions). The collagen was left in the tube for 24 h in a warm, moist environment to form a thin layer of <100 m. Following incubation, tubes were rinsed with 1x PBS (Fisher Scientific, Fair Lawn, NJ).

3.0.9.3 Whole Porcine Blood/ Whole Human Blood

Whole porcine blood was collected directly from the aorta at an abattoir (Holifield Farms, Covington, GA). Whole human blood from donors was obtained at the Georgia Institute of Technology Phlebotomy Lab at Stamps Health Services in accordance with the IRB (Protocol H06190). Blood was drawn from a 21G butterfly needle directly into a syringe.

3.0.9.4 Image Processing and Histology

The test section was photographed through a 2x microscope objective using a high resolution digital CCD camera (Pixelfly, Keleim, Germany), with a 0.5x magnification, connected directly to the Zeiss Stemi 2000-C (Zeiss, Jena, Germany) stereo microscope as previously described.[11] Images were sequentially stored at a rate of approximately 1 s/frame for off-line analysis. The software programs for postprocessing image analysis were CamWare (Cooke Corporation, Romulus, MI) and Photoshop (Adobe, San Jose, CA).

Embolus was defined as a rapid increase in pressure and a sudden stoppage of flow within seconds. Embolus was verified visually and experiments which terminated with embolus were not included in this study.

As lower volumes of blood were used, RPA and not occlusion was used as an

endpoint, although it is reasonable to assume that occlusion would occur with additional blood. Rapid Platelet Accumulation (RPA) was defined as being any platelet deposition rate greater than 1.6 $\mu m^3\ \mu m^{-2}\ min^{-1}$ (the upper bound of the average initial deposition, [11]) and occlusion is defined as a pressure head of P = 30mmHg for syringe pump experiments. Deposition rates were calculated by taking a regression of consecutive time points during thrombus formation.

3.0.9.5 Statistics

All experiments were analyzed using an unpaired student's t-test where statistical significance is defined as $p<0.05$.

3.0.10 Results

Platelet deposition morphology, thrombus composition, initial platelet deposition rates and RPA are analyzed in the human syringe pump model using low volumes of blood (<30mLs). These are compared to previous results obtained using porcine blood in the gravitationally fed model and the syringe pump model. Species differences between human blood and porcine blood are also compared.

3.0.10.1 Human Syringe Pump Model

Thrombus formation to complete occlusion can be seen in the human blood syringe pump model. Initial visible adhesion (Figure 10 A), or the first noticeable platelet deposition, is minimal and occasionally located downstream. Some spots of thrombus deposition form upstream or within the throat of the stenosis.

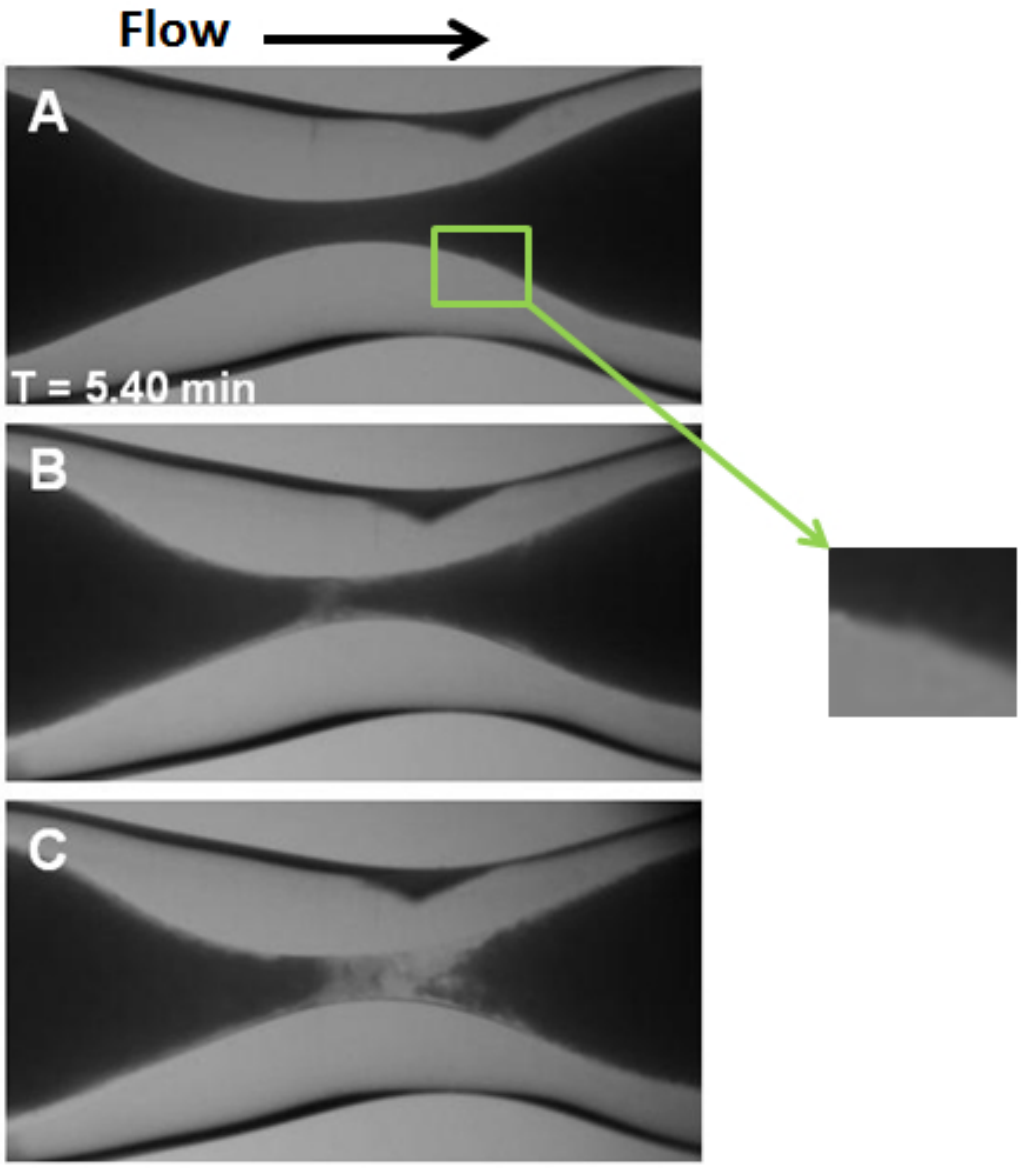

Figure 10: Thrombus formation using human blood in an 86% stenosis. Initial visible formation in this stenosis is seen as very slight formation which occurred in 5.4 minutes (A) and is highlighted by the green box. Following initial formation, subsequent platelet deposition occurs (B) until complete occlusion (C).

Following visible initial adhesion, thrombus deposition became more diffuse, with

platelets forming finger-like projections into the flow (Figure 10 B). Platelets deposited rapidly onto this surface, showing visible morphological changes in real time until occlusion (Figure 10 C).

Histological staining of human thrombus in the syringe pump apparatus reveals that it is composed predominantly of platelets (Figure 11). Red blood cells are trapped downstream of the occlusive plug and some small pockets are trapped within but do not contribute to the bulk of the platelet-rich thrombus plug (Figure 11).

Figure 11: Human thrombus stained using Carstairs staining highlights platelets in navy blue. It can be seen from this stain that an occlusive thrombus formed from human blood is predominantly platelets.

Platelet deposition to occlusion in human blood in the syringe pump model occurs in two phases: initial visible adhesion, which is the rate at which the first deposition

of platelets to the thrombogenic surface occurs. This is followed by RPA, a fast regime of platelet-to-platelet deposition, which precedes occlusion (Figure 12). Prior to initial visible adhesion, there is a lag time of 7.4 ± 3.8 min and requires 3.1 ± 2.0mLs to occur (n=21). This constitutes the deposition of the first $5.7 \pm 7.0 * 10^{-6}$ cm^3 of thrombus volume (n=21).

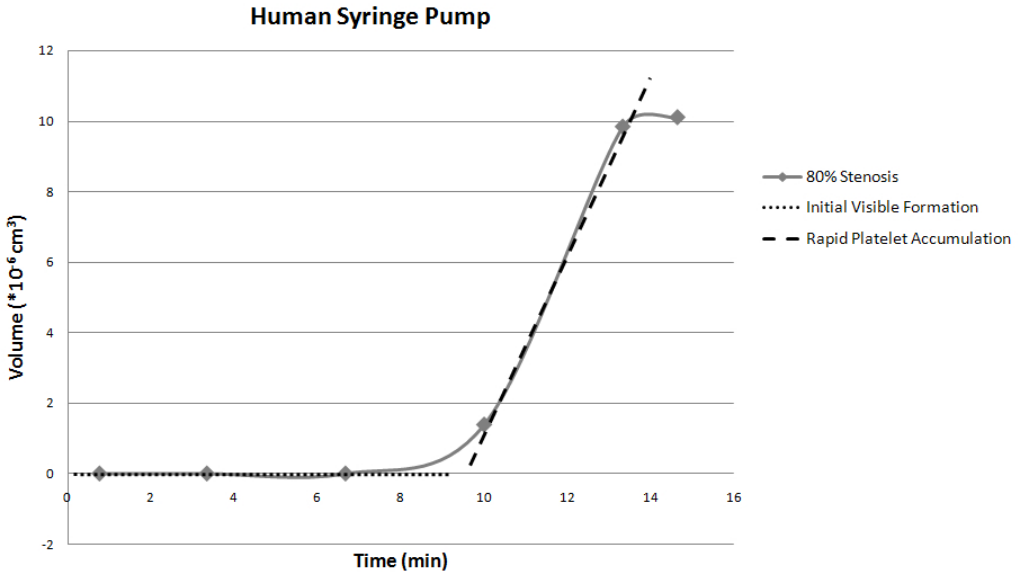

Figure 12: Human blood deposits in the stenosis in two phases -initial visible formation followed by a faster Rapid Platelet Accumulation.

Initial deposition occurs at rates of 0.8 ± 1.0 μm^3 μm^{-2} min^{-1} (n=21, Figure 13). This is significantly slower than RPA which occurs at rates of 4.5 ± 2.4 μm^3 μm^{-2} min^{-1} (n=21, $p<0.05$).

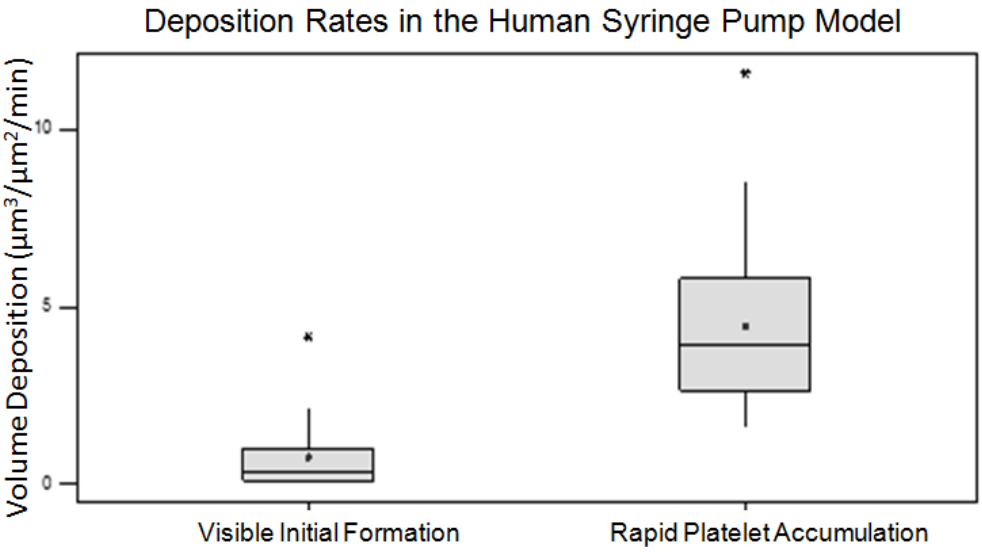

Figure 13: Thrombus deposits significantly slower during visible initial deposition ($p<0.05$) than RPA. The mean is denoted with a black circular dot and outliers are marked with an *.

The disparity between the two rates can also be seen in the full range of values (Figure 14), with the mean of initial visible adhesion below the lowest value of RPA and only 5/21 data points above the mean.

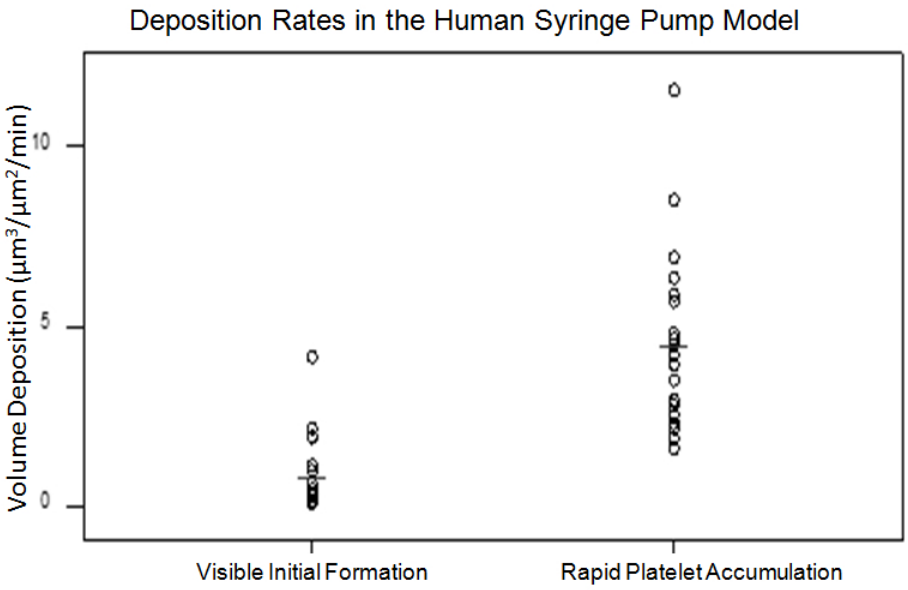

Figure 14: Thrombus deposits significantly slower during visible initial deposition ($p<0.05$) than RPA.

3.0.10.2 Porcine Syringe Pump and Porcine Gravitationally Fed Experiments

Thrombus deposition to occlusion occurred similarly in porcine experiments. Following initial visible adhesion, thrombus deposited throughout the throat of the stensosis (Figure 15 AI, BI). Subsequent platelet-to-platelet deposition filled the throat of the stenosis until occlusion of the lumen (Figure 15 AII, BII).

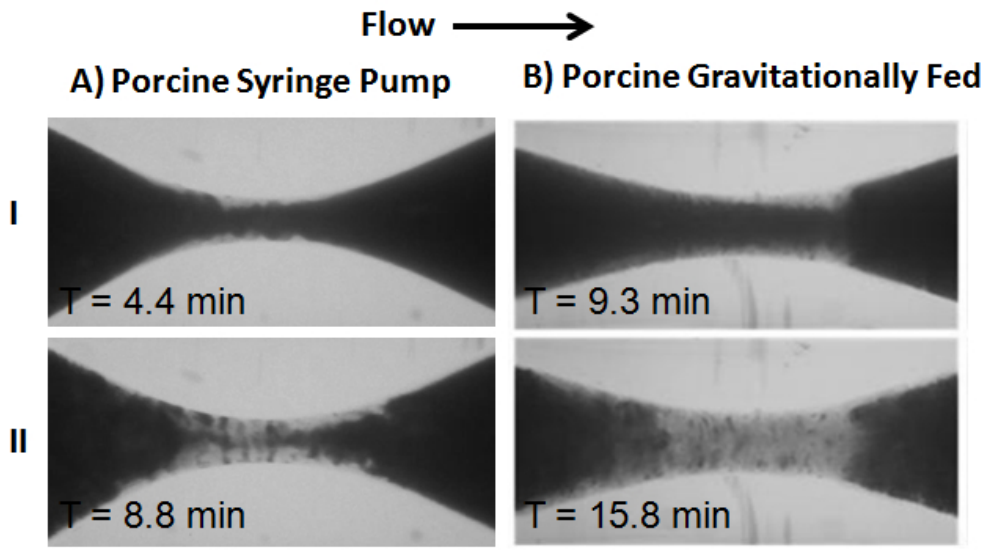

Figure 15: Porcine blood forms similarly in both the syringe pump (A) and the gravitationally fed (B) models. Following visible initial adhesion, more diffuse deposition (I) and, ultimately, occlusion occur (II).

For both the gravitationally fed and syringe pump models, thrombus formation occurred in the throat of the stenosis, where shear was highest.

Histological staining of occlusive thrombus of porcine blood in both the syringe pump model (Figure 16 B) and the gravitationally fed model (Figure 16 A) showed that thrombus was composed mainly of platelets. Red blood cells can also be seen in the sample (stained as red), likely trapped after flow cessation.

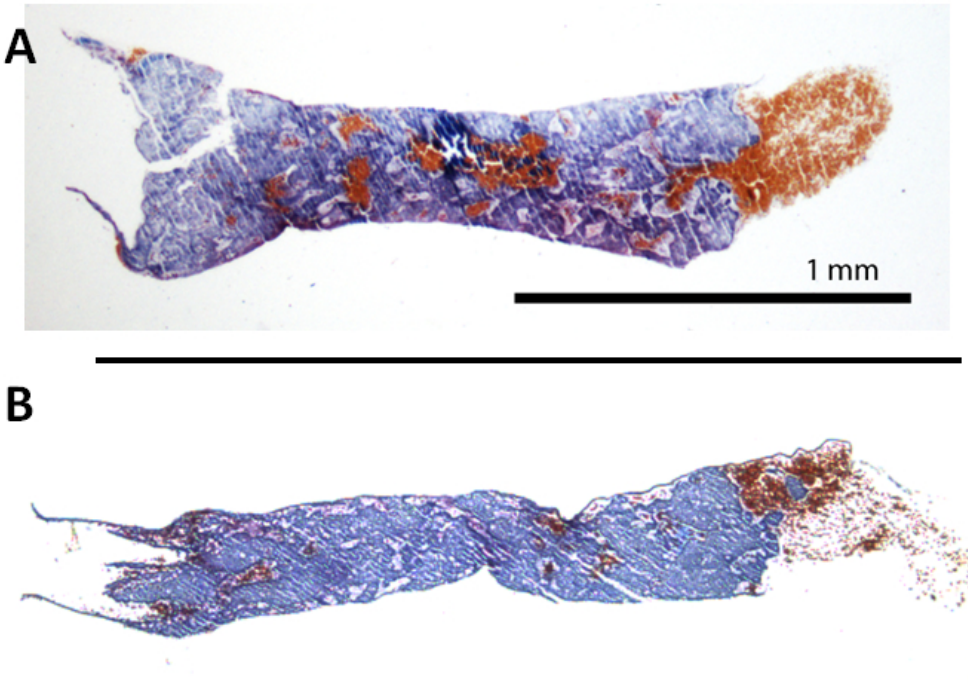

Figure 16: Thrombus formation in both the gravitationally fed (A) and syringe pump models (B) are dominated by platelets (navy) in porcine blood. Platelets are stained using Carstairs Staining protocol and flow during formation was from left to right. The scale for both samples is indicated above.

3.0.10.3 Comparison of Human and Porcine Models

The amount of blood to occlusion was 43 ± 24mLs (n=6) for the porcine gravitationally fed experiments. A significantly lower amount of blood, 6.1 ± 2.7mLs was required for occlusion for the porcine syringe pump model (p=0.05, n=7).

In the porcine gravitationally fed model, visible initial formation, the first measurable thrombus volume, is $5.0 \pm 2.0 * 10^{-6} cm^3$. In the porcine syringe pump model, visible initial formation is $3.8 \pm 3.6 * 10^{-6} cm^3$. In the human syringe pump model, visible initial formation is $5.7 \pm 7.0 * 10^{-6} cm^3$.

Visible initial formation occurs within 1.3 ± 0.8mLs in the pocine syringe pump (n=7) and within 3.1 ± 2.0mLs for the human syringe pump model (n=21, Table 2).

Table 2: Initial visible formation occurred significantly faster in the porcine gravitationally fed model than either the porcine syringe pump model ($^{\gamma}$,p<0.05) or the human syringe pump model ($^{\beta}$, p<0.05). The porcine syringe pump model formed initial visible formation significantly faster than the human syringe pump model ($^{\alpha}$, p<0.05).

	Amount of Blood to Visible Initial Formation (mLs)	Amount of Time to Visible Initial Formation (min)	N
Human Syringe Pump	3.1 ± 2.0	$7.4 \pm 3.8^{\alpha,\beta}$	21
Porcine Syringe Pump	1.3 ± 0.8	$2.7 \pm 0.5^{\alpha,\gamma}$	7
Porcine Gravitationally Fed	3.9 ± 3.2	$1.0 \pm 0.9^{\beta,\gamma}$	6

A similar volume of blood is required for visible initial formation in the porcine gravitationally fed model (3.9 ± 3.2mLs, n=6). Due to the different initial flow rates of the models, with gravitationally fed being faster than constant volume, visible initial formation occurs significantly faster (1.0 ± 0.9 min) in the porcine gravitationally fed model (p<0.05) than both the porcine syringe pump model (2.7 ± 0.5 min) and human syringe pump model (7.4 ± 3.8 min, Table 2). The porcine syringe pump model also forms visible initial formation significantly faster than the human syringe pump model (n=7, n=21, p<0.05).

In the porcine gravitationally fed model (10 ± 3.5 $\mu m^3\ \mu m^{-2}\ min^{-1}$, n=5) and the porcine syringe pump model (9.6 ± 6.1 $\mu m^3\ \mu m^{-2}\ min^{-1}$, n=7), Rapid Platelet Accumulation (RPA) rates are significantly higher than the human syringe pump model (4.5 ± 2.4 $\mu m^3\ \mu m^{-2}\ min^{-1}$, n=21, p<0.05, Figure 17). The maximum RPA rate for the porcine gravitationally fed model is 15 $\mu m^3\ \mu m^{-2}\ min^{-1}$ and the porcine syringe pump model is 17 $\mu m^3\ \mu m^{-2}\ min^{-1}$, while the human syringe pump model had a maximum RPA rate of 12 $\mu m^3\ \mu m^{-2}\ min^{-1}$.

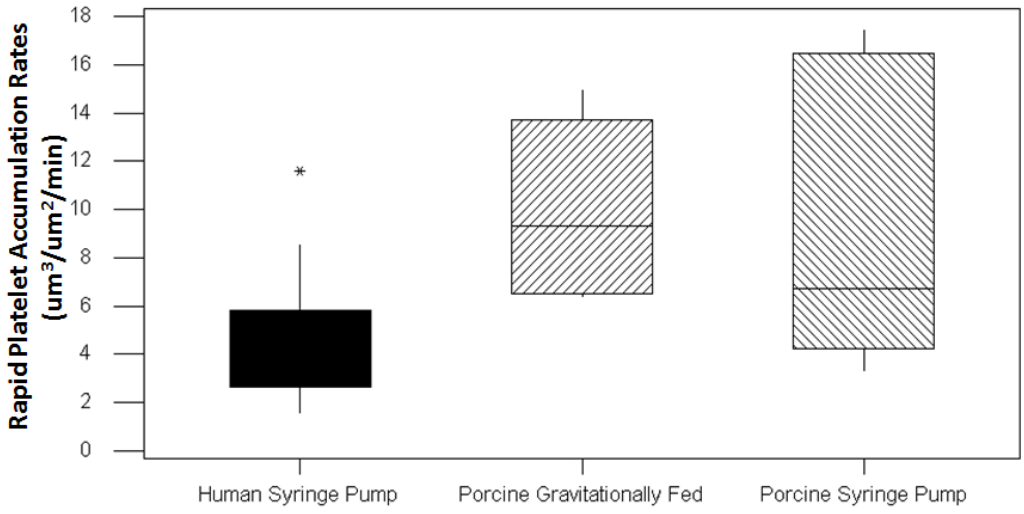

Figure 17: Rapid Platelet Accumulation Rates in the human syringe pump model are significantly lower ($p<0.05$, n=21) than either the porcine gravitationally fed model (n=6) or the porcine syringe pump model (n=7).

While the RPA rates for human blood is slower than that for porcine blood, there is a minimal difference between visible initial formation rates for the porcine gravitationally fed model ($1.1 \pm 0.5\ \mu m^3\ \mu m^{-2}\ min^{-1}$) and the human syringe pump model ($0.8 \pm 1.0\ \mu m^3\ \mu m^{-2}\ min^{-1}$).[11]

3.0.11 Discussion

Our studies demonstrate that thrombus formation to RPA occurs in a low volume (<30 mLs), single pass, syringe pump fed system using whole, human blood. RPA occurred in the syringe pump with human blood following the first 7.4 ± 3.8 min (n=21) and averaged $4.5 \pm 2.4\ \mu m^3\ \mu m^{-2}\ min^{-1}$ (n=21) with a maximum of 12 $\mu m^3\ \mu m^{-2}\ min^{-1}$. Thrombus formation morphology was similar as was composition of occlusive thrombus between species, with thrombus consisting of predominantly platelets for both porcine and human models. Porcine blood had a shorter time to initial formation, with visible thrombus occurring within 2.7 ± 0.5 min (n=7, $p<0.05$)

of experimentation for the syringe pump model. Porcine RPA was also faster in the porcine syringe pump model (9.6 ± 6.1 μm^3 μm^{-2} min^{-1}, n=7, p<0.05) than the human syringe pump model 4.5 ± 2.4 μm^3 μm^{-2} min^{-1} (n=21). However, the rate of visible initial formation in the human syringe pump model (0.8 ± 1.0 μm^3 μm^{-2} min^{-1}) is similar to the porcine gravitationally fed model (1.1 ± 0.5 μm^3 μm^{-2} min^{-1}).[11]

Differences in harvesting methods between porcine and human blood may account for differences in RPA rates in this syringe pump model. Pigs may release more stress hormones such as epinephrine during slaughter, creating a more thrombogenic blood than humans, who experience minimal stress during a routine blood draw. Alternatively, differences in desposition rates may simply be due to species differences.

The human blood, syringe pump model presented here utilizes very high shear rates seen pathologically (>3,000s^{-1}), which are not used in clinical aggregometry such as the VerifyNow®. Longer experimental times (>10min) are also utilized. Models such as the PFA-100® and parallel-plate chambers terminate with experiments 5 minutes or less. Since human blood has a lag time of 7-10 min until RPA, it is unlikely that the PFA even tests for the pathologic platelet accumulation responsible for intravascular thrombotic occlusion.[15] The syringe pump model also uses a stenotic test section which exposes platelets to a region of high shear stress. The cone and plate viscometer subjects platelets to a sustained, high shear rate, which is non-physiologic. A model encompassing all of these requirements for high, pathologic shear, lengthened experimental times and a geometry which transiently exposes platelets to shear is the Flannery-Ku stenosis model.[8] However, due to its large requirement for blood (240mLs), makes it prohibitive as an assay for patient-specific testing.

Our human blood, single pass, syringe pump experiment has limitations. The first is the lack of physiologic pulsatility. Previous reports are inconclusive, suggesting

that there is either no change in thrombus growth or an increase in thrombus growth caused by pulsatility.[18, 21] Furthermore, most studies of pulsatility focus on initial deposition and do not explore pulsatile effects on platelet-platelet deposition.[13] This should be pursued in future experimentation using whole, human blood.

Another limitation is that the walls of the stenosis are rigid, unlike compliant, healthy arteries. However, atherosclerotic arteries are also more rigid, making compliance a minimal consideration for modeling the diseased hemodynamics.

3.0.12 Conclusions

In conclusion, we have created a steady, single pass model of RPA using low volumes (<30mLs) of whole, human blood which may be used for patient-specific testing. The human syringe pump model was developed following the reduction of the 240mL porcine gravitationally fed model of RPA to a low volume, syringe pump fed model of RPA also using porcine blood. As both models formed RPA using porcine blood at similar rates, 10 ± 3.5 $\mu m^3\ \mu m^{-2}\ min^{-1}$ (n=6) for the porcine gravitationally fed and 9.6 ± 6.1 $\mu m^3\ \mu m^{-2}\ min^{-1}$ (n=7) for the porcine syringe pump model, and with similar morphologies, we were able to transition the model to utilize human blood.

In the human syringe pump model, visible initial formation occurs in the first 3.1 ± 2.0 mLs when perfused through stenoses ranging from 75% to 92% at an initial shear rate of 3,500s^{-1}. For this initial stage, platelets deposit at a rate of 0.8 ± 1.0 $\mu m^3\ \mu m^{-2}\ min^{-1}$, similar to rates in the porcine gravitationally fed model (1.1 ± 0.5 $\mu m^3\ \mu m^{-2}\ min^{-1}$, n=21). RPA rates in human blood are less than those of porcine blood (9.6 ± 6.1 $\mu m^3\ \mu m^{-2}\ min^{-1}$, n=7), with human RPA rates measuring 4.5 ± 2.4 $\mu m^3\ \mu m^{-2}\ min^{-1}$ (n=21).

This whole, human blood model of RPA can be used for future clinical use to test patient-specific responses to therapies which will affect RPA under pathologic, hemodynamic conditions.

3.0.13 References

REFERENCES

[1] Arrieta Blanco, J. J., Bartolome Villar, B., Juzgado, A., and Mourelle Martinez, R., "Assessment of pfa-100 system for the measurement of bleeding time in oral surgery," *Medicina Oral Patologia Oral Cirugia Bucal*, vol. 11, pp. 514–519, 2006.

[2] Belval, T. and Hellums, J., "Analysis of shear-induced platelet aggregation with population balance mathematics," *Biophysical Journal*, vol. 50, no. 3, pp. 479 – 487, 1986.

[3] Davies, M. J. and Thomas, A., "Thrombosis and acute coronary-artery lesions in sudden cardiac ischemic death," *The New England Journal Of Medicine*, vol. 310, no. 18, pp. 1137–1140, 1984.

[4] Force, U. P. S. T., "Aspirin for the prevention of cardiovascular disease: U.S. preventative services task force recommendation statement," *Annals Of Internal Medicine*, vol. 150, no. 6, pp. 396–405, 2009.

[5] Giorgio, T. D. and Hellums, J. D., "A cone and plate viscometer for the continuous measurement of blood platelet activation," *Biorheology*, vol. 25, no. 4, pp. 605–624, 1988.

[6] Gum, P. A., Kottke-Marchant, K., Poggio, E. D., Gurm, H., Welsh, P. A., Brooks, L., Sapp, S. K., and Topol, E. J., "Profile and prevalence of aspirin resistance in patients with cardiovascular disease," *The American Journal Of Cardiology*, vol. 88, no. 3, pp. 230–235, 2001.

[7] Jackson, S. P., "The growing complexity of platelet aggregation," *Blood*, vol. 109, no. 12, pp. 5087–5095, 2007.

[8] Ku, D. N. and Flannery, C. J., "Development of a flow-through system to create occluding thrombus," *Biorheology*, vol. 44, no. 4, pp. 273–284, 2007.

[9] Lordkipanidze, M., Pharand, C., Nguyen, T. A., Schampaert, E., and Diodati, J. G., "Assessment of verifynow P2Y_{12} assay accuracy in evaluating clopidogrel-induced platelet inhibition," *Therapeutic Drug Monitoring*, vol. 30, no. 3, pp. 372–378 10.1097/FTD.0b013e3181757c59, 2008.

[10] Munster, A.-M. B., Olsen, A. K., and Bladbjerg, E.-M., "Usefulness of human coagulation and fibrinolysis assays in domestic pigs," *Comparative Medicine*, vol. 52, no. 1, pp. 39–43, 2002.

[11] Para, A., Bark, D., Lin, A., and Ku, D., "Rapid platelet accumulation leading to thrombotic occlusion," *Annals Of Biomedical Engineering*, vol. 39, pp. 1961–1971, 2011.

[12] Ruggeri, Z. M., Dent, J. A., and Saldivar, E., "Contribution of distinct adhesive interactions to platelet aggregation in flowing blood," *Blood*, vol. 94, no. 1, pp. 172–178, 1999.

[13] Sakariassen, K., Bolhuis, P., and Sixma, J., "Platelet adherence to subendothelium of human arteries in pulsatile and steady flow," *Thrombosis Research*, vol. 19, no. 45, pp. 547 – 559, 1980.

[14] Salles, I. I., Thijs, T., Brunaud, C., De Meyer, S. F., Thys, J., Vanhoorelbeke, K., and Deckmyn, H., "Human platelets produced in nonobese diabetic/severe combined immunodeficient (nod/scid) mice upon transplantation of human cord blood cd34+ cells are functionally active in an ex vivo flow model of thrombosis," *Blood*, vol. 114, no. 24, pp. 5044–5051, 2009.

[15] Savage, B., Saldivar, E., and Ruggeri, Z. M., "Initiation of platelet adhesion by arrest onto fibrinogen or translocation on von willebrand factor," *Cell*, vol. 84, pp. 289 – 297, 1996.

[16] Schoephoerster, R. T., Oynes, F., Nunez, G., Kapadvanjwala, M., and Dewanjee, M. K., "Effects of local geometry and fluid dynamics on regional platelet deposition on artificial surfaces," *Arteriosclerosis, Thrombosis, And Vascular Biology*, vol. 13, no. 12, pp. 1806–1813, 1993.

[17] Softeland, E., Framstad, T., Thorsen, T., and Holmsen, H., "Porcine platelets in vitro and in vivo studies: Relevance to human thrombosis research," *European Journal of Haematology*, vol. 49, pp. 161–173, 1992.

[18] van Breugel, H., Sixma, J., and Heethaar, R., "Effects of flow pulsatility on platelet adhesion to subendothelium," *Arteriosclerosis, Thrombosis, and Vascular Biology*, vol. 8, no. 3, pp. 332–335, 1988.

[19] Wang, T. H., Bhatt, D. L., and Topol, E. J., "Aspirin and clopidogrel resistance: an emerging clinical entity," *European Heart Journal*, vol. 27, no. 6, pp. 647–654, 2006.

[20] Wootton, D. M., Markou, C. P., Hanson, S. R., and Ku, D. N., "A mechanistic model of acute platelet accumulation in thrombogenic stenoses," *Annals Of Biomedical Engineering*, vol. 29, no. 4, pp. 321–329, 2001.

[21] Zhao, X. M., Wu, Y. P., Cai, H. X., Wei, R., Lisman, T., Han, J. J., Xia, Z. L., and de Groot, P. G., "The influence of the pulsatility of the blood flow on the extent of platelet adhesion," *Thrombosis Research*, vol. 121, no. 6, pp. 821 – 825, 2008.

CHAPTER IV

PREVENTING RAPID PLATELET ACCUMULATION IN WHOLE, HUMAN BLOOD UNDER HIGH SHEAR STRESS BY BLOCKING $\alpha_{IIB}\beta_3$ AND PLATELET ACTIVATION

4.0.14 Introduction

Intravascular thrombosis is arguably responsible for the highest percentage of morbidity and mortality in the developed world. Death by Myocardial Infarction (MI) or stroke due to thrombosis can occur within an hour of symptomatic onset.[10] Platelet accumulation to occlusion under high shear rate conditions causes most arterial thrombosis and occurs in two phases - an initial adhesion of platelets to the damaged subendothelium followed by Rapid Platelet Accumulation (RPA) where platelets adhere to other platelets, ultimately rapidly stopping blood flow.[21] Platelet thrombosis typically occurs in arteries in the regions of high shear stress.[12] Pathologically high shear rates are present in the arterial system when an atherosclerotic plaque creates a local stenosis. Stenoses greater than 25% in arteries can create shear rates exceeding $3{,}500s^{-1}$ that reach over $100{,}000s^{-1}$ as thrombus grows.[3] Previous studies indicate that, following initial platelet adhesion onto a thrombogenic surface in these high shear rate regions, platelet activation ensues.[9] Activation of the platelet causes a conformational change in Glycoprotein IIb/IIIa ($\alpha_{IIb}\beta_3$) which allows $\alpha_{IIb}\beta_3$ to bind other proteins and occurs through a multitude of pathways.[9]

Anti-platelet agents are therefore one approach to prevent thrombosis causing MI and stroke. Clinical studies of the efficacy of anti-platelet agents have been mixed, with some agents demonstrating more blockade than others. Acetylsalicylic Acid

(ASA, aspirin) is the most widely used therapy in patients with vascular disease due to its relative cheapness and effectiveness.[1] ASA functions by preventing the metabolism of arachadonic acid to thromboxane A_2. Thromboxane A_2 promotes platelet activation.[17, 25] Clopidogrel (Plavix®) is another popular pharmaceutical, seen by some as superior to ASA.[11] It prevents activation by competitively and irreversibly binding to $P2Y_{12}$, an ADP receptor.[27] Prostaglandin E_1 (PGE_1), yet another activation inhibitor, prevents activation by increasing cyclic-AMP which decreases Ca^{2+} rise in the cytoplasm and ultimately stabilizes the platelet membrane. Even though these treatments have an effect on thrombosis, there is still controversy as to the role of platelet activation under high shear stress. Recent studies by Ruggeri *et al.* indicate that platelet aggregation of <100 platelets is activation independent.[22] As there is success with activation inhibitors clinically, large scale thrombus formation may require activation.

Inhibiting the change in conformation of $\alpha_{IIb}\beta_3$ to its active form, a protein triggered by platelet activation, specifically may prevent platelet aggregation.[4] The most widely used inhibitor of $\alpha_{IIb}\beta_3$ activation is abciximab (Reopro®), a Fab fragment directed against $\alpha_{IIb}\beta_3$.[20] Eptifibatide (Integrilin®), another inhibitor of $\alpha_{IIb}\beta_3$, is a cyclic heptapeptide which reversibly binds the glycoprotein.[5, 7]

Patients do not have uniform response to these pharmaceuticals, with therapy-resistant patients having an increased risk of cardiovascular events.[24] This creates the need for a low-volume device which allows for patient-specific therapy testing.

Under pathologic high shear rate conditions, we have previously shown that platelets in whole blood can attach in large numbers on a collagen-coated surface causing rapid platelet accumulation (RPA) rates greater than 1.6 $\mu m^3\ \mu m^{-2}\ min^{-1}$. In our in-vitro hemodynamic assay, hundreds of millions of platelets attach in the throat of the stenosis during RPA, eventually causing total occlusion of blood flow in less than 30 minutes. To this end, a low volume (30mLs), high shear stress, capillary model

of RPA which utilizes whole, human blood for experimentation may be utilized for testing patient specific therapies.

The purpose of this study is to determine if current anti-platelet agents are effective inhibitors of thrombosis under high shear conditions in whole, human blood. Our hypothesis is that the mechanism of the anti-platelet agent influences the efficacy and uniformity of blockade in human blood. Thus, we test five different pharmaceuticals (PGE_1, ASA, 2-MeSAMPS, abciximab, and eptifibatide) on their ability to block thrombus growth in stenotic test sections.

4.0.15 Experimental Design and Methods

4.0.15.1 Syringe Pump Apparatus

A single pass, syringe pump fed, in-vitro system was created in which thrombus formation could be viewed under a microscope (Figure 18). Whole, human blood is perfused though at a shear rate of 3,500 s^{-1}, or just above 2,000s^{-1}, the lower threshold level of shear induced platelet activation.[6]

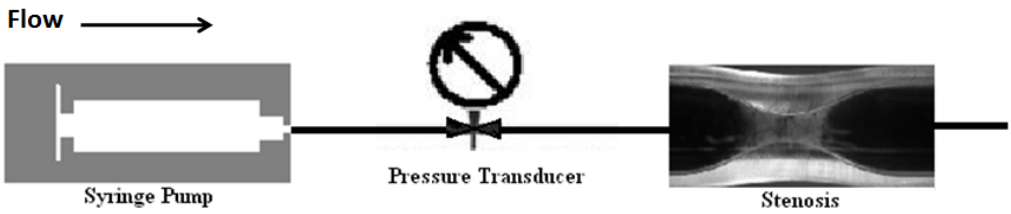

Figure 18: Whole blood is perfused from a syringe pump, past a pressure transducer and through a pyrex, collagen coated test section which is placed under a microscope. A high resolution camera takes images in real time through the microscope.

The test section through which the blood flows was created and collagen coated as previously described.[21] The original inner diameter of the tube is 1.5mm and the severity of stenosis used during experimentation range from 78% to 92%. To

attain the prescribed shear rate of $3{,}500s^{-1}$, flow rates were calculated using Poiseuille assumptions.

4.0.15.2 Whole Human Blood

Whole, human blood was drawn at the Georgia Institute of Technology's Health Center from consented subjects according to IRB protocol H06190. Blood was drawn directly into syringes containing 3.5 USP units/mL heparin (Sigma-Aldrich, St Louis, MO). This amount of heparin was chosen based on previous porcine experiments to prevent clotting during transport while still allowing thrombus formation during experimentation.[21] All blood was used within 8 hours of harvestm. Most of the experiments were conducted at the beginning of this 8 hour window, although no apparent differences were measured during experimentation time. During the flow experiments, excess blood was placed on an LS orbital mixer (Labnet, Woodbridge, NJ) to prevent blood separation.

4.0.15.3 Experimental Design

All of the experiments were conducted in three steps as seen in Figure 19. In the first step (Figure 19 A), up to 10mLs of untreated blood is perfused through a stenosis until initial visible deposition is seen. This allows for platelets to initially adhere to the surface. In the second step (Figure 19 B), up to 10mLs of blood treated with an anti-thrombotic therapy is perfused through the same stenosis. For the final step (Figure 19 C), up to 10mLs of untreated blood is perfused through the same stenosis. This ensures that the blood is thrombogenic. Experiments in which RPA did not occur in the second or third syringe were discarded as the effect of the treatment on RPA could not be determined on blood in which RPA did not occur.

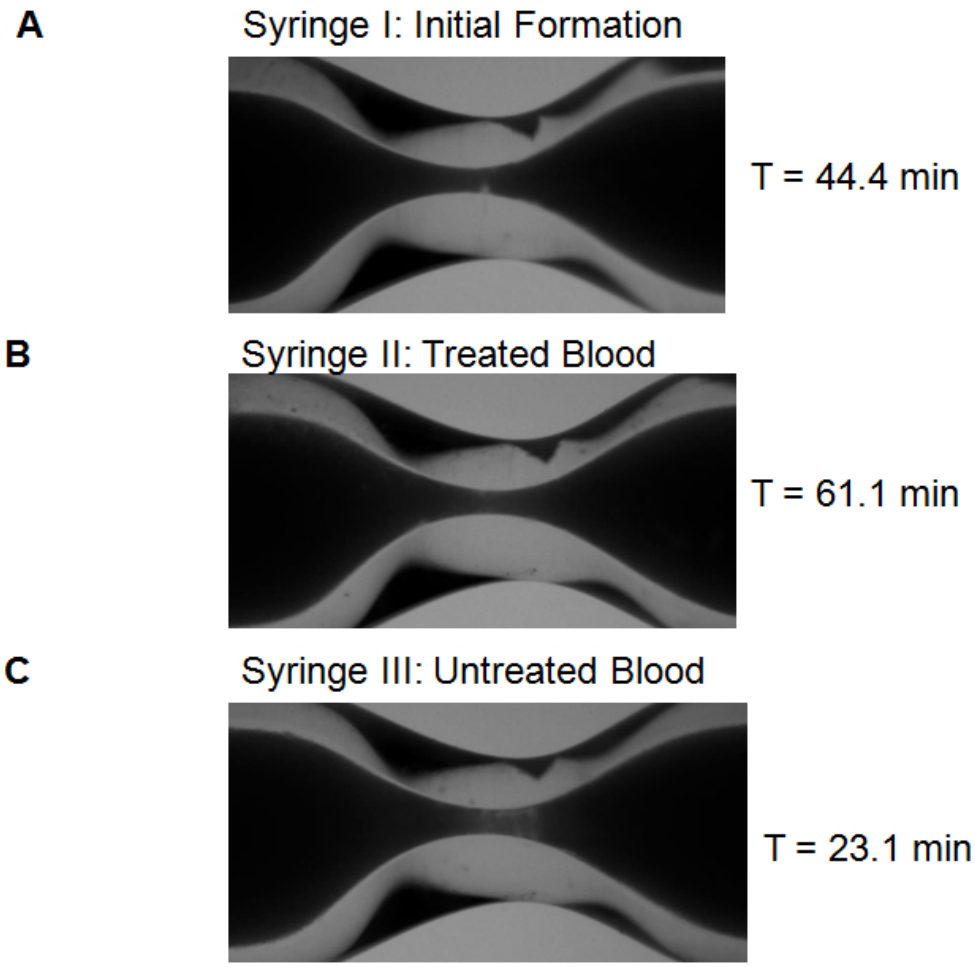

Figure 19: Experiments were completed in a three step approach. Initially, up to 10mLs of untreated blood was perfused through a collagen coated test section until visible initial thrombus deposition occurred (A). This was followed by perfusing up to 10mLs of blood treated with an anti-thrombotic agent through the same test section (B). Lastly up to 10mLs of untreated blood was perfused through the test section (C). Times shown are relative to the initiation of flow for that particular step.

4.0.15.4 Dosing

All pharmaceuticals and chemicals were reconstituted with a difference between the volume of chemical/drug used and saline to yield 1mL of total solution added to the 10mL syringe of blood. All chemicals were mixed according to manufacturer's

specifications.

Abciximab and Eptifibatide A 10x dose was calculated using the original recommended dose of 0.25mg/kg and 0.36mg/kg for abciximab and eptifibatide respectively. Assuming an average body weight of 70kg and a total blood volume of 5L, the final dose was determined to be 0.35mg of abciximab and 0.504mg of eptifibatide per 10mLs of whole blood used. The high dosage used was to ensure receptor blocking.

ASA A 10x dose was calculated for ASA (Sigma-Aldrich, St. Louis, MO) - based on a low-daily dose of 100mg and 5L of total blood volume.[16] This resulted in a mixture of 2mg of ASA and saline (1mL total added volume) which were added to 10mL of whole blood. The high dosage used was to ensure receptor blocking.

PGE_1 and 2-MeSAMPS Experimental doses for PGE_1 (Sigma-Aldrich, St. Louis, MO) and 2-MeSAMPs, a clopidogrel stand-in, (as it does not need to be metabolized to block $P2Y_{12}$, Sigma-Aldrich, St. Louis, MO) were 10μM and 50μM as previously described by Ruggeri *et al* and Andre *et al* respectively for blocking activation.[2, 18, 22]

4.0.15.5 Images

The test section was photographed through a 2x microscope objective using a high resolution digital CCD camera (Pixelfly, Keleim, Germany) connected directly to the Zeiss Stemi 2000-C (Zeiss, Jena, Germany) stereo microscope. The camera had a corresponding lens which had a 0.5x magnification, yielding a final magnification of 1x and a resolution of approximately 7μm/pixel. Images were taken sequentially in real time (1 frame/sec) and post processed using CamWare (Cooke Corporation, Romulus, MI) and Photoshop (Adobe, San Jose, CA).

4.0.15.6 Embolus

Embolus was defined as a visible mass seen entering the stenosis which caused an instantaneous increase in pressure. Two types of embolus seen during experimentation are shown below in Figure 20. Adherent embolus (Figure 20 A) was seen as a visible mass entering the stenosis which adhered to the stenotic test section and persisted for minutes during experimentation (Figure 20 A, 1, 2). In one case, the embolus changed position at the end of experimentation due to fluid forces (Figure 20 A, 3, 4). Adherent embolus volumes were not included in the thicknesses or deposition rates reported, with areas containing embolus being excluded from measurement as platelet deposition rates were equivalent prior to and following an embolic event. Transient embolus (Figure 20 B) was also not included during experimentation. Transient embolus was defined as the instantaneous, non adherent movement of a visible mass seen entering the stenosis and exiting within seconds (Figure 20 B, 1-4). Occasionally, the transient embolus would remove previously deposited thrombus. While decreases in thrombus thickness and volume were seen due to the mass pushing out adherent thrombus, the presence of embolus was deleted from the analysis due to rates prior to and after embolitic events being comparable.

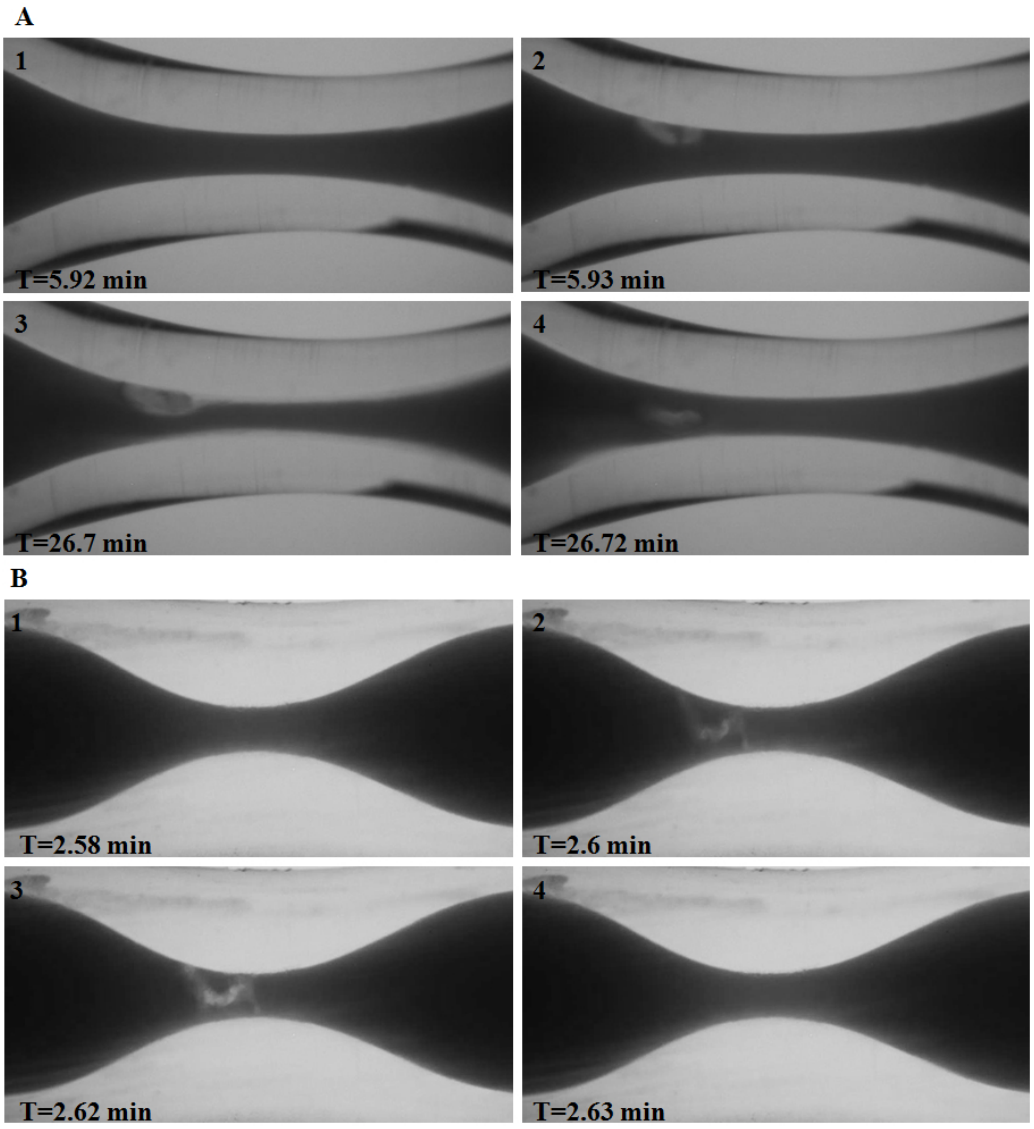

Figure 20: (A) Adherent embolus is debris which enters the test section quickly (A1,A2), but remains for minutes during experimentation (A3). In the event shown, the embolus shifted near the end of experimentation (A4). (B) Transient embolus also occurs during experimentation and is seen as rapidly transiting debris (B1-B4), which exits the tube within seconds.

4.0.15.7 Additional Thickness/Volume/Accumulation Rates

Thickness of platelet accumulation was measured as the difference between the stenosis inner diameter and the inner diameter of the thrombus protruding into the lumen. The increase in thickness is determined by subtracting the initial thickness at the beginning of each new 10mLs perfused. The maximum thickness reported was taken at a single location in the stenosis at the time when accumulation was greatest. Average thickness was calculated for each set of experiments by averaging the maximum thickness values over each position a distance $0.19 - 0.24$mm apart. The thickness reported for each stenosis in each set of experiments is from the time of maximum thickness during experimentation.

Volume was calculated from thickness using the equation below:

$$Volume(cm^3) = \sum_{i=1}^{n} (\frac{(D_{O,i}^2 - D_{I,i}^2}{4})\pi L \tag{3}$$

where D_O was the diameter of the inside of the glass stenosis and the inner diameter, D_I, was the diameter created by measuring the top of the thrombus growing from the bottom of the tube and the bottom of the thrombus growing from the top of the tube. By summing the cylinders, the volume was then integrated along the length of the thrombus, L, which was divided into equal segments which ranged in length for each set of images from $0.19 - 0.24$mm.

Surface area used was the total surface area that thrombus deposited on during experimentation and was calculated as:

$$SurfaceArea(cm^2) = \sum D_O \pi L \tag{4}$$

Where D_O is the inner diameter of the stenosis for each segment on which thrombus deposited on during experimentation.

Accumulation rates were calculated using the equation below:

$$AccumulationRate(\mu m^3 \mu m^{-2} min^{-1}) = (\frac{Volume/Time}{SurfaceArea}) \quad (5)$$

Volume/Time is a regression of the volume over at least three consecutive time points, with the three time points encompassing a minimum of 2 minutes of the volume growth of thrombus formation. For all experiments, the maximum accumulation rate was calculated using at least three points. If the maximum did not exceed RPA, or an accumulation rate $\geq$ 1.6 $\mu m^3 \mu m^{-2} min^{-1}$, a regression of the volumetric growth over the total time of experimentation was calculated.[21]

4.0.15.8 Statistics

Experiments were analyzed using a student's t-test where statistical significance is defined as $p<0.05$.

4.0.16 Results

Results are presented for the general activation inhibitors (PGE_1, 2-MeSAMPS, and ASA), followed by $\alpha_{IIb}\beta_3$ specific inhibitors (abciximab and eptifibatide).

4.0.16.1 RPA Requires Activation Mediated by PGE_1 Pathway

We explored the effects of blocking activation on RPA under high shear conditions.

PGE_1

The incremental thrombus thickness beyond the initial deposition is shown in Figure 21. The added thickness in each individual stenosis is shown for blood treated with PGE1 (Figure 21 A) as well as untreated blood which was subsequently perfused (Figure 21 B). This is followed by the thickness averaged by position (Figure 21, C and D) and is also shown with standard deviations (Figure 21, E and F). In general, little thrombus thickness was observed in the PGE1 group. There was significantly less added maximal thickness in blood treated with PGE_1 (11 $\pm$ 12 μm, n=5, Figure 21 C) than untreated blood (138 $\pm$ 84 μm n=5, $p<0.05$, Figure 21 D).

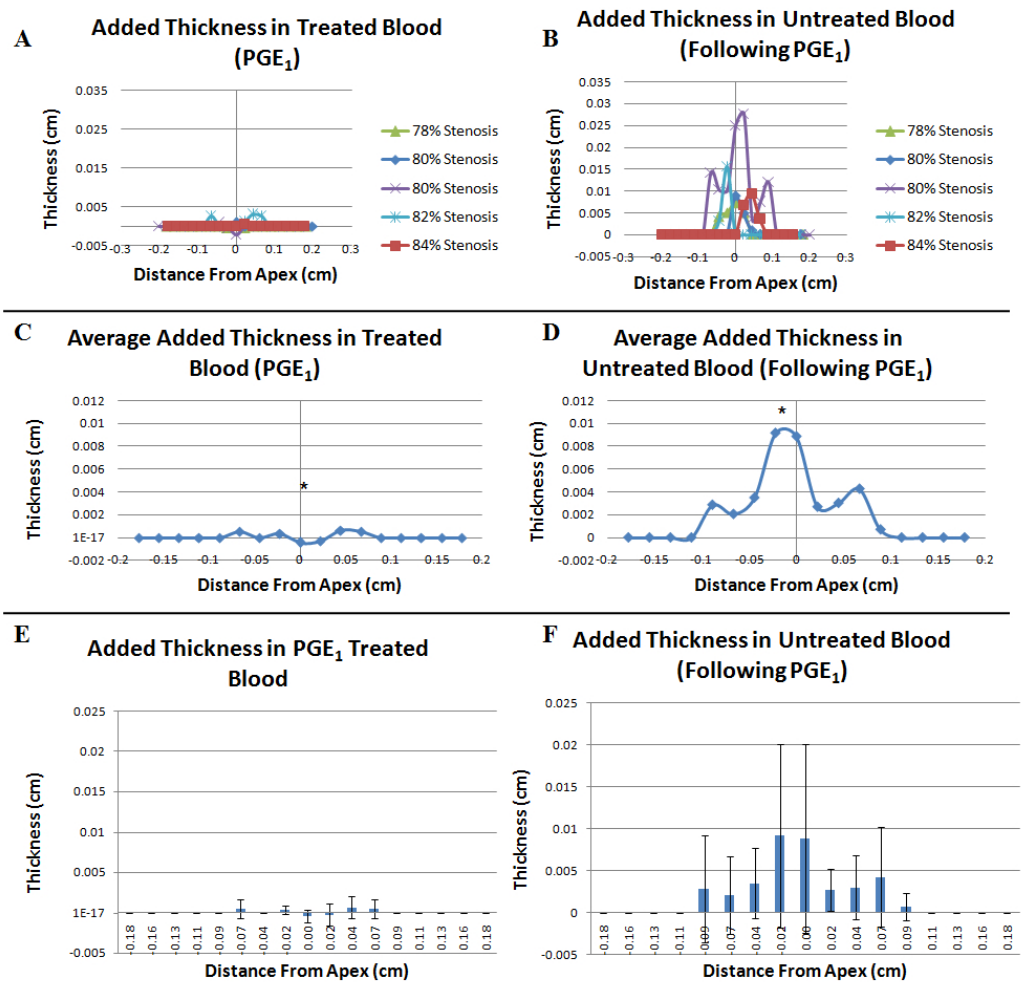

Figure 21: Measured thicknesses following the perfusion of blood treated with A) PGE_1 and the subsequent perfusion of B)untreated blood. There was a significant increase in maximum thicknesses (*, $p<0.05$) for D)untreated blood following the perfusion of treated blood when compared to C)blood treated with PGE_1. The averages with standard deviations for E)treated blood and F)untreated blood are also shown.

Individual volume growths are shown over time for blood treated with PGE_1 (Figure 22 A). For comparison, the amount of thrombus volume accumulation over time in the same test section with normal blood (control) immediately after is shown (Figure 22 B). The additional volume added during experimentation was 1.0 ± 7.0

$*10^{-6}cm^3$ (1.0 $\pm$ 7.0 $*10^6\mu m^3$)in PGE_1 treated blood (n=5), which was an order of magnitude lower than untreated blood 42 $\pm$ 52 $*10^{-6}cm^3$ (n=5).

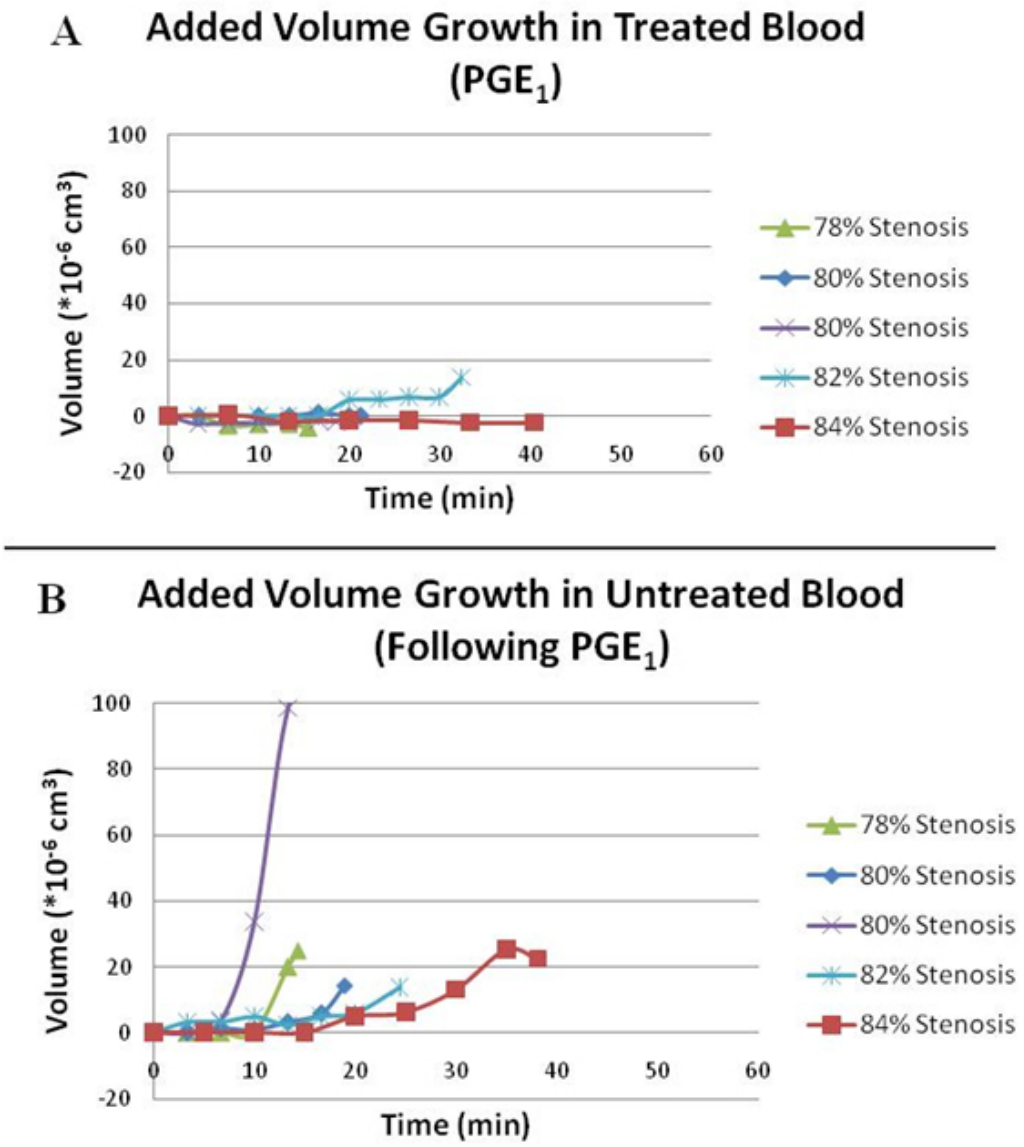

Figure 22: Calculated volumes are shown for blood treated with PGE_1 (A) and subsequently perfused untreated blood (B)

PGE_1 added to whole blood completely inhibited RPA, with RPA occurring in 0/5 samples of treated blood ($p<0.05$), whereas RPA occurred in the untreated

blood (n=5/5). Average deposition rates for the PGE_1 treated blood were -0.1 ± 0.3 $\mu m^3 \mu m^{-2} min^{-1}$ (n=5) and were significantly lower than the RPA rates for the untreated blood (3.2 ± 1.7 $\mu m^3 \mu m^{-2} min^{-1}$, n=5, $p<0.05$).

2-MeSAMPS 2-MeSAMPS blocks the $P2Y_{12}$ pathway of platelet activation and does not need to be metabolized like clopidogrel.

Figure 23 A depicts the 5 experiments using 2-MeSAMPS and is followed by untreated blood perfused immediately after (Figure 23 B). The average added thickness is shown in Figure 23 C for 2-MeSAMPS treated blood (n=5) and is followed by untreated blood which was perfused immediately following (n=4) and is also shown with standard deviations (Figure 23, E and F). The maximum thickness deposited in 2-MeSAMPS treated blood is significantly smaller (27 ± 21 μm, n=5) than the subsequent perfusion of normal blood (138 ± 55 μm, $p<0.05$, n=4, Figure 23 D).

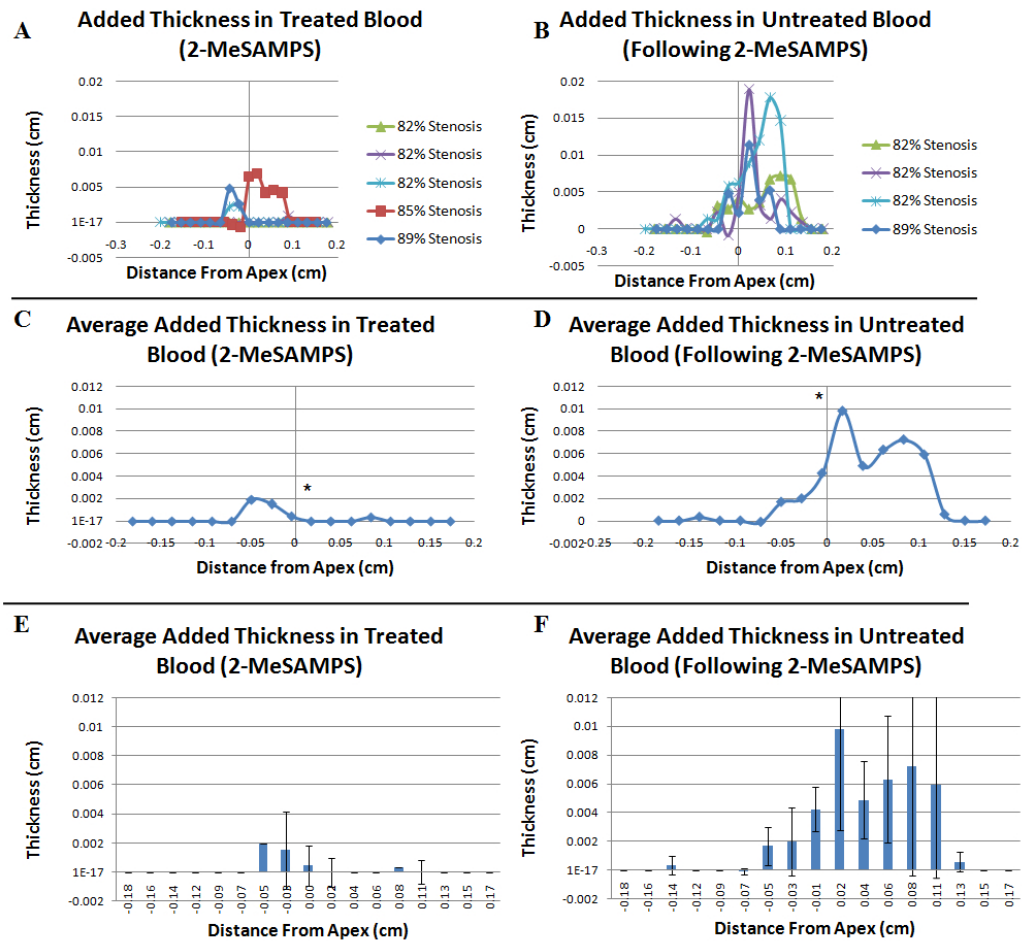

Figure 23: Measured thicknesses following the perfusion of blood treated with A) 2-MeSAMPS (n=5) and the subsequent perfusion of B)untreated blood (n=4). There was a significant increase in the maximum thicknesses (*, $p<0.05$) for D)untreated blood (n=4) following the perfusion of treated blood when compared to C)blood treated with 2-MeSAMPS (n=5). The averages with standard deviations for E)treated blood and F)untreated blood are also shown.

Treatment of whole blood with 2-MeSAMPS reduced the amount of thrombus formation over time (Figure 24 A) as compared to the control with normal blood (Figure 24 B). The additional volume added during experimentation was $4.8 \pm 4.5 * 10^{-6} cm^3$ in 2-MeSAMPS treated blood (n=5), which was lower than untreated blood

$59 \pm 44 * 10^{-6} cm^3$ (n=4).

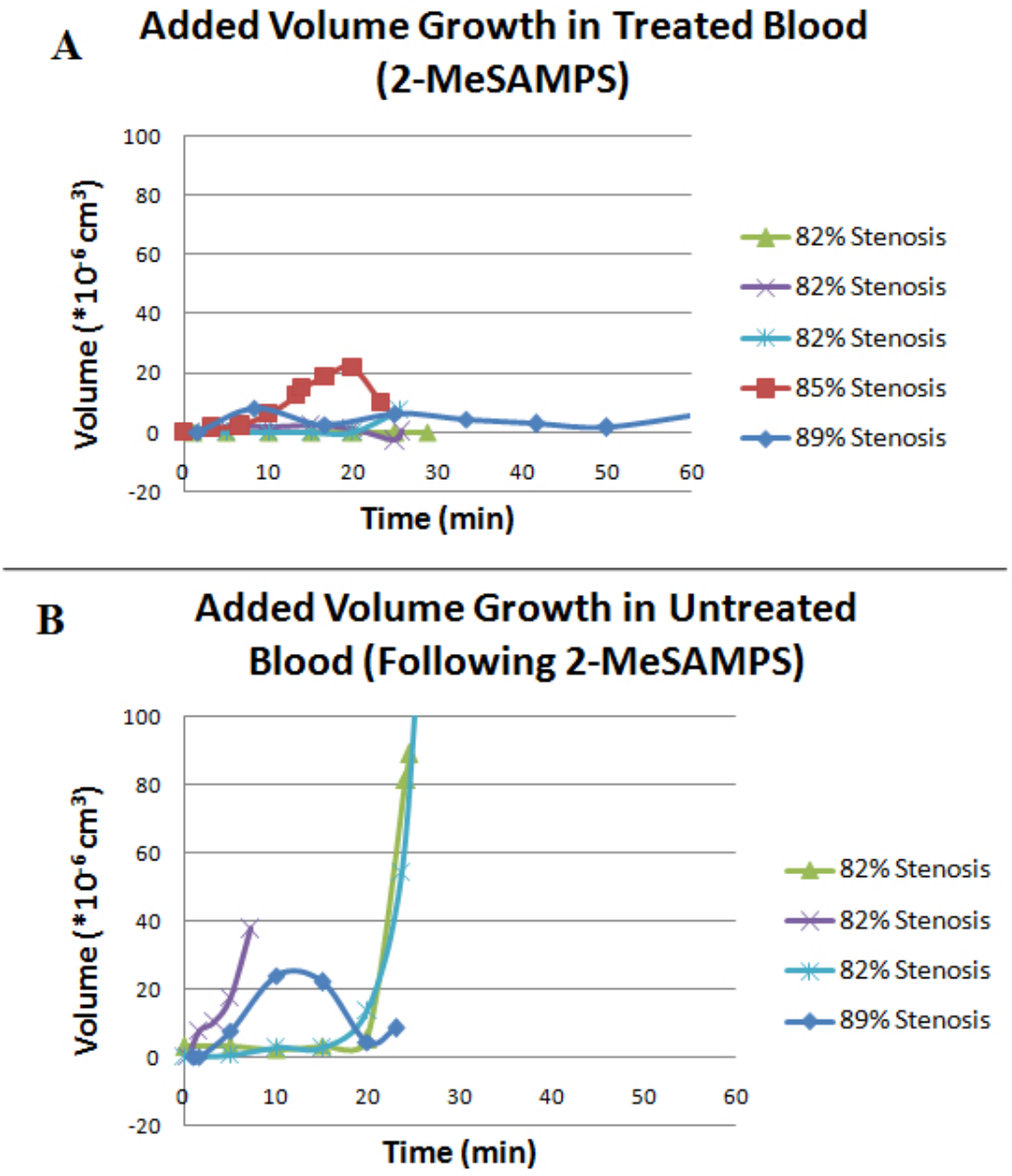

Figure 24: Calculated volumes are shown for blood treated with 2-MeSAMPS (A) and subsequently perfused untreated blood (B). Volumes are lower for treated blood.

In blood with 2-MeSAMPS, the average accumulation rates for samples which did not go to RPA were $0.002 \pm .22\ \mu m^3 \mu m^{-2} min^{-1}$ (n=4) and minimal volume

deposition can be seen during experimentation (Figure 25). The platelet deposition rate in the treated syringe which exceeded RPA was 3.7 $\mu m^3 \mu m^{-2} min^{-1}$ (n=1, 85% stenosis). Combined, the rates with 2-MeSAMPS were significantly slower than the RPA rates of the untreated syringe (4.1 ± 1.7 $\mu m^3 \mu m^{-2} min^{-1}$, n=4, $p<0.05$). One of the four samples of 2-MeSAMPS treated blood in which RPA was prevented was dosed with 30nM of epinephrine (a high physiologic amount) to increase thrombogenicity in the blood overall.[19, 8]

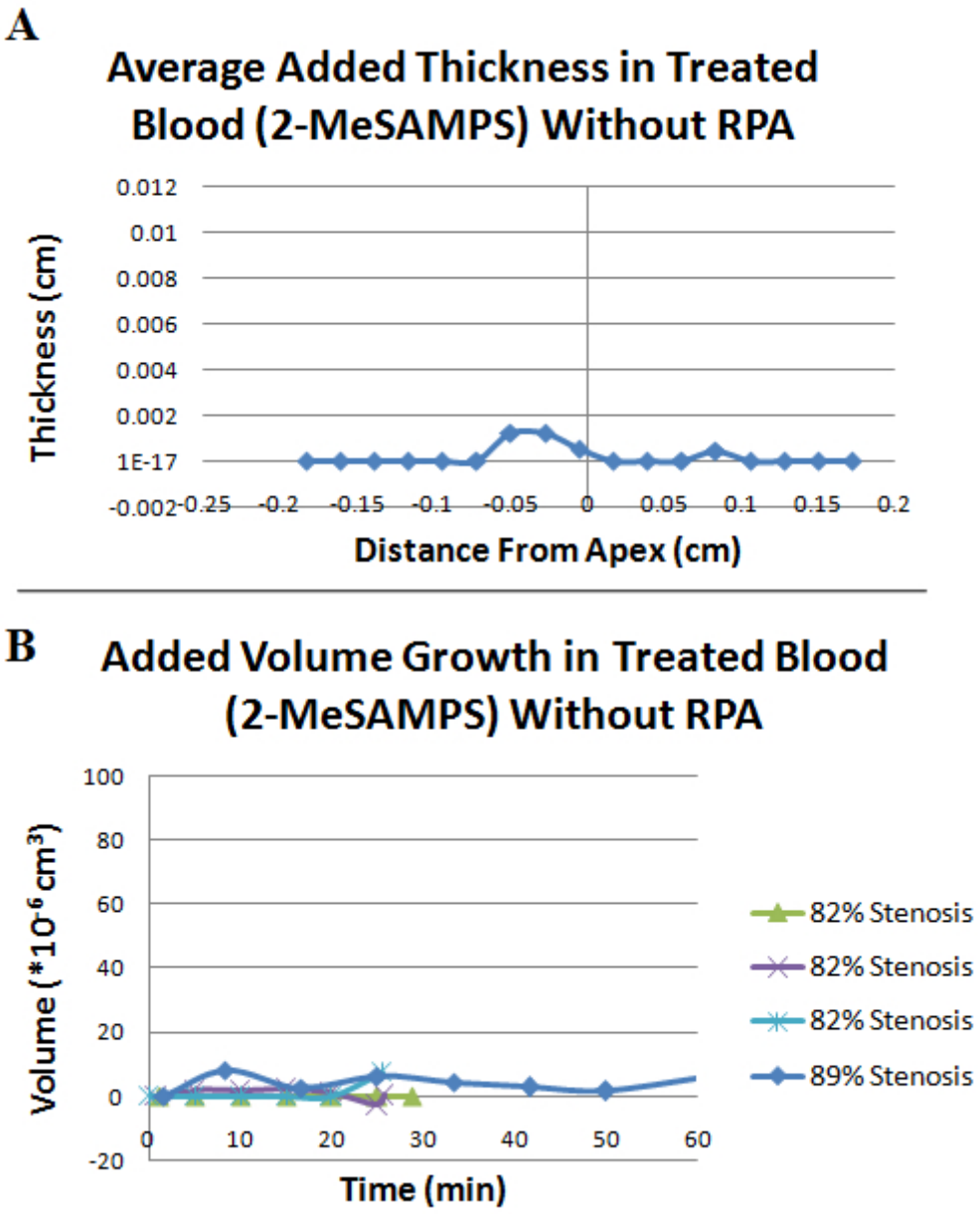

Figure 25: The average measured A)thickness and calculated B)volume of blood which was treated with 2-MeSAMPS (n=4).

RPA was present in 1/5 (20%) of samples with 2-MeSAMPS, although it was a significant inhibitor of RPA, with RPA occurring in only 1/5 of treated blood samples and in 4/4 of the following untreated samples ($p<0.05$). Thus, there was an example

of blood treated with a 10x dose of this $P2Y_{12}$ inhibitor which did not show adequate anti-platelet activity under high shear in our assay.

ASA

Acetylsalicylic acid is the active ingredient in aspirin. The maximum thicknesses are shown in Figure 26 A for ASA treated blood and in Figure 26 B for the untreated blood immediately following. Their averages with standard deviations can be seen in Figure 26, E and F. The maximum thickness for the ASA treated blood (66 $\pm$ 42 μm, n=7, Figure 26 C) was significantly less than the maximum thickness in the untreated blood (217 $\pm$ 158 μm, n=3, $p<0.05$, Figure 26 D).

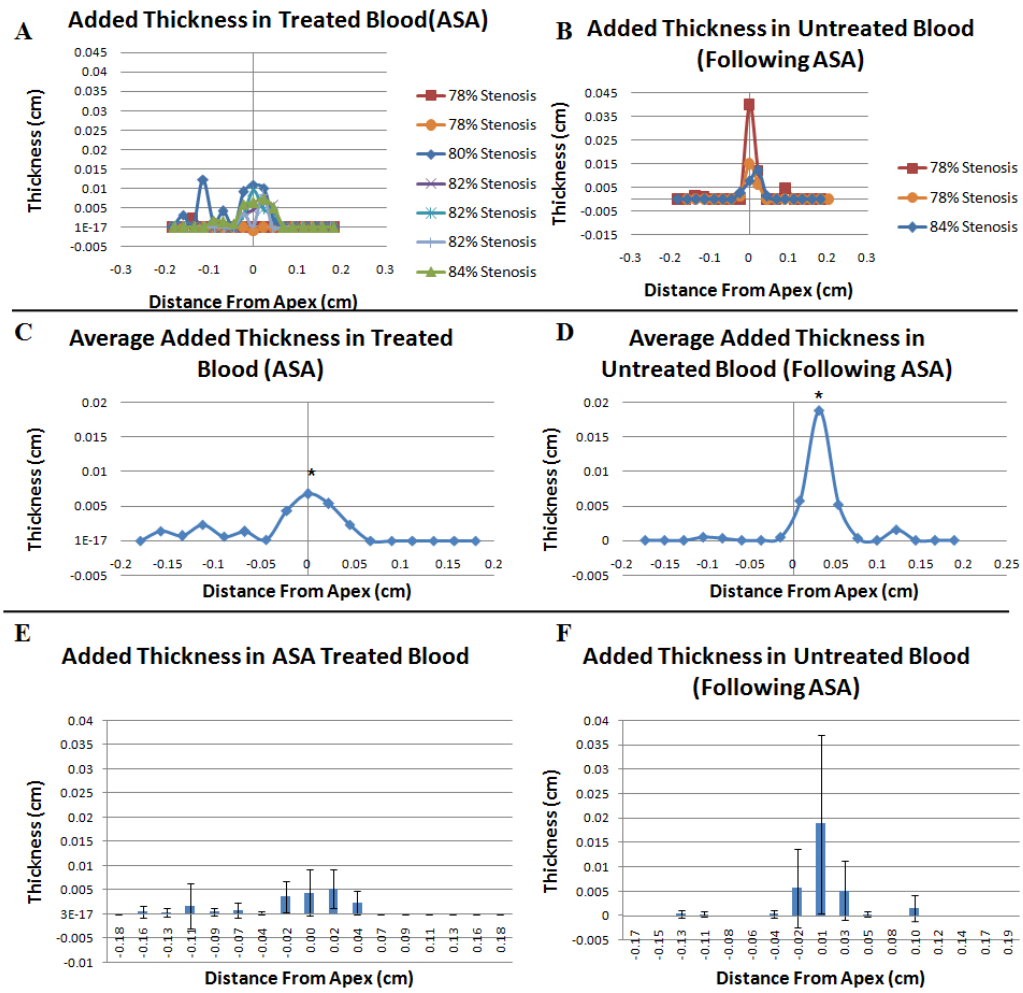

Figure 26: Measured thicknesses following the perfusion of blood treated with A) ASA (n=7) and the subsequent perfusion of B)untreated blood (n=3). There was a significant increase in maximum thickness(*, $p<0.05$) for D)untreated blood following the perfusion of ASA treated blood (n=3) and C)blood treated with ASA (n=7). The averages with standard deviations for E)treated blood and F)untreated blood are also shown.

The amount of thrombus volume growth over time is shown in Figure 27 A for ASA, as compared to the control growth seen in Figure 27 B. The additional volume added during experimentation was $26 \pm 35 * 10^{-6} cm^3$ in ASA treated blood (n=7)

and $62 \pm 86 * 10^{-6} cm^3$ (n=3) in untreated blood.

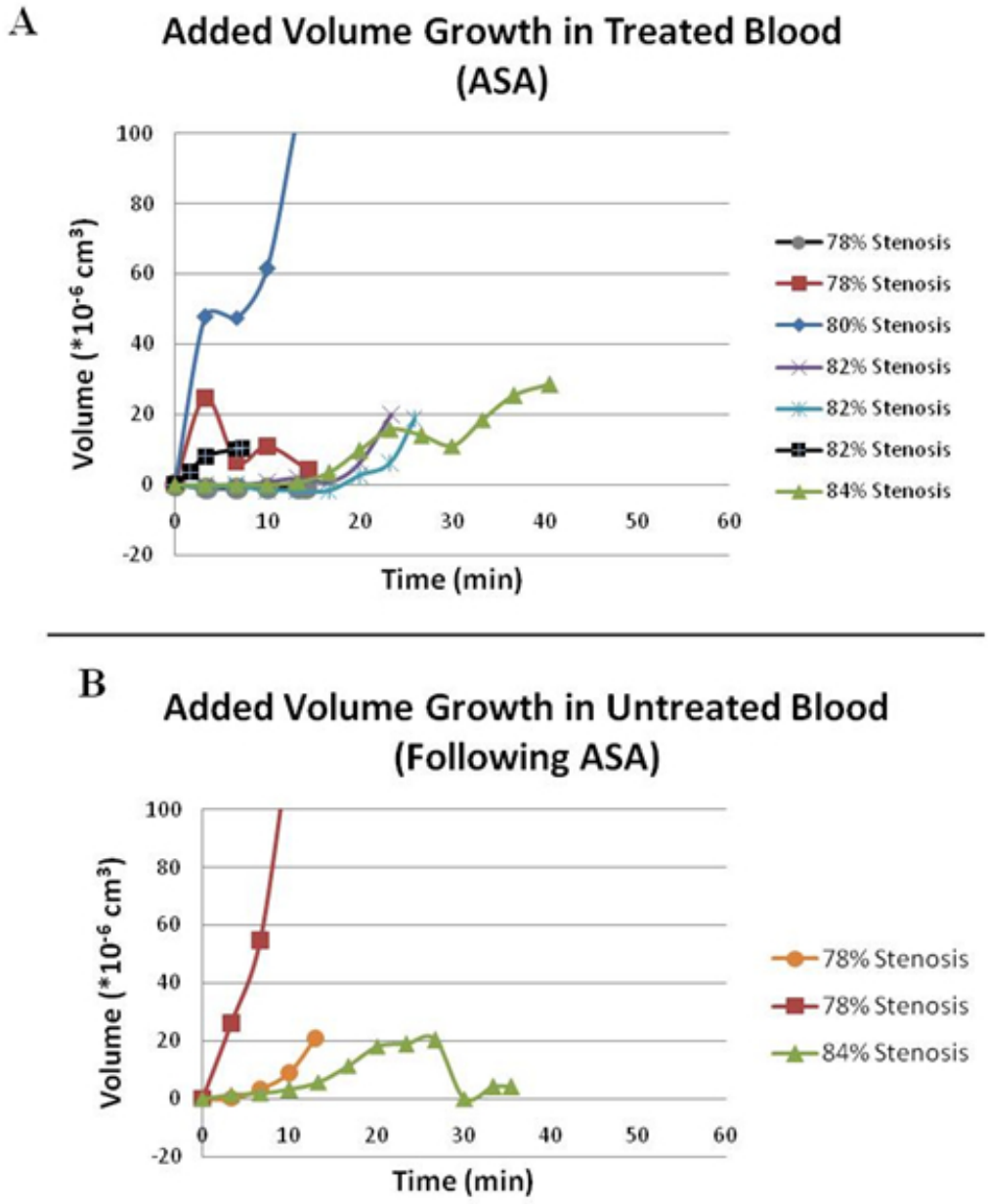

Figure 27: Calculated volumes are shown for blood treated with ASA (A) and subsequently perfused untreated blood (B).

RPA was present in 4/7 (57%) of ASA treated samples. In the samples in

which RPA was prevented average deposition rates in ASA treated blood were -0.01 ± 0.3 $\mu m^3 \mu m^{-2} min^{-1}$ (n=3). RPA rates in the untreated blood were 3.7 ± 1.1 $\mu m^3 \mu m^{-2} min^{-1}$ (n=3). ASA treated blood which went to RPA had rates of 2.8 ± 0.8 $\mu m^3 \mu m^{-2} min^{-1}$ (n=4).

Thus, there were several examples of blood treated with ASA that did not show adequate anti-platelet activity under high shear in our assay, indicating that that ASA treated blood was not as effective in preventing RPA and exhibited more thrombus volume deposition under high shear.

4.0.16.2 $\alpha_{IIb}\beta_3$ Blocking Agents

Abciximab

Abciximab (Reopro®) is a Fab fragment of a monoclonal antibody against $\alpha_{IIb}\beta_3$. Following visible initial adhesion, added thickness was measured for the following syringes containing blood treated with abciximab and untreated blood respectively (Figure 28, A and B). There was a significant increase in the maximal thicknesses in untreated blood (154 ± 30 μm, n=6, Figure 28 D) versus the maximal thickness in blood treated with abciximab (28 ± 19 μm, n=6, $p<0.05$, Figure 28 C).

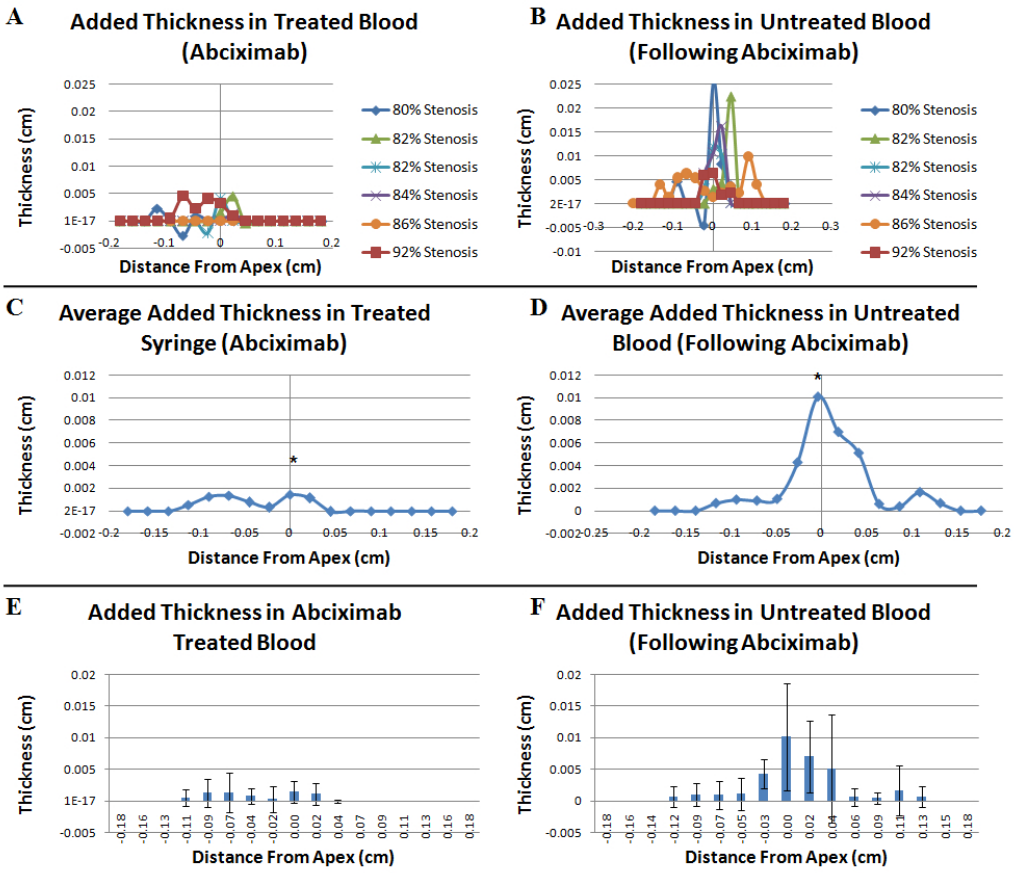

Figure 28: Measured thicknesses following the perfusion of blood treated with A) abciximab and the subsequent perfusion of B) untreated blood. There was a significant increase in thickness (*, $p<0.05$) in the average maximal thickness for D)untreated blood following the perfusion of treated blood when compared to C) blood treated with abciximab. The averages with standard deviations for E) treated blood and F) untreated blood are also shown.

Treatment of blood with abciximab prevented the formation of large amounts of thrombus volume as shown in Figure 29 A (n=6). For comparison, the volume of platelets deposited over time is shown for the control blood in Figure 29 B (n=6). There was a significant increase in the added volume during experimentation in the untreated blood, which averaged $32 \pm 22 * 10^{-6} cm^3$ ($p<0.05$, n=6), than the blood

treated with abciximab which averaged $1.4 \pm 7.0 * 10^{-6} cm^3$ (n=6).

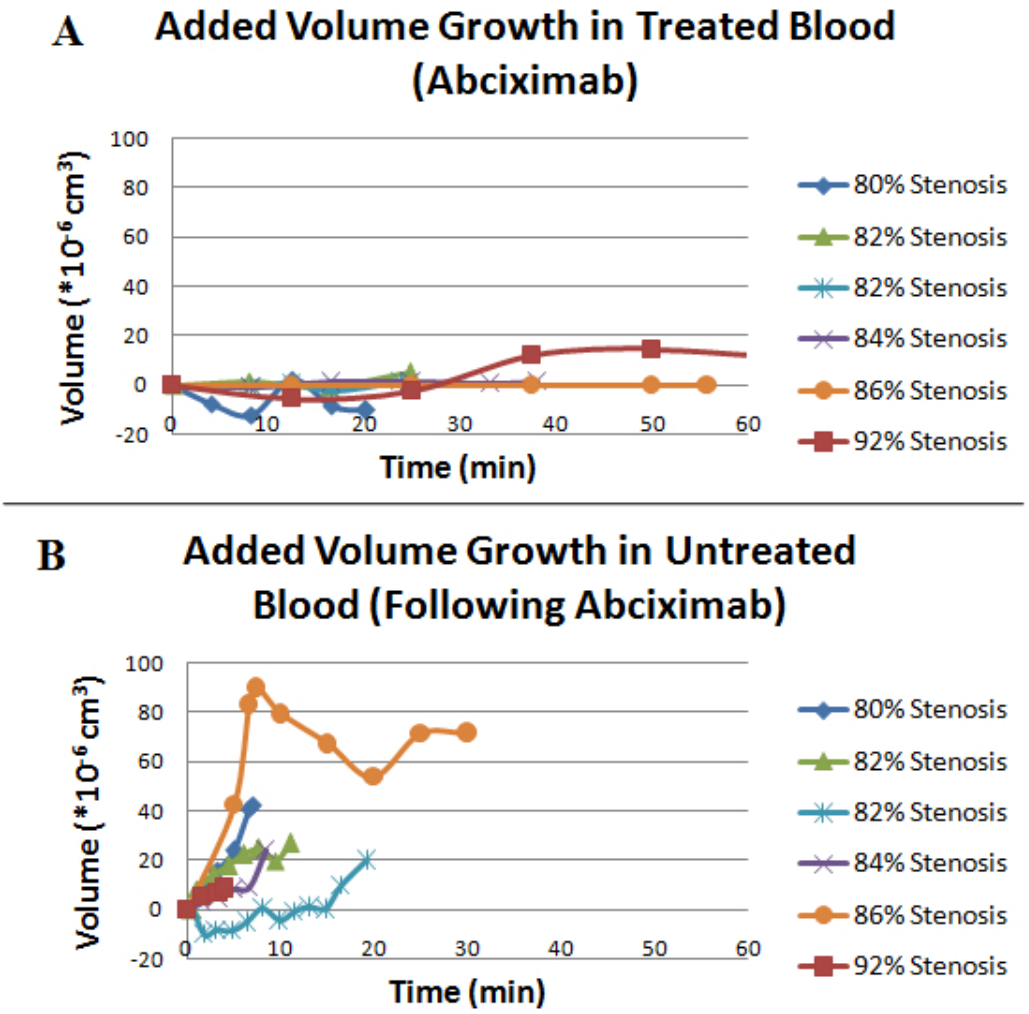

Figure 29: Volume deposition over time was calculated for blood treated with abciximab (A) and untreated blood which was subsequently perfused (B). The average added volume deposited in the untreated blood ($32 \pm 22 * 10^{-6} cm^3$, n=6) was significantly greater than the average maximal added volume in the blood treated with abciximab ($1.4 \pm 7.0 * 10^{-6} cm^3$, n=6, $p<0.05$).

Rapid platelet accumulation did not occur in any blood sample treated with abciximab (n=0/6), with a significantly higher occurrence of RPA occurring in untreated

blood ($p<0.05$, n=6/6). As RPA did not occur in blood treated with abciximab, average deposition rates of the treated blood were compared with RPA rates in the untreated blood resulting in a significant increase in the final thrombus volume deposition in untreated blood ($6.2 \pm 2.4 \pm 0.8\ \mu m^3 \mu m^{-2} min^{-1}$, $p<0.05$, n=6) versus treated blood ($0.1 \pm 0.1 \pm 0.8\ \mu m^3 \mu m^{-2} min^{-1}$, n=6).

Eptifibatide

Eptifibatide (Integrilin®) functions as a competitive small molecule against the binding site.

Added maximal thickness measurements for all blood treated with eptifibatide (Figure 30 A) and the subsequently perfused untreated blood (Figure 30 B) are shown below. An eptifibatide treated, 84% stenosis shows a marked increase in thickness deposition compared to the other treated syringes (Figure 30 A), causing the average added maximum thickness for the treated blood ($167 \pm 19\ \mu$m, n=5, Figure 30 C) to exceed those of the untreated samples ($121 \pm 38\ \mu$m, n=4, Figure 30 D).

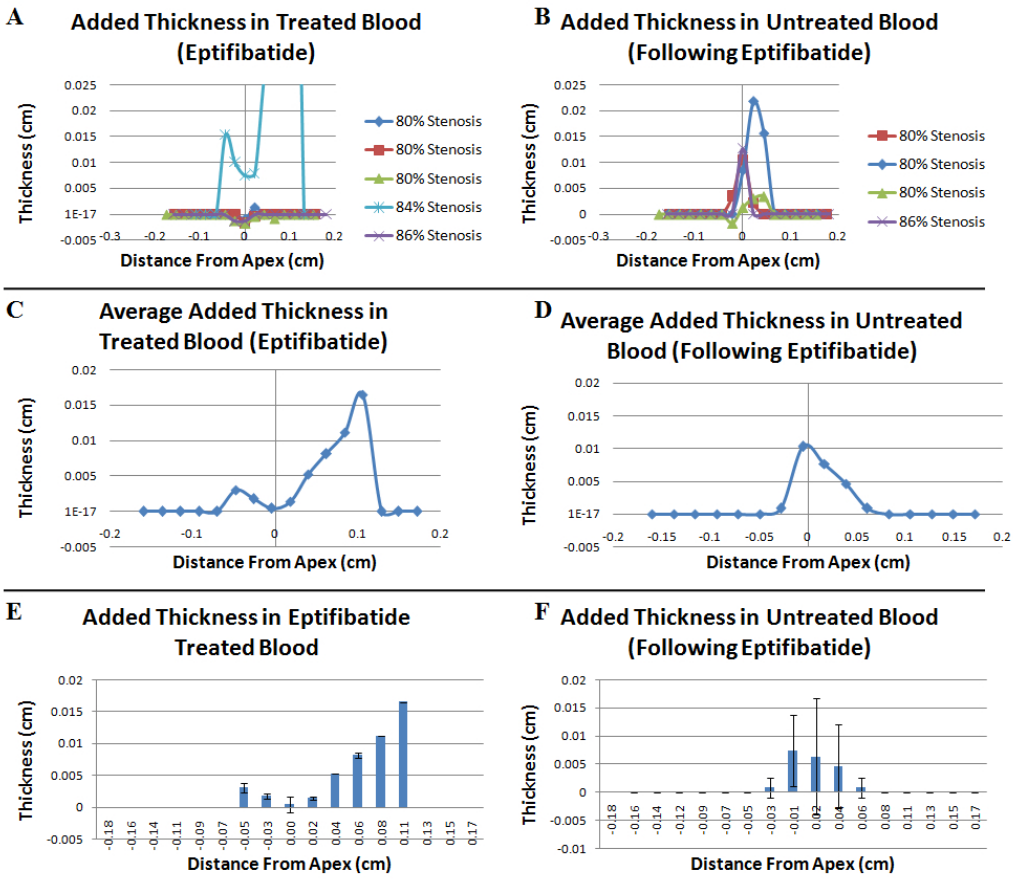

Figure 30: Measured thicknesses following the perfusion of blood treated with A) eptifibatide and the subsequent perfusion of B)untreated blood. The average maximal thickness was also represented for blood treated with eptifibatide (n=5, C) and untreated blood perfused following (n=4, D). The averages with standard deviations for E)treated blood and F)untreated blood are also shown.

Excluding this one sample, the effect of effective eptifibatide treatment can be seen below (n=4, Figure 31) for average maximum thrombus deposition (Figure 31 A) and volume growth (Figure 31 B). Overall, there is a net negative volume growth in eptifibatide-responsive blood treated during experimentation.

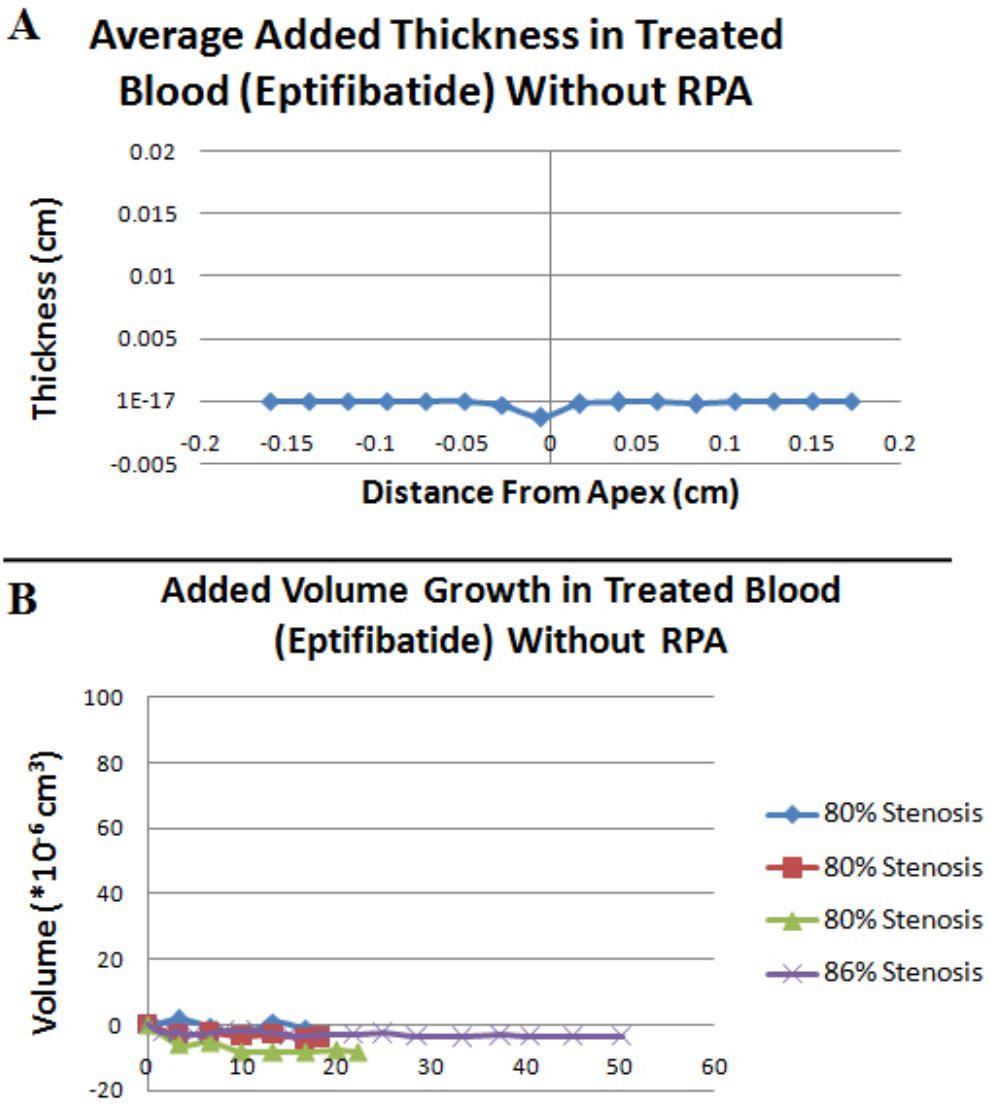

Figure 31: The average measured A)thickness and calculated B)volume of blood which was treated with eptifibatide in which RPA was prevented (n=4).

In 4/5 (80%) experiments, Eptifibatide showed no thrombosis volume growth following initial adhesion (Figure 32 A). The average added volume in eptifibatide treated blood was -10 $\pm$ 12 $*10^{-6}cm^3$ (n=5, Figure 32 A). The average added volume in the subsequently perfused untreated blood was 16 $\pm$ 16 $*10^{-6}cm^3$ (n=4, Figure 32 B). There is a marked increase in additional thrombus volume (Figure 32 A) in the

treated stenosis in which RPA occurred versus the other treated samples in which RPA was prevented (Figure 32 A).

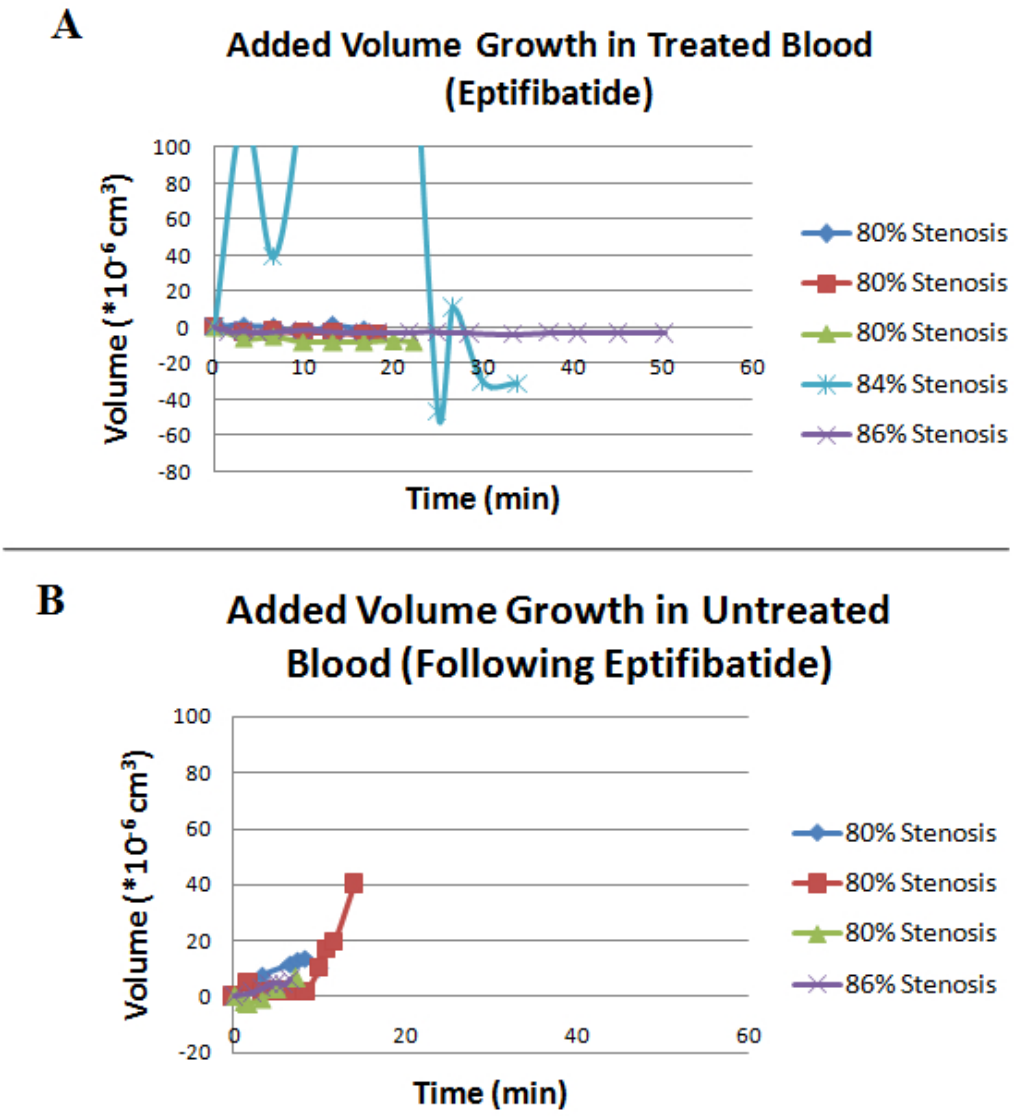

Figure 32: The added maximal thrombus volume deposited was calculated for both blood treated with eptifibatide (A) and untreated blood (B).

Significant prevention of RPA occurred in blood treated with eptifibatide (n=4/5, $p<0.05$), with RPA occurring in an 84% stenosis (n=1/5).

RPA rates averaged 5.9 $\pm$ 4.3 $\mu m^3 \mu m^{-2} min^{-1}$ for untreated blood (n=4) and

average deposition rates of eptifibatide treated blood in which RPA did not occur averaged -0.3 ± 0.1 $\mu m^3 \mu m^{-2} min^{-1}$ (n=4). In the sample of treated blood which achieved RPA, the RPA rate was 12.5 $\mu m^3 \mu m^{-2} min^{-1}$ (n=1, 84% stenosis).

Overall, abciximab and PGE_1 were the only therapies which completely prevented RPA and significantly inhibited maximal thickness deposition. Eptifibatide and 2-MeSAMPS were also significant inhibitors of RPA, but not of thickness deposition. ASA was the least successful at preventing RPA.

4.0.16.3 Response to therapies is patient/time specific

Patient Specific Results

It is possible that blood drawn at different times from the same individual may react differently over time. We compared the results of treatment for two subjects to evaluate variations within an individual. The responses listed in Table 3 show that responses to treatment can depend on the person or change over time. For subject 1, PGE_1 and abciximab prevented RPA, while 2-MeSAMPS, ASA, and eptifibatide did not. In the case of subject 2, all pharmaceuticals worked. However, a repeat of ASA in Subject 2 was performed one month later that showed less susceptibility to ASA and the presence of RPA. This time variation in the blood of Subject 2 suggests that testing of a patient for high shear thrombosis may be needed periodically.

Table 3: The ability of each investigatory drug to inhibit RPA is shown above for two subjects. A (+) indicates RPA prevention. Otherwise, (−) is shown.

	Abciximab	Eptifibatide	2-MeSAMPS	PGE_1	ASA
Subject 1	+	−	−	+	−
Subject 2	+	+	+	+	+ and −

4.0.17 Discussion

We have evaluated the efficacy of five anti-platelet agents to block thrombosis in a collagen coated tubular stenosis test section where shear stress exceeds $3500s^{-1}$. Blockade of high shear thrombus formation by PGE_1 was complete, whereas ASA was not uniformly effective. A Plavix® analog called 2-MeSAMPS generally worked with most blood with a failure in the blood from only one subject. Blockade of $\alpha_{IIb}\beta_3$ by abciximab, completely blocked thrombus under high shear, whereas eptifibatide had a notable failure. The endpoints of thrombus volume, thickness and growth rate yielded similar results in our assay.

Clinically, it is common to evaluate an entire cohort for treatment and efficacy. Thus, we can combine all treatments together and compare these results to the control, normal blood. Treatment by any means had a net overall reduction in thrombosis that was statistically significant. RPA was prevented in 22/28 (79%, $p<0.05$) If RPA did not occur, an average deposition rate during the duration of experimentation was used. Treatment significantly slowed accumulation rates to $0.9 \pm 2.6\ \mu m^3 \mu m^{-2} min^{-1}$ (n=28) Untreated blood had RPA rates of $4.7 \pm 2.6\ \mu m^3 \mu m^{-2} min^{-1}$ (n=22, $p<0.05$). This indicates that treatment is globally better than nothing, but serving as a reminder that patient-specific treatment would be a more effective course of action. Activation blockade by the different agents work by different mechanisms and pathways. Blockade of $P2Y_{12}$ receptors and treatment with ASA were not effective against RPA in all blood samples, consistent with clinical findings.[1, 13, 15] Similarly, we found that certain blood may be resistant to eptifibatide while being responsive to abciximab. In comparison, the clinical data on the differences between these two therapies are not conclusive.[5]

The blockade of large scale thrombosis by activation in our flow system may appear to contradict findings by Ruggeri *et al* for very high shear conditions.[22] There

are differences which may be important between these assays. While Ruggeri utilized platelet-surface deposition measurements, our experiment evaluated endpoints of thickness, volume and accumulation rates which would be due to platelet-platelet accumulation. There was not always a correlation between significance found for volume and thickness, potentially due to any measurement errors being squared. Further, as the therapies tested may slow accumulation without preventing it, the maximum thickness deposited may be the most clinically relevant endpoint measured. The platelet-platelet accumulation may require activation and stabilization of mural platelets for very high shear attachment by released vWF.[26] Our thrombosis persisted for ten minutes after initial adhesion, requiring stabilization by activated $\alpha_{IIb}\beta_3$ that would persist long after the short GPIb binding observed in the Ruggeri very high shear study.[22] Thirdly, our initial shear rate was 3,500 s^{-1} versus the 10,000s^{-1} used by Ruggeri *et al.* The lower initial shear may require more activation than very high shear conditions.

The susceptibility of blood to antiplatelet agents appears to be patient specific. We evaluated only one 10x dose or described in vitro doses for blocking of each of these drugs. We did not perform a dose-response curve. The testing of blood with a variety of pharmaceutical agents may be important in establishing patient-specific anti-platelet therapy instead of giving all patients the same anti-platelet drug and dosage.

Our human, single pass, syringe pump experiment has several limitations. The first is that it requires 30mLs of blood for each trial. As only 500mLs can be taken from a patient within 6 weeks, this would allow for approximately 16 different therapy regimens to be tested. Depending on the patient's platelet response, 16 permutations of therapies could potentially prove limiting. Further, there is no physiologic pulsatility in the system, which could be added in future testing. The addition of pulsatility has unclear implications on deposition rates.[23, 28] Another limitation of the system

is the use of heparin which may impair platelet deposition rates.[14] While it does not prevent RPA, it may decrease the actual rate of accumulation.

4.0.18 Conclusion

An in vitro hemodynamic system of high shear thrombosis is adapted to test patient-specific responses to a variety of anti-platelet therapies in an effort to develop more effective patient-specific treatments.

PGE_1, 2-MeSAMPS, ASA, abciximab and eptifibatide were evaluated for the prevention of RPA in a collagen coated stenosis at shear rates $>3{,}500s^{-1}$. The effectiveness of each pharmaceutical in reducing the amount and rate of thrombosis was different. Blockade of activation, mediated by PGE_1 was most effective in our high shear system while 2-MeSAMPS and ASA were less effective at preventing thrombus growth and RPA. $\alpha_{IIb}\beta_3$ blockade via abciximab prevented RPA and permanent thrombus accumulation in all tested blood whereas eptifibatide was less effective. Further, we note in one patient that ASA was effective one month, but not the next month. The time variation suggests that patients may need to be tested periodically to accommodate physiological changes in platelet behavior.

Overall, inhibition of $\alpha_{IIb}\beta_3$ using abciximab and blocking platelet activation using PGE_1 in human blood effectively prevented thrombosis in this high shear, stenosis model.

4.0.19 References

REFERENCES

[1] Alberts, M. J., Bergman, D. L., Molner, E., Jovanovic, B. D., Ushiwata, I., and Teruya, J., "Antiplatelet effect of aspirin in patients with cerebrovascular disease," *Stroke*, vol. 35, no. 1, pp. 175–178, 2004.

[2] Andre, P., LaRocca, T., Delaney, S. M., Lin, P. H., Vincent, D., Sinha, U., Conley, P. B., and Phillips, D. R., "Anticoagulants (thrombin inhibitors) and aspirin synergize with P2Y_{12} receptor antagonism in thrombosis," *Circulation*, vol. 108, no. 21, pp. 2697–2703, 2003.

[3] Bark, David Ku, D., "Wall shear over high degree stenoses pertinent to atherothrombosis," *Journal of Biomechanics*, vol. 43, pp. 2970–2977, 2010.

[4] Bassler, N., Loeffler, C., Mangin, P., Yuan, Y., Schwarz, M., Hagemeyer, C. E., Eisenhardt, S. U., Ahrens, I., Bode, C., Jackson, S. P., and Peter, K., "A mechanistic model for paradoxical platelet activation by ligand-mimetic (gpIIb/IIIa) antagonists," *Arteriosclerosis, Thrombosis, and Vascular Biology*, vol. 27, no. 3, pp. E9–E15, 2007.

[5] Batchelor, W. B., Tolleson, T. R., Huang, Y., Larsen, R. L., Mantell, R. M., Dillard, P., Davidian, M., Zhang, D., Cantor, W. J., Sketch, M. H., Ohman, E. M., Zidar, J. P., Gretler, D., DiBattiste, P. M., Tcheng, J. E., Califf, R. M., and Harrington, R. A., "Randomized comparison of platelet inhibition with abciximab, tirofiban and eptifibatide during percutaneous coronary intervention in acute coronary syndromes," *Circulation*, vol. 106, no. 12, pp. 1470–1476, 2002.

[6] Belval, T. and Hellums, J., "Analysis of shear-induced platelet aggregation with population balance mathematics," *Biophysical Journal*, vol. 50, no. 3, pp. 479 – 487, 1986.

[7] Biondi-Zoccai, G. G., Valgimigli, M., Sheiban, I., Margheri, M., Marzocchi, A., Prati, F., Vischi, M., Lettieri, C., Violini, R., Sardella, G., Stabile, A., Clementi, F., Romeo, F., Colombo, A., and Sangiorgi, G., "A randomized trial comparing eptifibatide vs. placebo in patients with diffuse coronary artery disease undergoing drug-eluting stent implantation: design of the integrilin plus stenting to avoid myocardial necrosis trial," *Journal of Cardiovascular Medicine*, vol. 9, no. 9, pp. 957–962 10.2459/JCM.0b013e3282ffd3a6, 2008.

[8] CLARK, R. B., FRIEDMAN, J., JOHNSON, J. A., and KUNKEL, M. W., "β-adrenergic receptor desensitization of wild-type but not cyc lymphoma cells unmasked by submillimolar mg^{2+}," *FASEB Journal*, vol. 1, pp. 289–297, 1987.

[9] Coller, B., "Blockade of platelet gpIIb/IIIa receptors as an antithrombotic strategy," *Circulation*, vol. 92, pp. 2373–2380, 1995.

[10] Davies, M. J. and Thomas, A. C., *Plaque fissuring-the cause of acute myocardial infarction, sudden ischaemic death, and crescendo angina*, vol. 53. London, ROYAUME-UNI: BMJ Publishing Group, 1985.

[11] Diener, H.-C., Ringleb, P. A., and Savi, P., "Clopidogrel for the secondary prevention of stroke," *Expert Opinion on Pharmacotherapy*, vol. 6, no. 5, pp. 755–764, 2005.

[12] Fuster, V., Badimon, L., Cohen, M., Ambrose, J. A., Badimon, J. J., and Chesebro, J., "Insights into the pathogenesis of acute ischemic syndromes," *Circulation*, vol. 77, no. 6, pp. 1213–1220, 1988.

[13] Grundmann, K., Jaschonek, K., Kleine, B., Dichgans, J., and Topka, H., "Aspirin non-responder status in patients with recurrent cerebral ischemic attacks," *Journal of Neurology*, vol. 250, pp. 63 – 66, 2003.

[14] Heras, M., Chesebro, J., Penny, W., Bailey, K., Badimon, L., and Fuster, V., "Effects of thrombin inhibition on the development of acute platelet-thrombus deposition during angioplasty in pigs heparin versus recombinant hirudin, a specific thrombin inhibitor," *Circulation*, vol. 79, pp. 657–665, 1989.

[15] Labarthe, B., Throux, P., Angio, M., and Ghitescu, M., "Matching the evaluation of the clinical efficacy of clopidogrel to platelet function tests relevant to the biological properties of the drug," *Journal of Americal College of Cardiology*, vol. 46, pp. 638 – 645, 2005.

[16] Lorenz, R. L., Weber, M., Kotzur, J., Theisen, K., Schacky, C. V., Meister, W., Reichardt, B., and Weber, P. C., "Improved aortocoronary bypass patency by low-dose aspirin (100 mg daily)," *The Lancet*, vol. 323, no. 8389, pp. 1261–1264, 1984.

[17] McDonald, J., Ali, M., Morgan, E., Townsend, E., and Cooper, J., "Thromboxane synthesis by sources other than platelets in association with complement-induced pulmonary leukostasis and pulmonary hypertension in sheep," *Circlation Research*, vol. 52, pp. 1–6, 1983.

[18] Mendolicchio, G. L., Zavalloni, D., Bacci, M., Corrada, E., Marconi, M., Lodigiani, C., Presbitero, P., Rota, L., and Ruggeri, Z. M.,

"Variable effect of P2Y_{12} inhibition on platelet thrombus volume in flowing blood," *Journal of Thrombosis and Haemostasis*, vol. 9, no. 2, pp. 373–382, 2011.

[19] Mustonen, P. and Lassila, R., "Epinephrine augments platelet recruitment to immobilized collagen in flowing blood–evidence for a von willebrand factor-mediated mechanism," *Thrombosis and haemostasis*, vol. 75, no. 1, pp. 175–81, 1996.

[20] Nurden, A. T., Poujol, C., Durrieu-Jais, C., and Nurden, P., "Platelet glycoprotein IIb/IIIa inhibitors : Basic and clinical aspects," *Arteriosclerosis, Thrombosis, And Vascular Biology*, vol. 19, no. 12, pp. 2835–2840, 1999.

[21] Para, A., Bark, D., Lin, A., and Ku, D., "Rapid platelet accumulation leading to thrombotic occlusion," *Annals Of Biomedical Engineering*, vol. 39, pp. 1961–1971, 2011.

[22] Ruggeri, Z. M., Orje, J. N., Habermann, R., Federici, A. B., and Reininger, A. J., "Activation-independent platelet adhesion and aggregation under elevated shear stress," *Blood*, vol. 108, no. 6, pp. 1903–1910, 2006.

[23] van Breugel, H., Sixma, J., and Heethaar, R., "Effects of flow pulsatility on platelet adhesion to subendothelium," *Arteriosclerosis, Thrombosis, and Vascular Biology*, vol. 8, no. 3, pp. 332–335, 1988.

[24] Van Werkum, J. W., Van Der Stelt, C. A. K., Seesing, T. H., Hackeng, C. M., and Ten Berg, J. M., "A head-to-head comparison between the VerifyNow® P2Y_{12} assay and light transmittance aggregometry for monitoring the individual platelet response to clopidogrel in patients undergoing elective percutaneous coronary intervention," *Journal of Thrombosis and Haemostasis*, vol. 4, no. 11, pp. 2516–2518, 2006.

[25] Vane, J. and Botting, R., "Inflammation and the mechanism of action of anti-inflammatory drugs," *The FASEB Journal*, vol. 1, no. 2, pp. 89–96, 1987.

[26] Wellings, P. and Ku, D., "Mechanisms of platelet capture under very high shear," *Cardiovascular Engineering and Technology*, vol. Online, 2012.

[27] Wiviott, S. D., Antman, E. M., Winters, K. J., Weerakkody, G., Murphy, S. A., Behounek, B. D., Carney, R. J., Lazzam, C., McKay, R. G., McCabe, C. H., Braunwald, E., and for the JUMBO-TIMI 26 Investigators, I., "Randomized comparison of prasugrel (CS-747, LY640315), a novel thienopyridine P2Y_{12} antagonist, with clopidogrel in percutaneous coronary intervention," *Circulation*, vol. 111, no. 25, pp. 3366–3373, 2005.

[28] Zhao, X. M., Wu, Y. P., Cai, H. X., Wei, R., Lisman, T., Han, J. J., Xia, Z. L., and de Groot, P. G., "The influence of the pulsatility of the blood flow on the extent of platelet adhesion," *Thrombosis Research*, vol. 121, no. 6, pp. 821 – 825, 2008.

CHAPTER V

THROMBOSIS IS INCREASED BY EXCESS AMOUNTS OF VON WILLEBRAND FACTOR AT VERY HIGH SHEAR RATES

5.0.20 Introduction

High shear occlusive thrombosis occurs in two stages. Initial adhesion constitutes the attachment of platelets on the damaged subendothelium and is followed by the subsequent accumulation of platelets onto platelets previously adhered to the surface. If the subsequent platelet-to-platelet thrombosis is massive (millions of platelets), then we refer to this large thrombus growth as Rapid Platelet Accumulation (RPA).[5] RPA occurs when volume accumulation rates exceed 1.6 $\mu m^3 \mu m^{-2} min^{-1}$.[5] Following platelet activation, Glycoprotein IIb/IIIa ($\alpha_{IIb}\beta_3$) can contribute to the formation of mural thrombus under high shear conditions.[6, 7, 14]

vWF is a multimeric protein that allows for the attachment of platelets to the vessel wall following injury as well as platelet-to-platelet interaction necessary for occlusion.[7, 10] vWF is present after platelet activation on the surface of thrombus formation with a 50x higher concentration than in plasma.[2, 15] vWF is shear dependent, elongating at shear rates greater than 6,000s^{-1}.[9] In a patient study of 9,758 men and women between the ages of 50-59, there was a three-fold increase in ischemic heart disease in subjects who had high vWF levels in the top quartile when compared to those in the bottom quartile.[3, 4] This increase in risk for ischemic heart disease coincided with approximately a 2x increase in vWF levels on average.[4]

Conversely, patients who are suffering from von Willebrand Disease (vWD) and have a deficiency of vWF, tend to have longer bleeding times.[8] Bleeding times can

be (partially) corrected by the addition of purified vWF in patients with VWD, suggesting that thrombus deposition may be influenced by vWF concentration.[11]

It is the goal of this study to determine if excessive amounts of vWF in whole, human blood will increase thrombus deposition under high (3,500s^{-1}) and very high shear stress (10,000s^{-1}). Our hypothesis is that addition of vWF to whole blood or the surface of thrombus formation will increase thrombus thickness and increase RPA rates.

5.0.21 Experimental Design and Methods

5.0.21.1 Syringe Pump Apparatus

A single pass, syringe pump fed, *in-vitro* system was created in which thrombus formation could be viewed under a microscope (Figure 33). Whole, human blood is perfused though at either a shear rate of 3,500 s^{-1} (just above 2,000s^{-1}, the lower level of shear induced platelet activation) or 10,000 s^{-1}, above the level of vWF elongation. [1, 9]

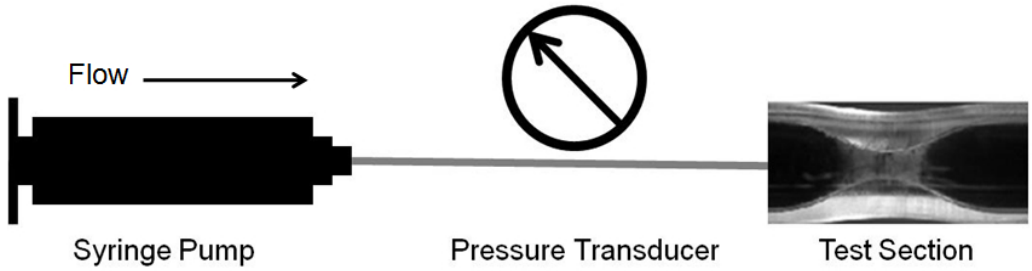

Figure 33: Whole blood is perfused from a syringe pump, past a pressure transducer and through a pyrex, collagen coated test section which is placed under a microscope. A high resolution camera takes images in real time through the microscope.

The test section through which the blood flows was created and collagen coated as previously described.[5] The original inner diameter of the tube is 1.5mm and the severity of stenosis used during experimentation range from 80% to 93%. Flow rate

for each experiment was prescribed using Poiseuille assumptions.

5.0.21.2 Whole Human Blood

Whole, human blood was drawn at the Georgia Institute of Technology's Health Center from consented subjects according to IRB protocol H06190. Blood was drawn directly into syringes containing 3.5 USP units/mL heparin (Sigma-Aldrich, St Louis, MO). This amount of heparin was chosen based on previous porcine experiments to prevent clotting during transport while still allowing thrombus formation during experimentation.[5] All blood was used within 8 hours of harvest. During the flow experiments, excess blood was placed on an LS orbital mixer (Labnet, Woodbridge, NJ) to prevent blood separation.

5.0.21.3 Experimental Design

All experiments were conducted in multiple steps utilizing the same stenosis. In the first step, up to 10mLs of untreated blood was perfused through a stenosis until visible initial deposition is observed. This allows for platelets to initially adhere to the surface. The second step is determined by the type of experiment run (see below).

vWf Enriched Blood

For the second step in vWF saturated blood, 35IU of vWF from Humate-P® (CSL Behring, LLC, King of Prussia, PA) and saline (for a total added volume of 1mL) was added to 10mLs of whole blood and mixed using a rotating motion. Humate-P® is a homogenized, purified plasma vWF product which contains factor VIII.[16] 1 IU is the activity of vWF in 1mL of healthy plasma.[11] Through experimentation (not shown here), it was determined that there were approximately 3.5mLs of plasma in 10mLs of whole blood. A 35IU dose of vWF would therefore increase the concentration of vWF to 8.6x. Blood was used immediately for experimentation.

vWF Coated Surface

For the second step of a vWF coated surface, 35 IU of vWF from Humate-P®

(CSL Behring, LLC, King of Prussia, PA) were incubated in the stenosis following initial visible adhesion for 1 hour at room temperature, similar to methods previously described by Sixma.[11] Up to 10mLs of untreated, whole blood was then perfused over the surface.

5.0.21.4 Images

The test section was photographed through a 2x microscope objective using a high resolution digital CCD camera (Pixelfly, Keleim, Germany) connected directly to the Zeiss Stemi 2000-C (Zeiss, Jena, Germany) stereo microscope. The camera had a corresponding lens which had a 0.5x magnification, yielding a final magnification of 1x. Images were taken sequentially in real time and post processed using CamWare (Cooke Corporation, Romulus, MI) and Photoshop (Adobe, San Jose, CA).

5.0.21.5 Additional Thickness/Volume/Accumulation Rates

Thickness of platelet accumulation was measured as the difference between the stenosis inner diameter and the inner diameter of the thrombus protruding into the lumen. The increase in thickness is determined by subtracting the initial thickness at the beginning of each new 10mLs perfused. The maximum thickness reported was taken at a single location in the stenosis at the time when accumulation was greatest. Average thickness was calculated for each set of experiments by averaging the maximum thickness values over each position a distance $0.19 - 0.24$mm apart. The thickness reported for each stenosis in each set of experiments is from the time of maximum thickness during experimentation.

Volume was calculated from thickness using the equation below:

$$Volume(cm^3) = \sum_{i=1}^{n} (\frac{(D_{O,i}^2 - D_{I,i}^2}{4})\pi L \tag{6}$$

where D_O was the diameter of the inside of the glass stenosis and the inner diameter, D_I, was the diameter created by measuring the top of the thrombus growing

from the bottom of the tube and the bottom of the thrombus growing from the top of the tube. By summing the cylinders, the volume was then integrated along the length of the thrombus, L, which was divided into equal segments which ranged in length for each set of images from $0.19 - 0.24$mm.

Surface area used was the total surface area that thrombus deposited on during experimentation and was calculated as:

$$SurfaceArea(cm^2) = \sum D_O \pi L \tag{7}$$

Where D_O is the inner diameter of the stenosis for each segment on which thrombus deposited on during experimentation.

Accumulation rates were calculated using the equation below:

$$AccumulationRate(\mu m^3 \mu m^{-2} min^{-1}) = (\frac{Volume/Time}{SurfaceArea}) \tag{8}$$

Volume/Time is a regression of the volume over at least three consecutive time points, with the three time points encompassing a minimum of 2 minutes of the volume growth of thrombus formation. For all experiments, the maximum accumulation rate was calculated using at least three points. If the maximum did not exceed RPA, or an accumulation rate $\geq 1.6\ \mu m^3 \mu m^{-2} min^{-1}$, experiments were not included in this study.

5.0.21.6 Embolus

Embolus was defined as a rapid increase in pressure and a sudden presence in the tube. Embolus intrusion into the stenosis was excluded from thrombus volume deposition measurements regardless of whether it was a transient or permanent event.

5.0.21.7 Statistics

Experiments were analyzed using a student's t-test where statistical significance is defined as $p<0.05$.

5.0.22 Results

We compared thrombus formation with i) normal whole blood, ii) whole blood with added Humate-P, and iii) whole blood over surfaces of Humate-P that was additionally deposited on the surface. As we were focusing on Phase II of massive thrombosis, 10 ml of normal blood was perfused through each test section prior to the study conditions to lay down an initial layer of platelets on the raw collagen surface. Whole blood was perfused at two shear rates, 3,500s^{-1} (high shear) and 10,000s^{-1} (very high shear). The endpoints for thrombus formation were thrombus thickness, thrombus volume, and rate of accumulation.

The thrombus thickness in the 6 different test sections with vWF enriched blood is shown in Figure 34 A for a shear rate of 3,500 s^{-1}. The average thickness for these test sections is shown in Figure 34 B. The additional 1mL volume of vWF solution may affect the amount of thrombosis. As a control, Figure 34 C illustrates the thickness of 4 experiments where an additional 1 ml of saline was added to the blood. Note that the individual and average thrombus thicknesses were the same with the added saline. There were no significant differences between the average thicknesses for samples with vWF added to blood and the control with saline (Figure 34, B and D).

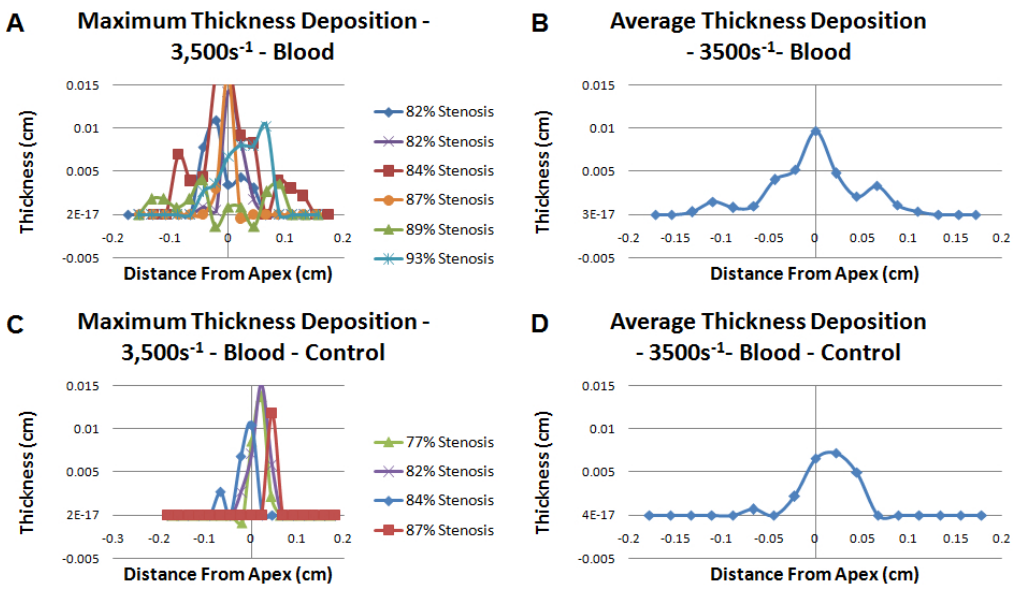

Figure 34: Thicknesses for each sample were measured in the stenosis for vWF enriched blood (A). Average thicknesses was also calculated for vWF enriched blood samples (B). Thickness was also measured for control blood in which saline was added (C). Average thickness for the control was also calculated (D). All started at an initial shear rate of 3,500s^{-1}.

The second study condition was to deposit excessive amounts of vWF directly on the thrombus surface. Figure 35 A illustrates the thrombus thickness results with excess vWF on the surface. Figure 35 C shows the normal control with saline on the surface. No significant differences were measured between the average thicknesses at the apex between the vWF surface (Figure 35 B) and the control with saline (Figure 35 D). Likewise, no differences were seen with the average thickness by position (Figure 35 B and Figure 35 D).

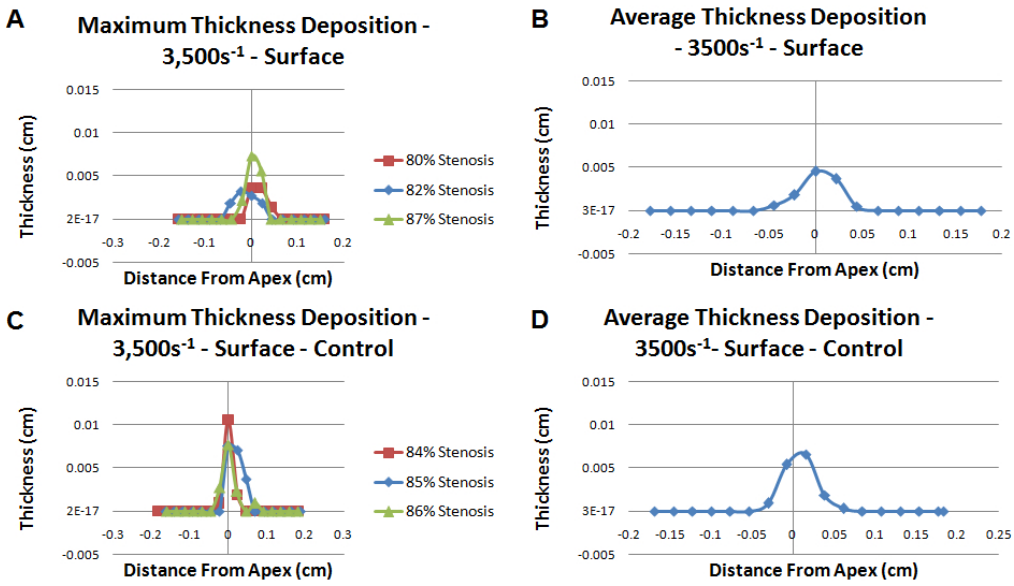

Figure 35: Thicknesses for each sample were measured in the stenosis with a vWF enriched surface (A). Average thicknesses were calculated for vWF enriched surface samples (B). Thickness was also measured for the control in which saline was added to the surface (C). The average for the control is also shown (D). All flow experiments started at an initial shear rate of 3,500s^{-1}.

5.0.22.1 Addition of vWF to blood increased thickness at the apex over adding vWF to the surface at 3,500s^{-1}.

A significantly greater maximum thickness was measured for samples in which vWF was added directly to the blood (n=6) than those in which vWF was added directly to the surface (n=3, $p<0.05$, Figure 36).

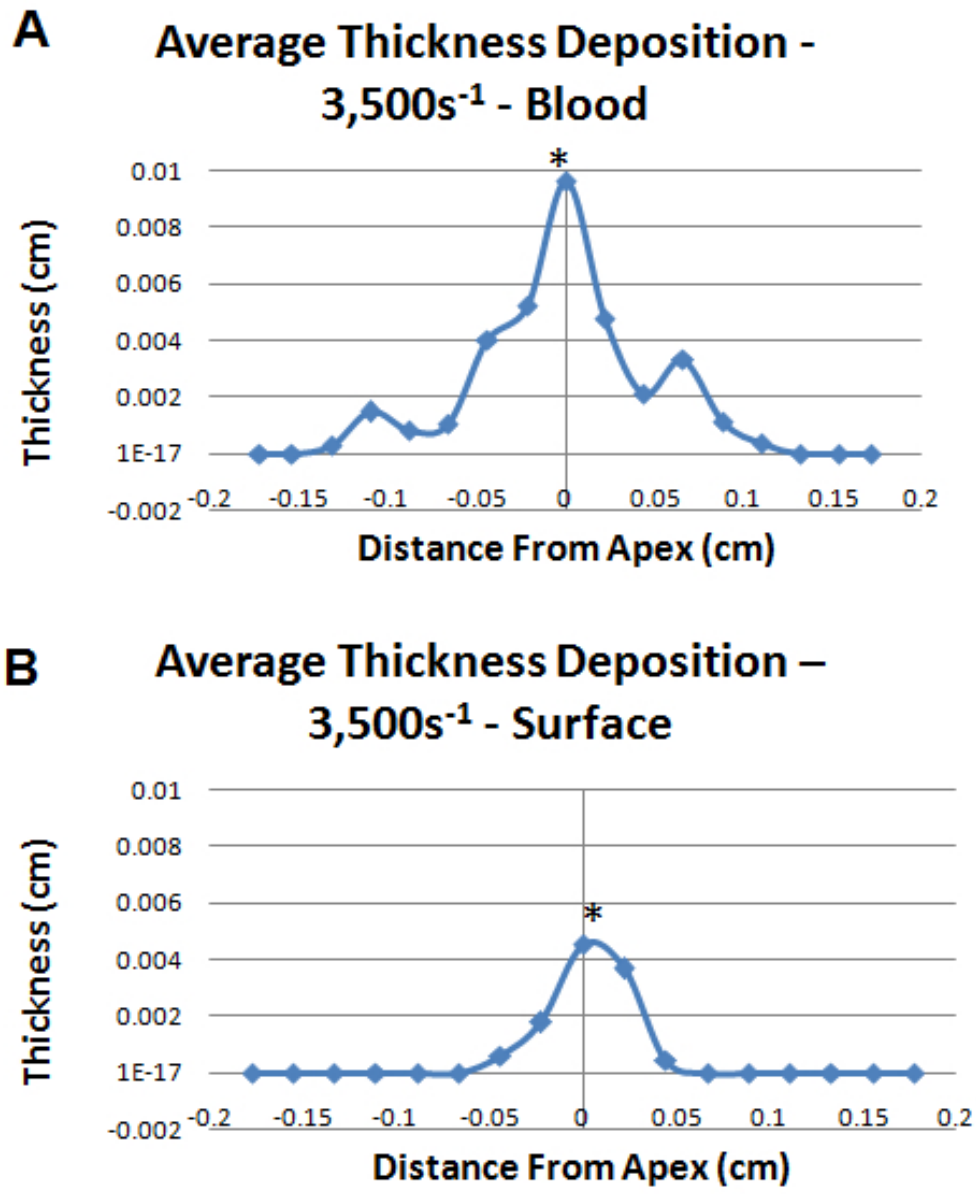

Figure 36: Thrombosis thickness formed at high shear rates (3,500s^{-1}), with vWF enriched Blood (above) and vWF enriched surfaces (Below) There is a significantly greater average thickness in vWF enriched blood (n=6) versus a vWF enriched surfaces (n=3, $p<0.05$).

Thrombus volume was also calculated for the treatments and their controls at 3,500s^{-1} (Figure 37). Maximum volume was $35 \pm 26 * 10^{-6} cm^3$ (n=6, Figure 37 A)

for samples in which vWF was added directly to the blood and 22 $\pm$ 3.3 $*10^{-6}cm^3$ (n=4, Figure 37 B) for the controls containing saline. In the samples with the coated surface, the maximum volume was 10 $\pm$ 0.3 $*10^{-6}cm^3$ (n=3) for the vWF coated surface (Figure 37 C) and 12 $\pm$ 4.6 $*10^{-6}cm^3$ (n=3) for the saline coated control (Figure 37 D).

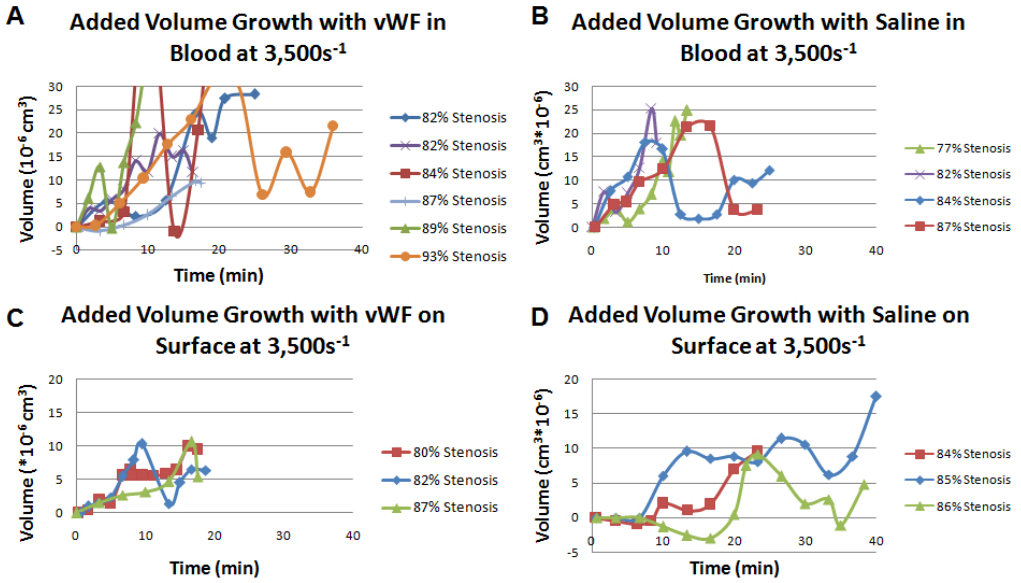

Figure 37: Volume growth of thrombus over time at 3,500s^{-1} for individual experiments. (A) Blood enriched with vWF, (B) saline enriched blood, (C) Surface enriched with vWF, (D) and the saline surface controls.

5.0.22.2 Increasing the vWF concentration in blood at 10,000s^{-1} increases the maximum thickness deposited

Following vWF addition into whole blood, thickness of thrombus in the stenosis was measured at an initial shear rate of 10,000s^{-1} (Figure 38 A). Thickness was measured for the control to which saline was added rather than vWF (Figure 38 C). Blood which had been enriched with vWF had a significantly greater average thickness (n=5, Figure 38 B) than its control in which saline was added to blood (n=3, Figure 38 D, $p<0.05$).

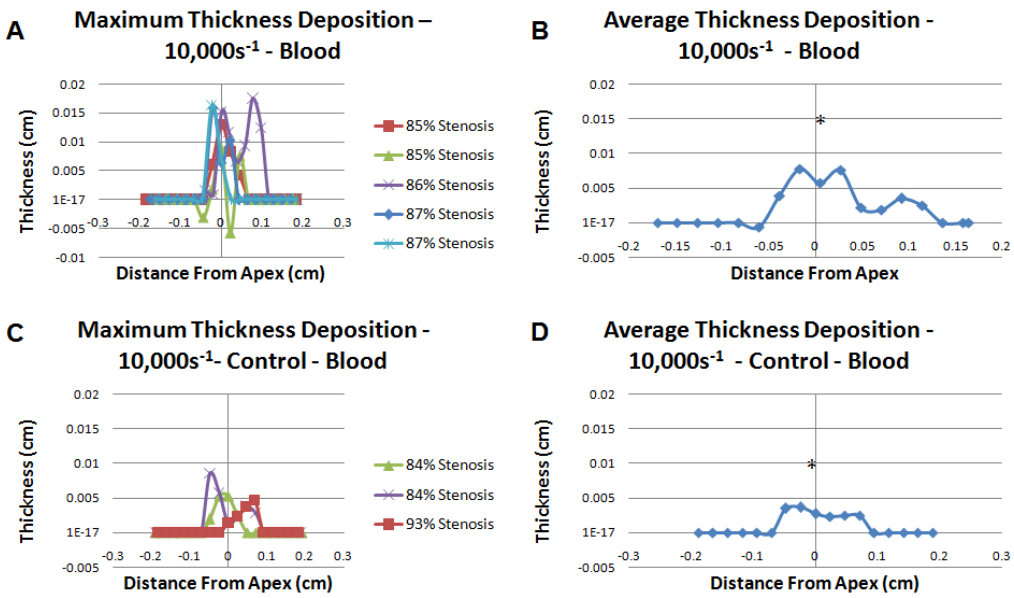

Figure 38: Thrombus thicknesses for vWF enriched blood at an initial shear rate of 10,000s^{-1}. (A) Individual thickness. (B) Average thickness. (C) Thickness for control blood in which saline was added. (D) Average thickness for saline control. The average thickness with vWF enriched blood (n=5) was greater than the saline control (n=3, $p<0.05$).

Thickness of thrombus formation at very high shear was measured for the surface coating experiments in which vWF was incubated in the stenosis (Figure 38 A) and its saline control (Figure 39 C). No significant differences were found between thicknesses at the apex between the vWF surface (Figure 39 B) and the control (Figure 39 D).

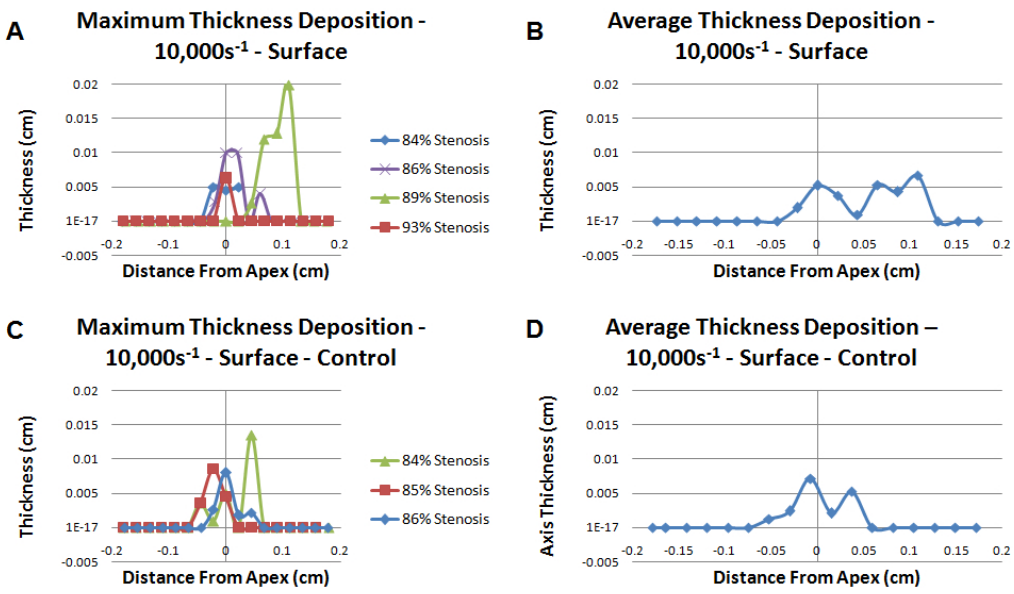

Figure 39: Thrombosis thicknesses at a shear rate of 10,000s^{-1}: (A) vWF enriched surface. (B) Average thickness for the treated samples . (C) Thickness for the control in which saline was added to the surface. (D) Average thickness for the control.

No significant differences were found between average thicknesses for vWF enriched blood at shear rates of 3,500s^{-1} versus vWF enriched blood at 10,000s^{-1} (p=0.971).

The average thickness for vWF treated blood and the vWF treated surface were compared (Figure 40), showing no significant difference between the two at shear rates of 10,000s^{-1} (p>0.05). Although, when compared to the vWF treated surface at 3,500s^{-1} (n=3), there was suggestive evidence indicating that that the higher shear rate of 10,000s^{-1} yielded a thicker deposition (n=4, p=0.159).

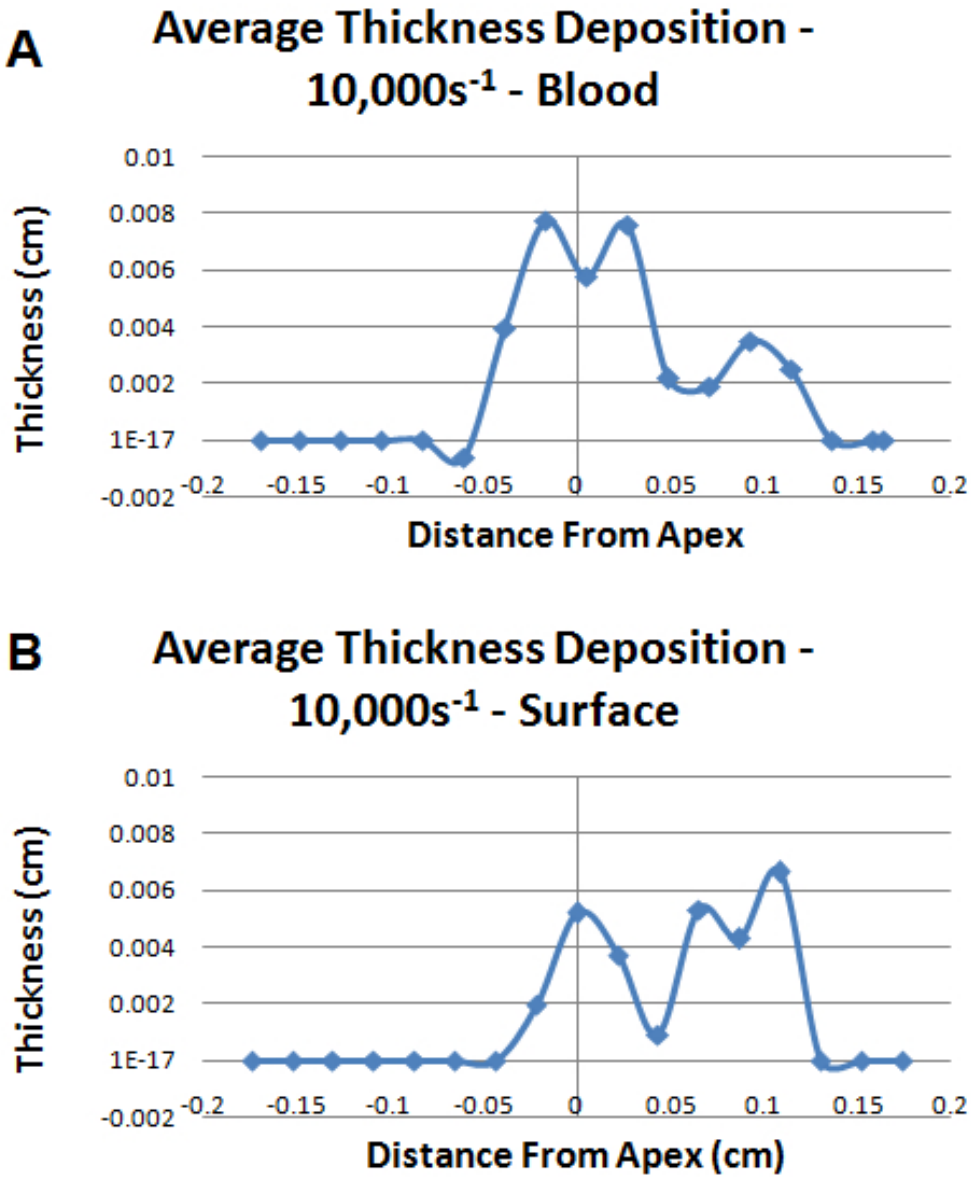

Figure 40: Thrombus average thickness at very high shear rates (10,000s^{-1}) from vWF enriched blood (above) and vWF enriched surface (below). There was no significant difference in average thickness on a surface coated with vWF versus the control surface coated with saline (p=0.525).

Maximum volume was also calculated for the treatments and their controls at 3,500s^{-1} (Figure 41). Maximum volume was 25 $\pm$ 20 $*10^{-6}cm^3$ (n=5, Figure 41 A)

for samples in which vWF was added directly to the blood and 16 ± 11 $*10^{-6}cm^3$ (n=3, Figure 41 B) in the controls with saline in the blood. In the samples with the coated surface, the maximum volume was 30 ± 40 $*10^{-6}cm^3$ (n=4) for the vWF coated surface (Figure 41 C) and 10 ± 3.9 $*10^{-6}cm^3$ (n=3) for the saline coated control (Figure 41 D).

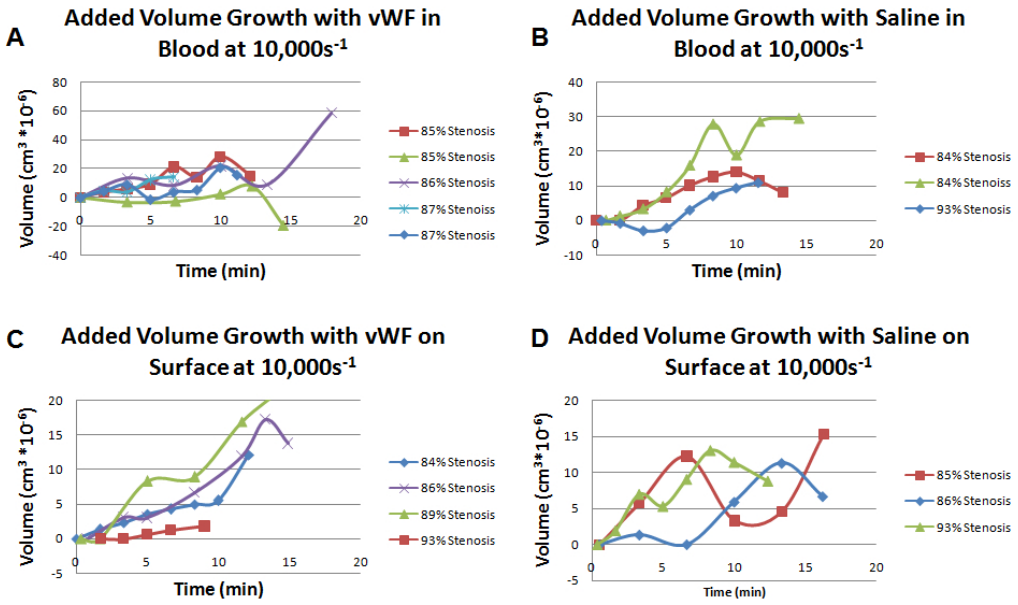

Figure 41: Volume over time is shown for vWF enriched blood (A), saline enriched blood (B), vWF enriched surface (C) and the saline enriched surface (D) at 10,000s^{-1}.

5.0.22.3 Increasing the vWF concentration in blood at 10,000s^{-1} may increase the max thrombus/surface area coverage.

A maximum volume of thrombus over the entire stenosis at any point in time was obtained from the volume plots. The maximum volume per surface area was calculated for all of the treatments and their controls (Table 4). The maximum volume of thrombus per surface area at 10,000s^{-1} for blood enhanced vWF was 3.16 ± 1.50 cm (n=5). The maximum volume of thrombus per surface area at 10,000s^{-1} for the saline control was 1.44 ± 0.40 cm (n=3). This maximum was two times larger, but

failed to reach statistical significance (p=0.073).

Table 4: The maximum volumes are shown in this table for all experiments and saline controls. The p values for the vWF enhanced blood just missed statistical significance.

	vWF Volume/SA ($*10^{-3}$cm)	Control Vol/SA ($*10^{-3}$cm)
Blood 3,500s^{-1}	1.95 ± 0.70	0.26 ± 0.66
Surface 3,500s^{-1}	1.33 ± 0.72	1.41 ± 0.39
Blood 10,000s^{-1}	3.16 ± 1.50	1.44 ± 0.40
Surface 10,000s^{-1}	2.19 ± 1.90	1.57 ± 0.71

Thrombus thickness increases may stem from an increase in the rate of accumulation. The calculated rates of accumulation were high (RPA) in every case, shown in Table 5. At very high shear rates, the vWF enriched blood exhibited a higher average rate, but failed to reach statistical significance. There is suggestive evidence that adding vWF to blood at 10,000s^{-1}(n=5) may increase RPA more than adding vWF to the surface at 10,000s^{-1} (n=4, p=0.153), vWF to the blood at 3,500s^{-1} (n=6, p=0.122) and vWF to the blood at 3,500s^{-1} (n=3, p=0.107).

Table 5: The RPA rates for all of the vWF experiments and their controls are shown above.

	vWF RPA ($\mu m^3 \mu m^{-2} min^{-1}$)	Control RPA ($\mu m^3 \mu m^{-2} min^{-1}$)
Blood 3,500s^{-1}	2.09 ± 0.36	3.61 ± 1.53
Surface 3,500s^{-1}	1.89 ± 0.20	2.24 ± 0.79
Blood 10,000s^{-1}	5.42 ± 3.80	2.94 ± 0.77
Surface 10,000s^{-1}	2.35 ± 0.78	2.97 ± 0.53

In general, the experiments exhibited a large range of accumulation rates fom 1.6 to 10 μm^3 μm^{-2} min^{-1}. The RPA rates for all treatment types are shown below as compared to human untreated blood at 3,500s^{-1} (n=21, Figure 42).

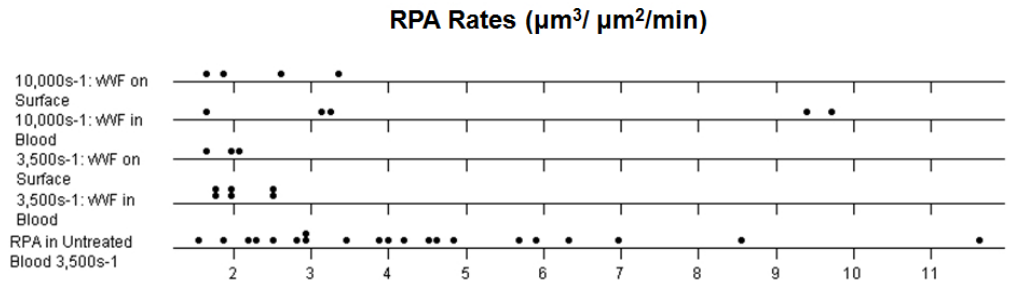

Figure 42: The RPA rates for all vWF experiments are shown above as compared with previous experiments with untreated blood at 3,500s^{-1} (n=21). illustrating the wide range of accumulation rates seen in individuals. Note that the entire range of accumulation rates is much greater than the initial deposition rates that average 0.8 ± 1.0 μm^3 μm^{-2} min^{-1} (n=21)

5.0.23 Discussion

Our experiments show that whole blood enriched with vWF at 8.6x concentrations increases thrombus thickness deposition at very high shear stress. The vWF enriched blood created larger thrombus thickness compared with vWF deposited on the surface. While some experiments showed higher RPA rates with blood enriched vWF, the group as a whole did not reach the level of statistical significance. The in vitro increase in thrombus thickness from high concentrations of vWF at very high shear rates agrees with the clinical observation that high concentrations in blood levels of vWF are associated with a 3 fold increase in ischemic heart disease.[3]

It is possible that only suggestive evidence indicates that RPA is increased as thrombus growth may be limited by the arrival of platelets at the wall and not vWF once normal vWF concentration levels have been reached.[17] Studies done by Sixma where a normal amount of vWF was added to vWD blood show that the addition of vWF increased thrombus formation, although it did not bring it back to normal levels.[11] Ruggeri notes that additional soluble vWF enhances platelet adhesion and rolling at higher shear rates on a vWF surface consistent with pathologic conditions.[7] Excessive vWF in blood has not been tested. Similarly, a 8.6x concentration may not be a sufficient concentration to influence thrombus formation beyond its normal levels, potentially requiring a 50x concentration for a measurable change.[2, 15] There may be a threshold for vWF where, once normal levels are met, a significantly larger (potentially 50x) local concentration is required to push platelet deposition beyond their normal rate at very high shear rates. Alternaatively, vWF may not be the rate limiting protein for RPA once normal concentrations of vWF are attained.

Mere incubation of vWF in the test section may not bind the vWF to the surface (immobilization). The vWF added to the surface may have washed off with the first few mLs of blood perfusion. The vWF may also not have elongated, due to being

applied under static conditions, and retained its globular form during experimentation. This would limit vWF's ability to bind due to domains being sterically covered in the globular formation.[7, 10]

We did not correct our results for subject-related factors, such as patient habits (e.g. smoking, NSAID use, etc) or test for diseases such as von Willebrand Disease which would alter platelet accumulation. Further, there may be a large interpersonal variation which was not accounted for in this study. Our in vitro blood perfusion system has several limitations. The studies are run at room temperature and not at 37^{o}C, which may decrease platelet deposition rates.[12] The temperature may be corrected for in the future by using a heating coil to surround the syringe during perfusion. Further, we did not impose arterial pulsatility. The literature is unclear about the effects of pulsatility on platelet deposition.[13, 18]

5.0.24 Conclusion

This study finds that an increase in concentration of vWF in the blood increases thrombus thickness at pathologic shear rates (10,000s^{-1}). Blood enhanced vWF also increases thickness over surface vWF at 3500s^{-1}. The increase in thrombus thickness with higher concentrations of vWF may be important for patients with stenotic atherosclerotic lesions with very high shear rates. Local concentrations of vWF from the blood or from local release by platelets or damaged endothelial cells may trigger a large thrombus growth instead of a benign platelet coating.

5.0.25 References

REFERENCES

[1] Belval, T. and Hellums, J., "Analysis of shear-induced platelet aggregation with population balance mathematics," *Biophysical Journal*, vol. 50, no. 3, pp. 479 – 487, 1986.

[2] Harrison, P. and Cramer, E., "Platelet alpha-granules," *Blood Review*, vol. 7, pp. 52–62, 1993.

[3] Lippi, M. F. . G., "Von willebrand factor and thrombosis," *Annals of Hematology*, vol. 85, p. 415423, 2006.

[4] Morange, P., Simon, C., Alessi, M., Luc, G., Arveiler, D., Ferrieres, J., Amouyel, P., Evans, A., Ducimetiere, P., and Juhan-Vague, I., "Endothelial cell markers and the risk of coronary heart disease : The prospective epidemiological study of myocardial infarction (prime) study," *Circulation*, vol. 109, pp. 1343–1348, 2004.

[5] Para, A., Bark, D., Lin, A., and Ku, D., "Rapid platelet accumulation leading to thrombotic occlusion," *Annals Of Biomedical Engineering*, vol. 39, pp. 1961–1971, 2011.

[6] Peterson, D. M., Stathopoulos, N. A., Giorgio, T. D., Hellums, J. D., and Moake, J. L., "Shear-induced platelet aggregation requires von willebrand factor and platelet membrane glycoproteins Ib and IIb-IIIa," *Blood*, vol. 69, no. 2, pp. 625–628, 1987.

[7] Ruggeri, Z. M., "Von willebrand factor: Looking back and looking forward," *Thromb Haemost.*, vol. 98, pp. 55–62, 2007.

[8] Sadler, J. E., Mannucci, P. M., Berntorp, E., Bochkov, N., Boulyjenkov, V., Ginsburg, D., Meyer, D., Peake, I., Rodeghiero, F., and Srivastava, A., "Impact, diagnosis and treatment of von willebrand disease," *Thrombosis and Haemostasis*, vol. 84, pp. 160–174, 2000.

[9] Schneider, S. W., Nuschele, S., Wixforth, A., Gorzelanny, C., Alexander-Katz, A., Netz, R. R., and Schneider, M. F., "Shear-induced unfolding triggers adhesion of von willebrand factor fibers," *Proceedings of the National Academy of Sciences*, vol. 104, no. 19, pp. 7899–7903, 2007.

[10] Siedlecki, C. A., Lestini, B. J., Kottke-Marchant, K., Eppell, S. J., Wilson, D. L., and Marchant, R. E., "Shear-dependent changes in the three-dimensional structure of human von willebrand factor," *Blood*, vol. 88, pp. 2939–2950, 1996.

[11] Stel, H., Sakariassen, K., de Groot, P., van Mourik, J., and Sixma, J., "Von willebrand factor in the vessel wall mediates platelet adherence," *Blood*, vol. 65, pp. 85–90, 1985.

[12] Turitto, V. and Baumgartner, H., "Effect of temperature on platelet interaction with subendothelium exposed to flowing blood," *Haemostasis*, vol. 3, p. 224236, 1974.

[13] van Breugel, H., Sixma, J., and Heethaar, R., "Effects of flow pulsatility on platelet adhesion to subendothelium," *Arteriosclerosis, Thrombosis, and Vascular Biology*, vol. 8, no. 3, pp. 332–335, 1988.

[14] Weiss, H. J., Hawiger, J., Ruggeri, Z. M., Turtto, V. T., Thiagarajan, P., and Hoffmann, T., "Fibrinogen-independent platelet adhesion and

thrombus formation on subendothelium mediated by glycoprotein lIb-Illa complex at high shear rate," *Journal of Clinical Investigation*, vol. 83, pp. 288–297, 1989.

[15] Wellings, P. and Ku, D., "Mechanisms of platelet capture under very high shear," *Cardiovascular Engineering and Technology*, vol. Online, 2012.

[16] Wood, A. J., "Drug therapy," *New England Journal of Medicine*, vol. 351, pp. 683–94, 2004.

[17] Yeh, C., Calvez, A. C., and Eckstein, E. C., "An estimated shape function for drift in a platelet-transport model," *Biophysical Journal*, vol. 67, pp. 1252–1259, 1994.

[18] Zhao, X. M., Wu, Y. P., Cai, H. X., Wei, R., Lisman, T., Han, J. J., Xia, Z. L., and de Groot, P. G., "The influence of the pulsatility of the blood flow on the extent of platelet adhesion," *Thrombosis Research*, vol. 121, no. 6, pp. 821 – 825, 2008.

CHAPTER VI

DISCUSSION OF THESIS RESULTS AND FUTURE STUDIES

This dissertation explored the formation of intravascular thrombosis in a stenosis with high shear rates. Initially, thrombosis was created in vitro with a collagen-coated stenosis perfused with whole porcine blood (Chapter 2). We observed three distinct phases: Phase I of slow deposition of platelets on the collagen surface lasting for several minutes; Phase II with large thrombus thickening where platelets accumulated rapidly at rates exceeding 1.6 μm^3 μm^{-2} min^{-1}, and a Phase III of total occlusion with cessation of blood flow.[2] The length of time in Phase I was called the "lag time" and represents the attachment of only a few thousand platelets. In contrast, Phase II represents the accumulation of hundreds of millions of platelets and is likely a different mechanism than Phase I attachment. It is difficult to distinguish between a single mechanism for both phases or two total mechanisms based on the sampling allowed for manual image processing. These experiments quantified the thrombus thickness and accumulation rates with much greater resolution than previous studies. However, our general findings are in good agreement with low-resolution observations made by previous investigators.

The first experiments used 240 ml of blood. A second system was devised to reduce the required blood volume to 30 ml. This second system was verified to yield similar thrombosis with porcine blood, then utilized to study human blood (Chapter 3). The human blood showed a similar Phase I and II, but with quantitative differences. Human blood shows a lag time that is over 7 minutes and an RPA rate that is 4.5 μm^3 μm^{-2} min^{-1}, half as fast as RPA in porcine blood. RPA occurred in approximately

22.4% (28/125) of experiments. These results are consistent with the perception that pigs are hypercoagulable compared to humans.

The system was then used to compare anti-platelet efficacy at reducing high shear thrombosis as measured by thrombus thickness and accumulation rate (Chapter 4). Our in vitro assay demonstrates features seen clinically, i.e. high shear platelet thrombosis is inhibited by activation and $\alpha_{IIb}\beta_3$ blockers. The test further demonstrates that different anti-platelet agents have different efficacy, consistent with clinical experience. Further, our findings provide an alternative view from Ruggeri's findings that high shear platelet aggregation does not require activation or $\alpha_{IIb}\beta_3$.[1] Instead, we find that large accumulation of thrombus under high shear is prevented by activation blockade or specific $\alpha_{IIb}\beta_3$ blockade. Both results may be resolved by defining a mechanism by which high shear circulating platelet attachment/adhesion occurs via GPIb without activation but high shear thrombus accumulation over several minutes requires stabilization from $\alpha_{IIb}\beta_3$ conformation change. An additional distinction may be that our high resolution thickness measurements allow the separation of Phase II accumulation from the Phase I attachment/aggregation that is more likely in the Ruggeri experiments. The results are clinically significant as we find in vitro quantification of thrombosis similar to previous literature describing patient response to the anti-platelets.

Lastly, we use our system to investigate whether excess (soluble or immobilized) vWF can increase either thrombus thickness or accumulation rate (Chap 5). In our system, the thrombus thickness increased by 100% with excess plasma (soluble) vWF for very high shear (10,000s^{-1}) but not at 3,500s^{-1}. In contrast, (immobilized) vWF deposited on the surface (under static conditions) did not have a significant effect at either high hemodynamic shear rates. As vWF may have more of an impact on Phase I, future experimentation may include the study of vWF immobilized to the stenosis surface prior to perfusion to measure the influence of vWF enrichment on Phase I.

The results of this dissertation indicate that thrombus formation within arterial stenosis is dominated by a Phase II rapid platelet accumulation. This formation is best characterized by an assay that can measure the thickness accumulation of millions of platelets rather than a surface attachment of a few platelets. Since clinical thrombosis arises from shear induced platelet accumulation (SIPA), patient-specific testing of whole blood at high shears may provide better titration of anti-platelet agents than static ristocetin or simple membrane occlusion assays. While high doses of some anti-platelet medications may prevent all thrombogenic effects in the blood, they may also create detrimental bleeding side effects for patients. Using a patient-specific assay would enable physicians to titrate anti-platelet medications to levels which prevent thrombosis only at very high shears without preventing all platelet deposition, thus preserving normal haemostasis.

Currently patients are being administered therapies based on recommendations via population studies and do not tailor their therapy regimes due to the patients themselves. Our findings in this thesis show that patients may benefit from patient-specific testing as one patient may not respond to all $\alpha_{IIb}\beta_3$ inhibitors or activation inhibitors equally. In the future, our system may be modified as a point-of-care system to provide accurate patient-specific titrations. Further, we find that patients may show a time dependent response, which may require adjustment of therapeutic doses within the time-span of a month similar to coumadin.

The hemodynamic system may be used for patient-specific testing of whole blood at high shear rates. The device would need to be modified so that the manual method of setup and measurement is automated. If the blood delivered upstream would be in a vacutainer, the device would be convenient with current phlebotomy practices. Multiple stenoses may also be placed upstream to simulate multiple plaques in a single artery and potentially preactivate platelets. An ideal model would also have a high throughput so that many therapies could be tested at once, decreasing the time

from blood draw to therapy formulation.

This BioEngineering thesis describes a method for quantifying the potential of human blood for high shear occlusive thrombosis, distinguishes a phenomenon of Rapid Platelet Accumulation, and demonstrates the utility of such a system to explore patient-specific responses to clinical anti-platelet agents.

6.0.26 References

REFERENCES

[1] Ruggeri, Z. M., Orje, J. N., Habermann, R., Federici, A. B., and Reininger, A. J., "Activation-independent platelet adhesion and aggregation under elevated shear stress," *Blood*, vol. 108, no. 6, pp. 1903–1910, 2006.

[2] Wootton, D. M. and Ku, D. N., "Fluid mechanics of vascular systems, diseases, and thrombosis," *Annual Review Of Biomedical Engineering*, vol. 1, pp. 299–329, 1999.

APPENDIX A

CH3 SUPPLEMENTARY FIGURES

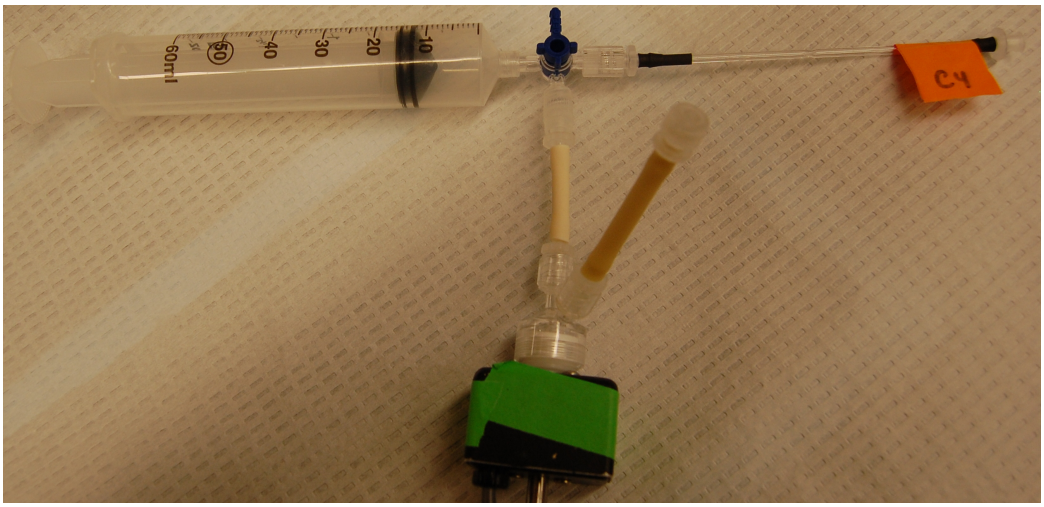

Figure 43: A detailed image of the syringe pump components are shown above. Flow is from left to right. Blood flows from the syringe pump, past the pressure transducer and into the stenotic test section. During experimentation there is usually a tube connected to the downstream end of the stenosis so that the blood cleanly flows into a waste container (not shown). The 3-way valve used posessed a 1.6mm inner diameter ensuring that the highest shear was located in the throat of the stenosis.

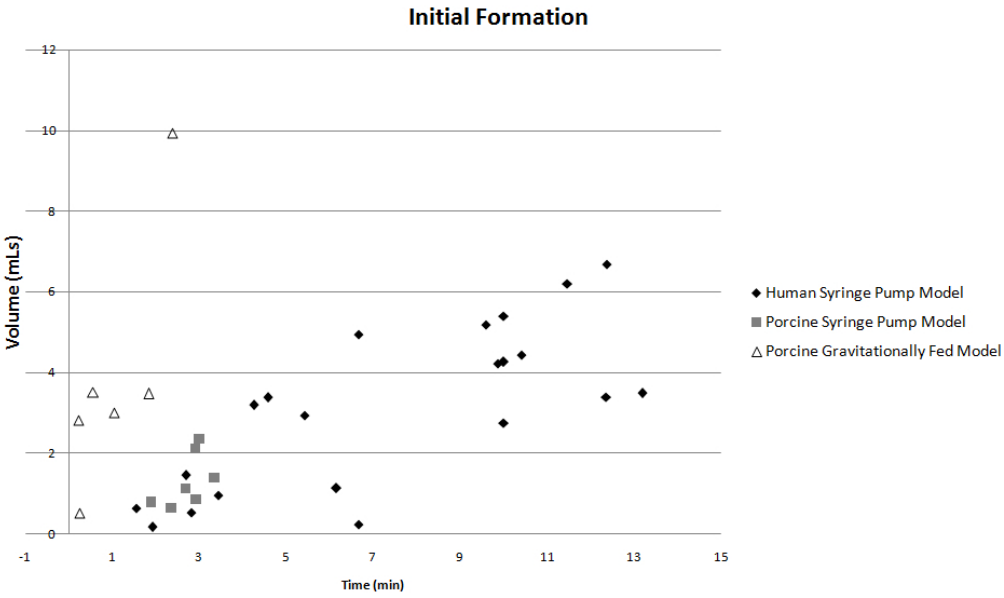

Figure 44: Scatter plot of time versus volume of blood required for visible initial formation in the human syringe pump model, the porcine syringe pump model and the porcine gravitationally fed model.

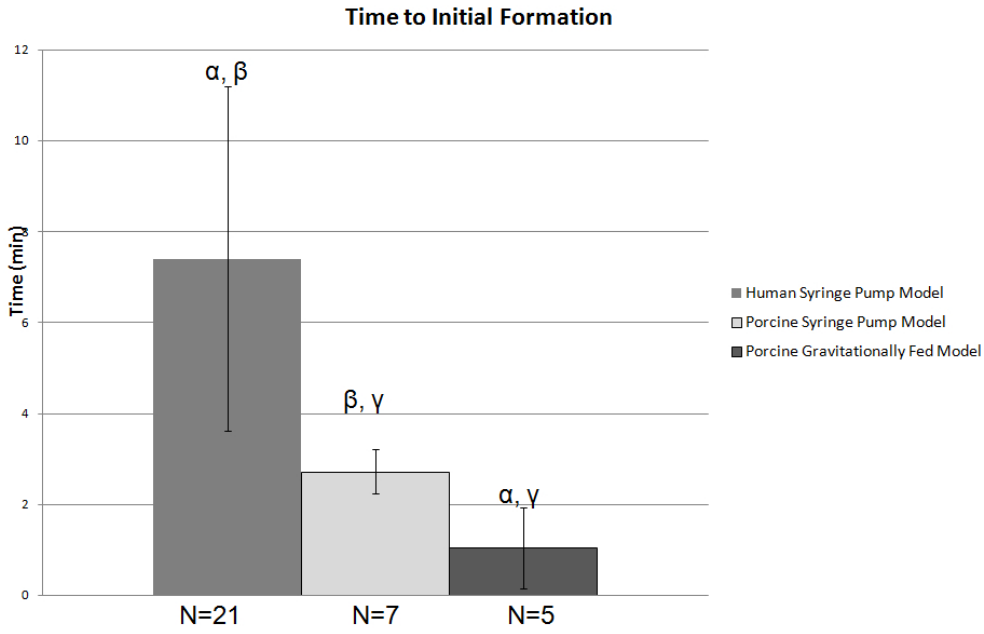

Figure 45: The average time to visible initial formation is shown above for the human syringe pump model, the porcine syringe pump model and the porcine gravitationally fed model. The bars denote the standard deviation. The time to initial formation for the human syringe pump model is significantly higer (7.4 $\pm$ 3.8 min) than the porcine syringe pump model (2.7 $\pm$ 4.9 min, α, $p<0.05$) and the porcine gravitationally fed model (1.0 $\pm$ 0.9min, β, $p<0.05$). The porcine gravitationally fed model is significantly faster (γ, $p<0.05$) then the porcine syringe pump model.